Investigating flood susceptibility and vulnerability through geospatial techniques in Kerala State, India

Navya Saira George-Mohan

GRGNAV001

Department of Architecture Planning and Geomatics: Division of Geomatics

Faculty of Engineering and the Built Environment

Thesis submitted in fulfilment of the requirements for the Degree of

Master of Science in Engineering (Geomatics) at the

University of Cape Town

Supervisor:

Associate Professor Patroba Achola Odera

September 2022

Copyright Declaration

Authorship Declaration

I know that plagiarism is wrong and that I cannot use another author's work and pretend that it is my own. This thesis is my own work.

Each significant contribution to, and quotation in this thesis from the work(s) of other people has been attributed and has been cited and referenced.

The work in this thesis has not previously been published in whole or in part for the award of any degree.

Signature: Signed by candidate **Date:** 06/09/2022

Research Ethics Declaration

Application for Approval of Ethics in Research (EiR) Projects
Faculty of Engineering and the Built Environment, University of Cape Town

APPLICATION FORM

Please Note:
Any person planning to undertake research in the Faculty of Engineering and the Built Environment (EBE) at the University of Cape Town is required to complete this form **before** collecting or analysing data. The objective of submitting this application *prior* to embarking on research is to ensure that the highest ethical standards in research, conducted under the auspices of the EBE Faculty, are met. Please ensure that you have read, and understood the **EBE Ethics in Research Handbook** (available from the UCT EBE, Research Ethics website) prior to completing this application form: http://www.ebe.uct.ac.za/ebe/research/ethics1

APPLICANT'S DETAILS		
Name of principal researcher, student or external applicant		Navya Saira George
Department		Department of Architecture, Planning and Geomatics
Preferred email address of applicant:		navgeo95@gmail.com
If Student	Your Degree: e.g., MSc, PhD, etc.	MSc
	Credit Value of Research: e.g., 60/120/180/360 etc.	180
	Name of Supervisor (if supervised):	Dr Patroba Odera
If this is a researchcontract, indicate the source of funding/sponsorship		
Project Title		Investigation flooding vulnerability through geospatial techniques in Kerala State (India).

I hereby undertake to carry out my research in such a way that:

- there is no apparent legal objection to the nature or the method of research; and
- the research will not compromise staff or students or the other responsibilities of the University;
- the stated objective will be achieved, and the findings will have a high degree of validity;
- limitations and alternative interpretations will be considered;
- the findings could be subject to peer review and publicly available; and
- I will comply with the conventions of copyright and avoid any practice that would constitute plagiarism.

SIGNED BY	Full name	Signature	Date
Principal Researcher/ Student/External applicant	Navya Saira George	Navya	**20 Mar 2019**

APPLICATION APPROVED BY	Full name	Signature	Date
Supervisor (where applicable)	Patroba Odera		22/3/2019
HOD (or delegated nominee) Final authority for all applicants who have answered NO to all questions in Section1; and for all Undergraduateresearch (Including Honours).	Simon Hull		22/03/2019
Chair : Faculty EIR Committee For applicants other than undergraduate students who have answered YES to any of the above questions.			

Page 1 of 1

Abstract

A flood is an overflow of water that submerges land that is usually dry. Flooding is a complex phenomenon caused by various meteorological, hydrological, geomorphological, and anthropogenic factors. Flood susceptibility identifies the most vulnerable areas that are flood prone based on the region's physical features. Flood vulnerability is the degree to which people or man-made structures are affected by, or unable to cope with the effects of flooding. One of the key factors in risk management and flood damage assessment is determining flood vulnerability. There has been an increased need to understand floods as they are recurring more frequently. The objectives of this study were to determine the land use/cover changes in Kerala State over the last 45 years, model flood susceptibility for the years 1973, 2001 and 2018 and finally determine flood vulnerability in Kerala for the year 2018. These objectives were achieved through Remote Sensing and GIS techniques. Image classification of Landsat images helped identify the change in land use/cover. The flood susceptibility model was attained by processing the physical characteristics and using the multi-criteria weighted analysis. The flood vulnerability model was achieved by processing the copying, social, infrastructure and physical vulnerability. Again, multi-criteria weighted analysis was used. Results show that in the year 2018, 50.31 % of the area had a medium flood susceptibility and 28.74% of the area had a high susceptibility. The areas of high flood susceptibility and medium flood susceptibility are visually seen to be around the high concentration of built-up area. The high susceptibility regions have only increased since 1973 as the built-up area increased. Regarding flood vulnerability, most of the State (60.59%) had a medium flood vulnerability in 2018, followed by high vulnerability areas taking up 28.48% of the land. The high vulnerability areas are found along the west coast of the State. This study brings awareness that the flood susceptibility regions are

increasing year by year and that the State has areas that are highly prone to flood vulnerability. The driving factors behind the increase in flood susceptibility and high flood prone areas are the increase in rainfall, population and the built environment.

Acknowledgements

To Arun:

Thank you, thank you, thank you. You have spent time explaining to me how to process data and where to attain it from. This thesis was possible because of you. You went above and beyond to send data to me and explain it to me. That data helped me complete my thesis. Your knowledge and understanding of GIS and Remote Sensing helped me greatly. I can't thank you enough for your time and effort.

To Jacqui:

Thank you for checking my language style and grammar.

To my husband, Jithin Zachariah Mohan:

Thank you for supporting me through this process. Your constant support, motivation and love has helped keep me motivated and driven me to complete this. You have been cheering me on since we met.

To my family:

You have been a great emotional support. The constant advice, motivation and reassurance has been necessary for me to attain my goal.

To my lecturers/staff:

Associate Professor Patroba Odera, thank you for taking me on as your student. You have always been available to guide and redirect me when I fumble. This journey has been enjoyable and tough, but you have constantly stood by me. Your knowledge and ability to guide has always left me in awe. Thank you, again. I do appreciate your guidance.

Nichholos Lindenberg, Thomas Slingsby and Mignon Wells, thank you for supporting me technically. You have helped me to understand, process and interpret the data. Without your advice this would not be possible.

Dedication

I dedicate this thesis to my parents- Mr Varkey George and Mrs Thara Thomas. I cannot thank you enough for all you have done for me.

You nurtured and protected me
And taught me with great care
And every time I needed you,
You were always there.

Thank you!

Table of Contents

List of Tables

List of Figures

List of Abbreviations

AHP: Analytical Heirachy Process

ASTER: Advanced Spaceborne Thermal Emission and Reflection Radiometer

CART: Classification and Regression Trees

CHIRPS: Climate Hazards groups Infarer Precipitation and Stations

CR: Consistency Ratio

DEM: Digital Elevation Model

DTM: Digital Terrain Model

ESA: European Space Agency

GIS: Geographical Information Systems

GLOBE: Global Land One-Kilometer Base Elevation

LIDAR: Light Detection and Ranging

InSAR: Interferometric Syntehtics-Aperture radar

MODIS: Modis resolution Imaging Spectroradiometer

NASA: National Aeronautics and Space Adminitration

NGA: National Geospatial- Intelligence Agency

NOAA: National Oceanice and Atmosphere Administartion

RADAR: Radio Detection and Ranging

RS: Remote Sensing

SAR: Synthetic Aperture Radar

SLAR: Side Looking AIborne Radar

SRL: Shuttle Radar Lab

SRTM: Shuttle Radar Topography Mission

TRMM: Tropical Rainfall Measuring Mission

USGS: United States Gelogical Survey

Chapter One

1 INTRODUCTION

1.1 Background

Flooding is water overflowing onto land that is usually dry (Doswell, 2003). Urban floods occur because of heavy rainfall where the riverbank over-flows due to high tides or storm surges (Tingsanchali, 2012). Insufficient drainage is one of the main reasons behind floods that occur during heavy rainfall. The floods occurring during riverbank over-flow transpire when the river level rises above the riverbanks. High runoff from upstream and high tides at river mouths cause river levels to increase (ibid). Flooding becomes dangerous when it effects crops and properties - people lose their lives and their livelihoods are affected (Harley & Samanta, 2018).

Flood vulnerability is one of the key factors in risk management and flood damage assessment (Nasiri, et al., 2016). The flood vulnerability assessment methods can be categorised into four main groups:

(i) The vulnerability indicator method: this method helps decision makers assess economic, social and environmental factors (Papathoma-Kohle, 2016). According to Birkmann (2007), it helps examine and discuss the root causes of risk and vulnerability. This method proves variables that are represented to secure information regarding susceptibility, coping capacity and resilience (Papathoma-Kohle, 2016). The vulnerability indicator method may help to facilitate mitigation, emergency management and communication. This method requires several steps such as indicator selection, normalisation, weighting and aggregation into a final index. Indicator weighting is the most sensitive step – it can be based on Principle Component

Analysis, Analytical Hierarchy Process or budget allocation approaches (Cristofari, et al., 2019). Nonetheless, this method has a higher chance of being misrepresented and could potentially be misleading. Even though this approach is statistical it needs expert judgement to interpret the data and the expert will need to choose the best indicator weighting system.

(ii) The disaster loss data method: the loss assessment plays a vital role in risk assessment and management (Emergency Management Australia, 2002). A rigorous approach to assess losses is needed for decision makers. An economical loss assessment helps in analysing and developing mitigation proposals. Social and environmental losses need to be considered too). A loss assessment is used for various reasons such as a guide to recovery management, support local or regional risk assessments or/and estimating the average annual damages etc. (ibid). This method is simple when compared to the other methods, but it could be somewhat inaccurate as the data may be unevenly recorded (Nasiri, et al., 2016).

(iii) The vulnerability curve method: this method focuses on the degree of loss rather than the likelihood or probability of loss (Papathoma-Kohle, 2016). Keiler, et al., (2012) states that the development of the curve is based on information and data provided by the local authorities or insurance companies. In order for this method to be concise, a substantial amount of empirical data is required. This process is useful for decision makers and cost analysis as the curve method can assess the potential cost of future events (ibid).

(iv) Modelling Method: this method looks at depth, elevation and velocity of flooding based on the frequency, magnitude and shape of the hydrograph (Nasiri, et al., 2016). Hydrodynamic models include one-dimensional, two-dimensional and three-dimensional models. These models solve equations to simulate water movements. Another method is also used to model large areas and provide data for sparse areas using a simplified conceptual model (Teng, et

al., 2017). This method represents the physical processes more moderately. These models are more suitable for large areas or stochastic modelling for probabilistic flood risk assessment.

Kerala is a State on the south-western region of India (Figure 1). This State roughly occupies 1 percent of the total area of the country (Noble, 2019). The State was formed in 1956 by combining the various Malayalam speaking regions as per the States Reorganisation Act. The languages spoken by the inhabitants of the State are Malayalam and English. This study looks at the vulnerability indicator method.

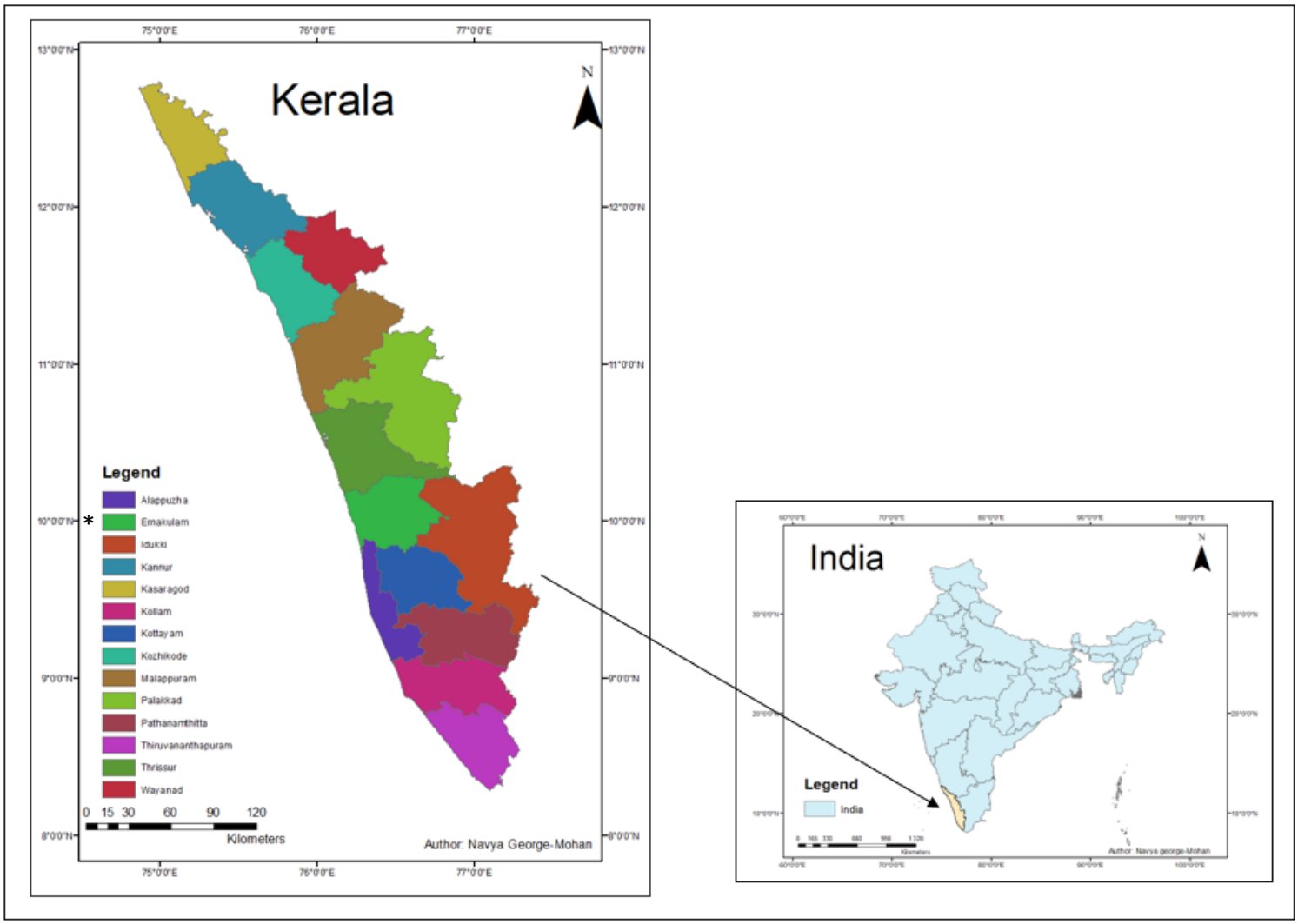

Figure 1: Region of interest

Kerala's location played a vital role in its development and growth as it connected the western part of the world to the eastern part of the world. Trade links between China and the Arab worlds as well as Europe existed. The traders who came from across the world included Jews, Christians and Muslims (Ramerini, 2016). Kerala's location has played a vital role in its development and growth as it connected the Western part of the world to the Eastern part of the world. Many traders were forced to stay in Kerala for long durations as sailing was impossible during the monsoon period. These settlements helped develop the State. The influence of the many different religions, beliefs, trade practices and languages exposed the people of Kerala to the wider world and has had a direct impact on their development as compared to other States in India (ibid).

Even though Kerala is closer to the equator than many of the other States in India, it experiences a constant temperature of $28 - 35^{\circ}C$ throughout the year (Thomas, 2000). The ocean on the east side and the Western Ghats on the west side is why the temperature remains within that range. Kerala has a tropical humid climate with intermittent wet and dry periods. The State experiences two monsoon periods – these are the South-West Monsoon and North-East Monsoons (Thomas, 2000). The rainy season is from early June, through to the middle of December. The South-West Monsoon rain brings the most rain and falls during the period of June to August, whereas the North-East Monsoon brings less rain and falls during the period of October to December. The average rainfall for Kerala is 3000 mm which can vary from 1000 mm in the low-lying areas and over 7600 mm on the hill side. The dry weather starts from mid-December to June (ibid).

Figures 2, 3 and 4 below depict the floods experienced in Kerala in 2018. Kerala experienced abnormally high rainfall during 1 June 2018 to 19 August 2018 (Government of India, 2018) Severe flooding was experienced in 13 of the 14 districts. The last major flooding event was in 1961 and 1924. All 14 districts in the state were red alerted (Gopikrishnan Unnithanan, 2018).

Figure 2: Flood in Kalissery

Source: Business Standard (https://www.business-standard.com/article/current-affairs/after-kerala-s-devastating-floods-how-lights-came-back-to-ravaged-homes-118111200078_1.html)

Figure 3: Landslides in Kozhikode, Kerala

Source:(https://www.theatlantic.com/photo/2018/08/devastating-monsoon-floods-in-kerala-india/568171/)

Figure 4: A dam gates being opened in Kerala

Source: (http://newstimenow.com/kerala-flood-situation-worsens-cochin-airport-shut-for-4-days/)

1.2 Statement of the problem

A previous study conducted in Kochi city, Kerala, only looked at the flood vulnerability of the city. The objective of this study was to find flood vulnerability zones within the city (Sowmya, et al., 2014). Another study looked at flood inundation in the Districts of Thrissur, Ernakulam, Alappuzha, Idukki and Kottayam in Kerala (Vishnu, et al., 2019). The latter study looks at very minimal variables, when determining the vulnerable zone, seven to be exact and it does not look at flood susceptibility and various vulnerability factors that contribute to flood vulnerability. Notable variables that are missing are land use/land cover, rainfall and the geological aspect which are included in this current study of Kerala. Another shortcoming is that this former study also only looks at one city within the entire State. The study conducted by Vishnu, et al., 2019 looked at satellite imagery before and during the flooding period to determine the rise in water bodies where a Modified Normalised Differential Water Index (MNDWI). The shortfall in this former study is that it does not look at any other factors that might cause an increase in inundation or vulnerability.

The study presented here on the State of Kerala fills an important gap as it covers the entire State in an attempt to help determine flood susceptibility and vulnerability within Kerala. In this instance, the focus is on flood susceptibility modelling and will include land use/land cover, elevation, slope, drainage density, soil, lithology and rainfall. Flood vulnerability is determined by exploring infrastructure, social, physical coping vulnerability that goes with flood susceptibility. This approach is therefore more holistic and considers many more variables than the previous studies. This will help in understanding if the state and cities are sustainable, how the climate affects the region and whether floods affect the wellbeing of the citizens. These factors tie in in with the sustainable Development Goals.

The study conducted by Sowmya, et al., 2014 used the same method as this current study- the layers were integrated through the multi-criteria approach. And, weighted overlay analysis was used in both studies to determine urban flood vulnerability and zoning. However, the study conducted by Vishnu, et al., 2019 used Modified Normalised Differential Water Index (MNDWI) to determine inundated areas. This method was not used in this study.

1.3 Objectives of this study

- To carry out a time series analysis of land use/land cover and related changes over Kerala State from 1973 to 2018.
- To model flood susceptibility over Kerala State from 1973 to 2018 using geospatial techniques.
- To model flood vulnerability for Kerala State by taking into account flood susceptibility, infrastructure, social and coping parameters.

1.4 Research Questions

1. How has the use of land changed between the years 1973 to 2018?
2. Have the flood susceptibility areas increased or decreased over time?
3. Which areas were highly vulnerable to floods in 2018?
4. What changes in land use/land cover have contributed to the increase or decrease in vulnerability/susceptibility?

1.5 Thesis structure

This thesis consists of five chapters. The first chapter gives a brief introduction of the study area, the problem statement, the objectives and research questions. The second chapter is the literature review, and it reviews the work that is pertinent to this study and that has been done in the past. It especially discusses the various types of floods and techniques around mapping flood vulnerability. Chapter three is the methodology chapter, and it discusses how the data was attained, the processing it underwent and how the calculations were performed. The results are then presented in chapter four, where the findings are discussed. Chapter five concludes the study and provides recommendations for future research.

Chapter Two

2 LITERATURE REVIEW

2.1 Types of Floods

Flooding is a complex phenomenon that can be caused by several meteorological factors such as intense or long-lasting rainfall, snowmelt, ice jam, glacial lake, coastland flooding and storm surge (Kundzewicz, et al., 2010). Other factors include hydrological and anthropogenic factors. Hydrological causes of flooding include infiltration rates and land erosion. Whereas the anthropogenic causes of flooding include population growth, urbanisation, climate change and global warming (Gaur, 2020). Floods can be categorised into riverine, pluvial, coastal and groundwater floods. This chapter examines these different types of floods.

2.1.1 Riverine floods

Riverine flooding usually occurs after long periods of rainfall or snowmelt within large catchment areas which results in slow rising of water levels (Lauda, et al., 2020). Riverine floods are seasonal and could last for many days and sometimes occur for many weeks (Gaur, 2020). The damages caused by riverine flooding have increased drastically in the last few decades. The contributing factors to these kinds of floods are terrestrial, socio-economic and climate systems. The climate change (heavy precipitation) is said to be the main contributing factor for the increase in riverine flooding, that is over and above human encroachment (Kundzewicz, et al., 2010).

There are two types of riverine flooding, one being slow onset floods and the second being rapid onset floods. The former flood type lasts longer whereas the latter flood type occurs in mountain or slope areas where the flood is at a high velocity. Harshit Gaur claims that riverine flooding is both

advantageous and disadvantageous. Although there is loss of property and crops, nutrients of the soil that have been lost due to agriculture are returned to the soil (Gaur, 2020).

It has been established that precipitation is the driving force behind riverine flooding. Precipitation is generated by different mechanisms (Blösch, et al., 2015). Large scale precipitation is related to the regional pressure and the influx of atmospheric humidity. An example of this can be seen in Western Europe during the period of winter floods. During this time, large quantities of humidity are transported across the Atlantic from the sub tropics. This shows that the precipitation rates are influenced by the changes in frequency and characteristics of global atmospheric circulation. Small scale precipitation produces higher intensity of rainfall due to the stability of the atmosphere. Stability of the atmosphere is when the air resists movement. Instability is when the air moves up, cools down, condensates and then precipitation occurs. This process occurs because the lower air warms up due to the radiation from the ground heat which decreases the density and thus allows for movement (ibid). If the air is warmer the atmosphere is able to hold more water. Hence, warmer regions are expected to have higher precipitation rates.

2.1.2 Pluvial Floods

Pluvial floods occur after short intense downpours of rainfall which cannot be evacuated by the drainage system or infiltration. These kinds of floods are often found in urban areas where there are many impermeable surfaces. The consequences of this kind of flood is thus greater in urban areas due to the density of buildings (Houston, et al., 2011). Surface runoff produced by rainfall is reliant on the drainage system, however, there is a limit to what the drainage system can handle in overbuilt areas and hence pluvial floods taking place when storms occur (Chen, et al., 2010).

Pluvial floods occur with very little warning and do not always happen in flood prone areas (Houston, et al., 2011). These floods are also both difficult to predict and to manage which makes it difficult to prepare warnings for the public. Falconer et al,. (2009) suggest that a trigger rainfall forecast combined with identifying locations prone to pluvial flooding should be used by organisations to warn their citizens of possible flooding.

Adebe et al, (2018) states that drainage infrastructure capacity, type and condition of the infrastructure together play a key role in influencing the occurrence of pluvial flooding. The drainage infrastructure consists of two systems - minor and major systems. The minor system is the underground sewer network while the overland flow route is the major system. The infrastructure has to be in good condition and perform according to the design to prevent pluvial flooding and also the design capacity as well as the performance condition has to be taken into account when determining pluvial flood vulnerability (ibid)

Houston et al. (2011), suggest that pluvial flood risk can be limited or even decreased if sustainable urban drainage systems, surface water management and flood proofing is put in place. According to these authors, separating the storm water and foul water systems will help to increase the drainage capacity and reduce the possibility of the sewage mixing with pluvial flood water. However, this often proves difficult to do as the systems are already in place. Houston et al. (2011) suggests that when building in built or renovated flood prone areas, flood proofing should be done on the building.

2.1.3 Coastal Floods

Coastal urban flooding is seen to be increasing, affecting mainly the coastal urban settlements. Diez et al. (2011) states that this is either due to sea level and/or climatic factors such as population increase. Changes in sea levels are affecting human activities in coastal areas which makes coastal

infrastructure more vulnerable to damage from storms. When the water rises above the expected levels, minor flooding may occur on streets causing many drains to become ineffective (United States Environmental Protection Agency, 2016). When this is a recurring phenomenon one will see frequent road closures, reduced storm-water capacity and the deterioration of infrastructure. Even though the sea level rise is slow, it is still significantly exponential as even a small rise in sea level can increase the frequency of coastal floods (Taherkhani, et al., 2020).

Population growth and migration from rural to urban areas means that low elevation coastal zones are holding higher population density and urban areas are being extended. This phenomenon is found particularly in developing countries such as Africa and Asia (Grases, et al., 2020). As a result there is an increase in both seashore erosion and inland flooding. According to Taherkhani et al. (2020) the sea level rise will redefine the coastline in the 21st century and for many coastlines the sea-level rise will be in the range of 0.5 – 2 meters by the year 2100. Changes in coastal flooding will be experienced – from events that occur only rarely today to more frequent flooding over time (Taherkhani, et al., 2020).

In the United States of America there are indicators that track coastal flooding based on measurements from tide gauges. The United States Environmental Protection Agency (2020) implemented these devices to measure water levels and this is also ideal for measuring the height of tides, tracking of sea level rise and detecting coastal floods.

2.1.4 Groundwater floods

Groundwater is a term used for water that is beneath the surface (Environment Agency, 2014). When water falls there are four possibilities for their destination – firstly water runoff into rivers, streams and drains, secondly some of the water will evaporate, thirdly plants may absorb it and lastly the soil

will absorb the water which seeps into deeper layers of soil and rocks. The Environment Agency (2014) explains that groundwater can be found in aquifers and that an aquifer exists when the saturated rock is permeable which allows the ground water to flow relatively easily. These aquifers are found underground and are usually large reservoirs.

Groundwater flooding is when the groundwater emerges at the ground surface away from the perennial river channels or the rising of ground water onto man-made grounds (Macdonald, et al., 2012). Similar to riverine flooding, groundwater flooding can cause extreme damage to infrastructure, especially to basements. Regrettably there is very little information available about groundwater flooding and this phenomenon is poorly understood (Abboud, et al., 2018). What we do know is that the areas prone to groundwater flooding are situated in low lying areas which are on or near an aquifer . It is often hard to differentiate between groundwater flooding and the other kinds of flooding as excess rain that falls will not be absorbed by the soil and will be seen to be flowing naturally across the surface similar to the groundwater which has emerged (Environment Agency, 2014). This type of flooding usually takes longer to subside as large volumes of water have to flow away in order for the water table to be lowered.

The United Kingdom has taken the approach to map out risk areas of groundwater flooding by acquiring historical evidence and developing procedures to capture data around future ground water floods. However, Macdonald et al. (2012) states that it is difficult to identify whether groundwater flooding was in fact the source of a particular flood. Similarly, the return periods of groundwater flooding are also difficult to assess. The method used to map out flood risk areas is to combine average groundwater levels over three months with the digital terrain model (DTM). This data is then used to create groundwater level contours to calculate the depth to groundwater. This data will then be translated to match areas with zero depth that are known for groundwater flooding. A warning

system, placed in boreholes, has also been established where local flood watches have been established to determine when groundwater levels increase (Macdonald, et al., 2012).

Majority of rains experienced in the state are during the monsoon period. The state experiences Pluvial and Coastal floods.

2.2 Flood Vulnerability

Vulnerability can be understood as the degree to which people or places are susceptible to, or unable to cope with, effects of climate change (Coninx & Bachus, 2007). As floods are increasing, public authorities and researchers have intensified their research in understanding the factors that contribute to the risk (Roder, et al., 2017). These various risk factors are social vulnerability, coping capacity, physical vulnerability and reaction.

2.2.1 Social vulnerability

Social Vulnerability can be broken down into gender, age, education, economic welfare and various other factors. It can also include community dynamics and support systems. Social vulnerability can be divided into population exposure and resistance which includes reaction capacity. These factors help determine the resilience of people in a given community (Tascón-González, et al., 2020).

Previous studies have always used a broad range scale when it comes to cartographic units, municipal districts and census blocks (Tascón-González, et al., 2020). However, spatial accuracy has improved with open access databases which provide high precision. The difficulty one faces is that classifying a general characteristic as vulnerable is not always accurate as the more complex social, economic and political context will have to be taken into account (Roder, et al., 2017).

Areas with higher population density are more vulnerable as the evacuation may be difficult (Tascón-González, et al., 2020). The elderly, over 75, is an at-risk group as they have limited mobility and might also experience visual and hearing impairment (Coninx & Bachus, 2007). Those aged above 75 often have limited access to financial and other resources making recovery and evacuation difficult. Another vulnerable age group that is affected by flooding is the cohort of children below the age of 15 as they will need adult supervision (Scheuer, et al., 2010). In Pakistan, women are greatly affected by floods and are therefore more vulnerable than men. Furthermore, the relief camps that are provided are often unhygienic or unsafe. Women who are pregnant and anaemic are often overlooked or not given the right care. Women are also vulnerable to abuse and there have been cases of women being ill-treated at camps. Women were often overlooked and their role in the case of a natural disaster has been minimised due to the belief that women are more insecure, illiterate, lack confidence and have specific social attitudes within the community (Bukhari & Rizvi2, 2015).

Those who are financially deprived are greatly affected by floods as they may struggle to afford insurance and flood protection material. It is also the case that the material of their buildings is likely to be of a lower quality which would mean that it would have greater damage. For the poorest of the poor, of even for those who are simply economically vulnerable, recovery is a long-term process due to their financial limitations (Coninx & Bachus, 2007). Furthermore, a high unemployment rate is likely to mean that they rely on the government for relief aid as they would be unable to carry financial losses after a disaster (Roder, et al., 2017)

2.2.2 Coping Capacity

Certain communities, social groups and ecological systems tend to cope better with the impact of natural disasters than others due to particular characteristics such as better care, infrastructure,

knowledge and shelters. Clearly then, vulnerability should take into account the coping capacity of a give society (Brito, et al., 2017). As stated above, evidence from the study completed in Bangladesh, shows that coping capacity refers to the capability of people, organisations and systems to manage the effects of disasters using the skills and resources available. Determining these strengths and weaknesses would help mitigate for disaster effects (Hoque, et al., 2019).

Vulnerability, according to certain experts, is the lack of coping capacity (Brito, et al., 2017). Various studies have looked at coping capacity in different ways. Table 1 below indicates the variables considered when determining coping capacity.

Table 1: Copying capacity variables

Variables	Source
Disaster prevention institutions	Adapted from Brito et al. (2017)
Evacuation drills and training	
Distance to shelters	
Existence of clearly marked escape routes	
Health care facilities	
Life expectancy	Adapted from Dunford et al. (2014)
Tertiary education	
Income inequality	
Assistance in time of threat	
Transport	
Produced Capitol	
Food shelter	Adapted from Hoque et al. (2019)
Distance to health complex	
Literacy rate	

The contributing factors stated in the study by Brito et al. (2017) were determined by scientists, policy makers and practitioners to identify the indicators to analyse flood vulnerability. The aim of the study was to involve stakeholders and to tap into their knowledge about the contributing factors around flood vulnerability. Dunford et al. (2014) looked at the climate impact and the capacity of the population to handle climate change vulnerability. There are many factors that mitigate for disasters

and Hoque et al. (2019) claim that some of these factors include access to shelters and hospital complexes which together decrease the negative impacts of the disaster.

2.2.3 Physical vulnerability

A natural disaster that has increased in occurrence is flooding (Mundhe, 2018). This has called for the need for a study of natural/physical factors (Hoque, et al., 2019) to better understand the reasons for these occurrences and to consider factors that might lessen their impact. There are many factors that can be taken into account such as land use/land cover, drainage density, rainfall, lithology, soil, elevation and slope. Land use affects the infiltration rate. The rate is determined by the interrelationships between surface and groundwater as well as debris flow (Mundhe, 2018). It has been found that forest and vegetation areas are more prone to infiltration, whereas urban areas have impermeable covers which cause water runoff (Lappas & Kallioras, 2019). A study undertaken in Slovakia, stated that ongoing climate change and the change in land use are contributing factors to flooding events (Vojtek & Vojtekova, 2019).

Drainage Density is the measure of stream spacing which expresses the length of river per unit of area. One attains the drainage density map by using the Line Density Tool which is found in ArcGIS. (Hammami, et al., 2019). Drainage Density plays a vital role in flood control as it reflects the length of rivers per unit. A study conducted by Mundhe states that permeable materials have a low drainage density whereas impermeable materials have a high drainage density. The same study also claims that a higher value of drainage density suggests a lower infiltration rate. The study conducted in Pune found that humid regions tend to have a lower density as thick vegetation promotes infiltration (Mundhe, 2018).

Other variables considered for physical vulnerability is elevation and slope. The vertical distance between a point of surface of the ground and a reference point which is usually the mean sea level is known as elevation (McVicar & Korner, 2012). The ways one can attain the elevation is either by reclassifying the DEM or by using the 3D Analyst Tool in ArcGIS on a topographical map with counter lines (Mundhe, 2018; Patrikaki et al., 2018). The use of a DEM to estimate slope is a common procedure for terrain analysis (Tang & Pilesjo, 2001).

Low lying areas are more susceptible to floods as flood frequency increases as elevation decreases. The elevation difference between two points is referred to as slope. Slope is also referred to as gradient which is represented as a percentage of a degree (Balasubramanian, 2007). There are various ways in which slope can be calculated. The calculation depends on the information provided such as whether one is working in 3D or 2D (Maidment & Tarboton, 2011). When working in a 2D land surface slope the x, y is on the earth's surface whereas the corresponding z value is the elevation value. The elevation value represents the vertical height of the land surface above the geoid surface at the location. The z value should be the same unit as the x and y. The gradient or slope can be defined by a 2D vector: Equations 1 and 2 are the land surface slope and the magnitude of land surface slope calculations.

Land Surface Slope:

$$Z = (x, y) = \left(\frac{\partial Z}{\partial X}, \frac{\partial Z}{\partial y}\right) \quad (1)$$

Magnitude of the land surface slope is given by:

$$|Slope| = \sqrt{\left(\frac{\partial Z}{\partial X}\right)^2 + \left(\frac{\partial Z}{\partial y}\right)^2} \quad (2)$$

This value is then multiplied by 100 to attain the percentage rise which can be computed using the slope function in an ArcGIS software (ibid). The slope of a pixel is attained by calculating the angle of the pixel plane with respect to the horizontal plane (Ritter, 1987). Ritter (1987) also claims that the slope is attained as a percentage of rise over run (Figure 5).

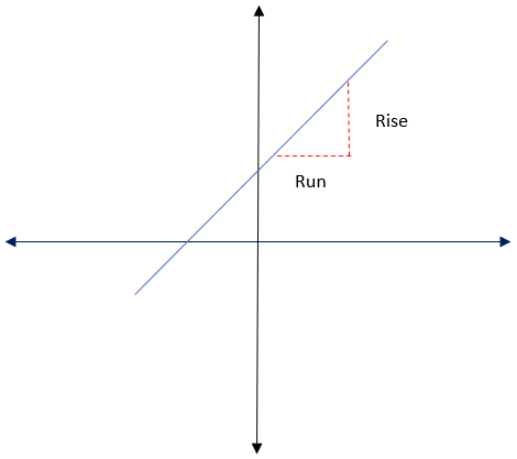

Figure 5: Rise over run

Adapted from ((Joy, et al., 2020)

Many researchers have included slope as an important factor in determining flood vulnerability. The lower the slope value the flatter the terrain and the higher the value the steeper the terrain (Getahun & Sintayehu, 2015). The steeper the terrain the lower the rate of water infiltration as these slopes are more susceptible to surface runoff (Lappas & Kallioras, 2019). This means the steeper the area

the higher the volume of run off, which indicates that these areas are less prone to flooding (Chapi, et al., 2017). The low-lying areas are therefore more vulnerable to floods (Mundhe, 2018).

Lithology is an important parameter that helps define flooding. Different rock types have varied water storage capacity and permeability. Impermeable rocks cause infiltration during rainfall which in turn, increases water runoff (Hammami, et al., 2019).

The texture and structure of soil influences the water storage capacity and the permeability of water. Impermeable soils often consist of clay which make them prone to flooding, whereas soils that are made up of sand are more permeable and have a higher infiltration rate (Lappas & Kallioras, 2019). Therefore, those soil types with sand in them tend to have a lower influence on flooding (Hammami, et al., 2019).

Rainfall is a triggering factor when it comes to flooding as it is often related to extreme precipitation. Local and regional scale analysis is more accurate than generalised national scale assessments (Vojtek & Vojtekova, 2019). A study in Pune found that flooding was caused in that region by increased rainfall causing surface runoff. The river channels could not cater for the increase in water load (Hammami, et al., 2019).

2.2.4 Infrastructure Vulnerability

Infrastructure is defined as basic facilities, services, transportation and communication systems, water and power line as well as public institutions. Infrastructure plays an important role in the functioning of industries, communities and the response against natural disasters (Len, et al., 2018). A study conducted in Ireland states that critical infrastructure is vulnerable and any damages may affect large areas over long periods of time (Bruijn, et al., 2016). The infrastructure is highly impacted

on by the network layout and level of dependency on this infrastructure by the society. Infrastructure is impacted on despite or irrespective of particular characteristics of floods (Len, et al., 2018).

It is important to identify first what networks exist and where they are located and then, once this has been determined, the resilience and resistance to flooding must be assessed. Once the resilience of the infrastructure and its potential to resist flood events has been determined the damage to one or more elements should be monitored to identify the ripple effects on other infrastructural networks (Bruijn, et al., 2016). Lastly, in the eventuality of the infrastructure collapsing, its impact on society and the extent to which the population relies on this infrastructure should be determined.

Rural areas flood control and defence is often very minimal in contrast to the flood hazards in urban areas, largely caused by development (Len, et al., 2018). The increase in flood hazards in urban areas are linked both to the rise in population and to increased infrastructure.

2.3 Techniques for mapping flood vulnerability

The assessment of flood hazards is critical for flood risk management, and it should include before, during and post flood events to better understand, prevent and mitigate flood hazards (Setler, 2014). This assessment helps to understand the impacts of floods on humans, the ecosystems and on natural resources. The methods that will be covered in the next section include Geomorphological, Historical, and geospatial techniques.

2.3.1 Geomorphological Method

Geomorphology when directly translated from Greek to English means “discourse from earths forms” (Huggett, 2011). Geomorphology is the study of landform and landform evolution. This type of study provides both qualitative and quantitative information (Setler, 2014). The former involves

descriptions of landform, and the latter is about processes which describe the forces acting on the earth's surface to produce landforms. It also describes landform changes.

Dordrecht (2007) explains that the modern study of geomorphology examines linkages between channels, floodplains, networks and the catchment area. Diverse approaches such as stratigraphic analysis, experimental studies of sediment transport in flumes, modelling of physical processes, comparison of landforms and sophisticated statistical approaches are undertaken to better understand the physical dynamics of river systems (Dordrecht, 2007). Fluvial geomorphology has been used from modern to millennial times to rigorously assess flood hazards on a local and a global scale (Benito & Hudson, 2017).

Geomorphology looks at flood hazard analysis through several angles. Horton, Strahler and Schumm, in the 1940s and 1950s, developed models relating to flood hydrograph characteristics, quantitative drainage network and shape indices (Benito & Hudson, 2017). Hydrographic characteristics include peak runoff and lag time, and shape indices include the catchment area, drainage network and stream network geometry. This estimates the hydrological response in small basins. The second method is to map out flood-related landforms and deposits, soil and plant associations and flood observations. The last approach involves energy based inverse hydraulic modelling of discrete paleo-floods which are deposited as slack water (ibid).

2.3.2 Historical Method

According to Macdonald (2019), historical flood data can be attained worldwide and this helps reconstruct flood magnitudes. The available data contributes to information relating to flood timing, the extent of damage, the way in which the society responded and what precipitated the flooding in the first place. Access to this information helps understand flood risk and decreases uncertainty as a

fuller picture is attained with reliable quantitative data and not just a qualitative rendering. However, the limitations of historical data are that it is not always reliable and it can also be subjective, excluding particular factual information that is needed. Nonetheless, according to Macdonald (2019), some believe that it is better to include these datasets, however uncertain they may be, rather than have no understanding at all.

The aim of collecting historical data is to improve flood frequency estimates and a review of this historical data should be conducted using diverse methods. Reviewing such data means applying historical and hydrological judgement (Bayliss & Reed, 2001). However, when it comes to historical flood information there will be variation between both the format and its reliability. The historical data includes accessing epigraphic marks, documentary sources, images, markers and sediments. Epigraphic marks are water levels found on structures such as bridges which mark the height of the flood. Documentary sources are often parish records, newspapers, economic reports, military sources, state records and diaries (Macdonald, 2019). Images include visual renderings such as woodcarvings, paintings and photographs (Macdonald, 2019). Flood stones have been used to mark the spatial extent of floods. Lastly, one needs to rely on the reconstruction of floods that occurs from sediment accumulation.

According to Bayliss & Reed (2001), to ensure a systematic approach is put in place to evaluate the data acquired, the following three questions are appropriate: 1) Does the information attained relate to the site of interest? 2) Does the information prove that an event did occur? 3) Can the peak flow or level of water be established? Establishing the exact dates of events is not essential but determining the year of occurrence is important as it helps anchor the event within the particular time period. If the flooding event is to be included in the flood frequency analysis the peak flow will need to be attained or otherwise at least estimated (ibid).

2.3.3 Geospatial Techniques

This section looks at different systems of flood vulnerability detection through Remote Sensing, GIS, Image classification and weighted overlay.

The integration of information through a Geographical Information Systems (GIS) and Remote Sensing (RS) with other datasets assists in identifying, monitoring and assessing flood disasters (Haq, et al., 2012). These two methods (GIS an RS) help to model and visualise the extent of floods.

GIS has a broad range of tools that can be used to determine and forecast areas that are likely to be flooded. Remote Sensing on the other hand, can be limiting, as some sensors do not have night and cloud vision. In these instances, active microwave remote sensing must be used (Aggarwal, et al., 2009).

Any changes in land use, such as urbanisation, may trigger flooding therefore it makes sense that land use and floods are closely related (Faisal, et al., 2018). The physical cover of the Earth's surface is described as land use or/and land cover. This includes vegetation and non-vegetation (Arseni, et al., 2017). To ensure effective management of natural resources the information around land use/land cover is essential (Faisal, et al., 2018). One can attain land use/land cover information from satellite imagery. Arseni et al. (2017) states that the economic loss of a flood is highly dependent on the type of land cover. The most economical and efficient method of obtaining land use/land cover information is using LANDSAT data. This helps overcome the issue of inadequate data particularly in the case of developing countries where far less data is available on land use and land cover.

Remote sensing is very useful in monitoring flood damage It helps in reconstructing the recent history of the land surface (Arseni, et al., 2017). Additionally, the remote sensing data can be used in

conjunction with ground-based network data and in this way both GIS and remote sensing contribute greatly to natural hazard analysis.

Vulnerability mapping has been used in multiple studies. Mundhe (2028), used GIS and remote sensing techniques to map out flood vulnerability in Pune City. This study focused on data mentioned in Chapiter 2.2. This data used remotely senses imagery. Once the data was processed the multi criteria approach was used to determine the vulnerability levels. A study conducted in Bangladesh used the AHP based geospatial multi-criteria assessment technique to determine flood vulnerability (Hoque, et al., 2019), Physical, social and coping vulnerability was taken into account in this study. The physical vulnerability aspect used remote sense imagery. A study in Tunisia looked at flood susceptibility which encompasses the physical vulnerability aspects. These images were processed using remote sensing and GIS (Hammami, et al., 2019).

Two methods have become popular over the last centuries, and these are using empirical and hydrodynamic models. Empirical methods are measurements, surveys, remote sensing and statistical models (Teng, et al., 2017). A hydrodynamic model explains flood behaviour by using precipitation, infiltration and runoff which is then integrated using various statistical approaches (Ozcelik & Gorokhovich, 2020). Teng et al. (2017) states that the models can be one-dimensional, two-dimensional and three-dimensional. There is a third approach which looks at modelling very large plains. This approach is known as simplified conceptual models which are suitable for large areas and for the modelling of an area which has a probable flood risk (ibid). Hydrological models explain flood behaviour by integrating precipitation, infiltration and runoff. This type of model integrates empirical, numeric and statistical approaches (Ozcelik & Gorokhovich, 2020).

Empirical methods can be a limited representation of reality as the data includes on-ground measurements, surveys, interviews, aerial photographs and satellite imagery. The results that are

derived are often based on assumptions which should be treated as model results. This modelling is based on past events. The results are often used in decision making as the results are considered robust and accurate (Teng, et al., 2017). The outputs from this type of model can often be used for different methods – for instance the remotely sensed flood extent is used in flood monitoring as well as for hydrodynamic modelling.

Hydrodynamic modelling looks at surface processes. This type of model has high accuracy and spatial capabilities for flood modelling (Ozcelik & Gorokhovich, 2020). However, this particular model is not very accurate in modelling rainfall induced flooding. It is a mathematical model that tries to replicate fluid motion which usually needs to be solved computationally. The dimension depends on the spatial representation of the floodplain. Hydrodynamic modelling requires highly accurate and precise data which may not necessarily be available in developing countries (ibid).

Teng et al. (2017) states that the simplified conceptual models do not simulate any physical processes of inundation and are based on simplified hydraulic concepts. These methods are “planar method”, “bathtub method” and Rapid Flood Spreading Method (RFSM). The first two methods define the flood extent by intersecting a series of planes with a high-resolution DEM. The water volume is instantly linked with the flood extent. The latter method, RFSM, represents topographic depressions by dividing the flood plain into elementary areas, after which, the flood volumes are spread by filling these areas with the filling and spilling process.

A combination of hydrologic and hydraulic models is being developed as European project and used as they have the capability to simulate rainfall-runoff and flood propagation simultaneously. This coupled model takes into account both hydrological and hydraulic processes and it is a two-dimensional model. (Sanz-Ramos & Amengual, 2018).

2.3.4 Remote Sensing

There are various applications for remote sensing that include hydrological modelling, watershed mapping, and change in energy and water monitoring as well as urban modelling and predicting drought . Passive and Active Remote Sensing are the two types of remote sensing sensors available. Passive sensors rely on radiation emitted from the sun or the target in question in order to capture the target of interest (Ali, 2010). On the other hand, active sensors can emit their own energy to capture the target. Figure 5 below depicts the passive remote sensing process.

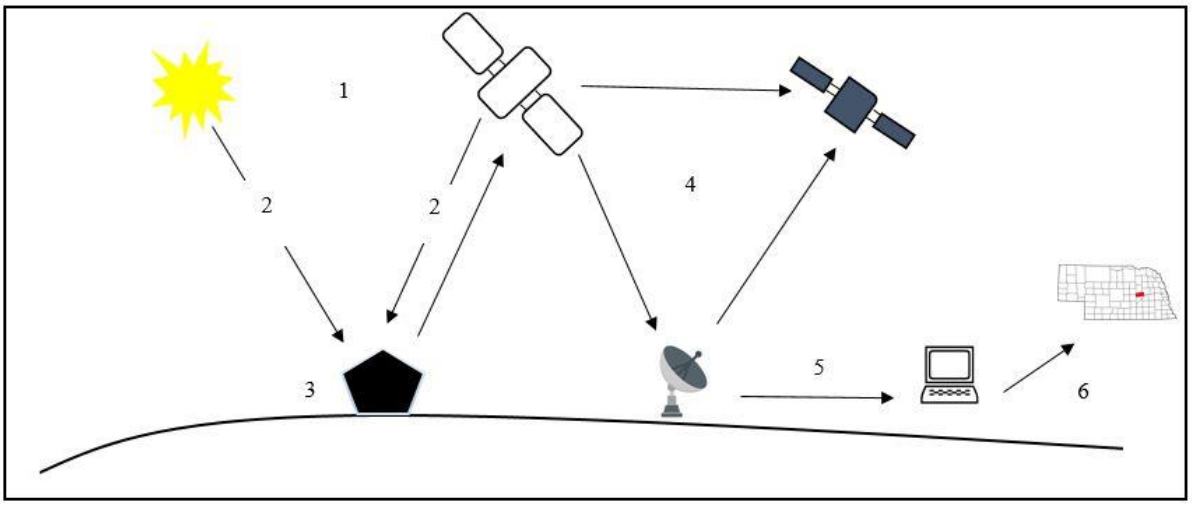

Figure 5: Passive remote sensing process

Source: Ali (2010)

Figure 5 above depicts the passive remote sensing procedure (Ali, 2010). To start a remote sensing process there needs to be a source of energy. The process in the image can be explained as the sun being the source of energy (1) . This energy then travels through the atmosphere (2) and experiences radiation. The radiation occurs again as it reflects to the sensor. This energy interacts with the target of interest (3). The type of interaction depends on the properties of the target (ibid). At stage four the energy is recorded by the sensor and directed to the processing station (5). The processed image then is analysed and interpreted which can reveal information that is useful (6).

It is important to identify various targets in the image in order to interpret and analyse the target. Targets are defined by the way they reflect and emit radiation (Ali, 2010). Reflection occurs when a ray of light is redirected as it strikes a non-transparent surface (Aggarwal, 2013). The three main earth features are vegetation, water and soil. Each of these have different spectral characteristics which effect how the target reflects the signal back. Vegetation has chlorophyll which absorbs blue and red wavelengths but reflects green wavelength. Water absorbs or transmits most of the radiation rather than reflecting it. Longer visible wavelengths and near infrared radiation is absorbed more than the visible wavelengths. However, this varies depending on the depth of the water, material in the water and surface roughness. Lastly, soil either reflects or absorbs waves and very little is transmitted. The amount of radiation reflected depends on the moisture of the soil, the organic matter content, texture and structure. The energy that is reflected from the targets are measured and this information is used to create a spectral signature. The response pattern for each surface will be different which helps differentiate one target from the other (ibid).

The images produced by remote sensing can either be analogue or digital. Satellite images are produced from electronic sensors which produces digital images whereas aerial photographs are analogue (Ali, 2010). Digital images are made up of pixels which have an intensity value and location address that is better understood by row and column locations. Multispectral images have several bands which produce a grey-scale images. If these images are placed in a combination of three bands a colour image will appear (ibid).

There are two types of image corrections which are radiometric and atmospheric corrections. The radiometric corrections rescale the monochromatic scale to their radiance values. The atmospheric correction rescales each frequency band so that it has a minimum value (ibid). This eliminates the atmospheric haze.

There are four types of resolutions which are spatial, spectral, temporal and radiometric. Spatial resolution refers to the size of the smallest object that can be identified. The resolution of an image is determined by the instantaneous field of view (IFOV) of the sensor. The IFOV is the measure of the ground area viewed by a single detector at a given moment. Issues such as improper focusing, atmospheric scattering and target motion can cause blurring of the image. A small resolution size implies that fine details can be seen whereas, a low resolution has a large resolution size (ibid).

Spectral resolution describes the sensor's ability to define fine wavelengths. High spectral resolution is achieved by narrow bandwidths (Kumar, 2000). Radiometric resolution refers to the smallest change in intensity which can be detected by the sensors. The resolution of this depends on the signal to noise ratio of the detector. Temporal resolution refers to repetitive coverage of the ground.

As remote sensing resolution has improved over time, the use has shifted from natural environments to urban areas (Ali, 2010). Urban areas have various facets such as roads, cars, sidewalks, gardens, soil and water. All these components have their own unique thermal, moisture, radiative and aerodynamic properties. Remote sensing has become popular to detect change in land use, but the classification accuracy is not always high as there is a mixed pixel problem where there might be a fuzzy area which causes difficulty in distinguishing the pixels (Ali, 2010). Remote sensing data used in this study are described in the subsequent subsections.

a. Landsat

The first satellite launched was Landsat-1 in 1972 which has a multi spectral scanner sensor. The next satellites to be launched were Landsat 2 to 3 which also carries MSS. Landsat 4 and 5 had Thematic Mapper Landsat 7 includes ETM + sensor. Landsat-8 was launched in the year 2011 (Melesse, et al., 2007).

The images obtained from these satellites are put to various uses such as forecasting of crops, agricultural needs and demands, crop insurance, evaluating water resources and many others. These images help in decision making in the various sectors mentioned above. It is to be noted that Landsat images are unique compared to other imagery provided as they were the first to provide earth imagery of 30m resolution for free and offering images over 4 decades. Landsat-1 was the first satellite to be able to observe the earth at human scale (Wulder, et al., 2015).

In the 1970's the capturing and use of images faced various challenges such as gaps in data, satellites that were always not functioning and the recording capacity was limited. In the year 1999, Landsat 5 was changed to Landsat 7. This system failed in May 2003, which caused a switch back to Landsat 5. Landsat 7 provided an improved coverage of the globe. Landsat 8 takes images of the earth every 16 days and has a lower signal to noise ratio (ibid).

The United States Geographical Science archive is where these images can be obtained. There are more than 5.5 million images. Many of these images are sourced from Landsat-5 (TM) and Landsat -7 (ETM+) sensors. The archive is increasing in size as Landsat 7 and 8 combined are now attaining 1200 scenes per day (ibid)

b. RADAR

RADAR is an acronym for Radio Detection and Ranging (Bhatta & GeethaPriya, 2016). This system is used to sense, detect and locate objects. It was initially used to measure range. Later, in World War II, RADAR was used to identify the approach of aircrafts. Now, it has multiple applications, and it can extract an extensive amount of information. This is because RADAR signals can penetrate through

rain, snow, darkness, fog and any other atmospheric conditions that might prevent the human eye to see a target. RADAR can also measure the instantaneous velocity of an object travelling towards or away from the observer (ibid).

The way in which RADAR operates is very similar to sound wave reflection. Electromagnetic energy pulses are used to detect and locate objects. The electromagnetic waves are released through the antenna in all direction. The targets then reflect these waves back in all directions. Some of these signals are then received by the receiver in the RADAR system. Once the signal has been received, the signal goes through the digital processing and amplification. The reception output then decides on the presence of reflected signal from the target (Bhatta & GeethaPriya, 2016).

The earliest scanning method used was Side Looking Airborne radar (SLAR) in the 1950's (Chan & Koo, 2008). A fixed beam pointed to the side while the aircraft moved. Initially SLAR was developed for military purposes, and it was only after the mid 1960's that this data was made available for scientific purposes. The biggest draw back with SLAR is that it has a poor azimuth resolution. In order to rectify this one would have to use a long antenna (ibid). However, this is not possible as antenna size and weight are restricted in airborne applications.

Signal processing is used in Synthetic Aperture radar (SAR) to improve the resolution. SAR allows longer wavelength and reasonable antenna structures in order to achieve high resolution (Chan & Koo, 2008). In this system microwave pulses are transmitted by an antenna towards the earth's surface (Reddy, 2008). SAR can operate during the day and night as it is an active sensor which means it produces its own illumination. Radar Interferometry is used to detect phase difference between measurements. This process helps with the detection of change in topography (Chan & Koo, 2008). SAR can be put to multiple uses such as sea and ice monitoring, mining, monitoring of oil pollution and so forth. The images below depict how the radar pulse transmits from the antenna to the ground

and how the radar pulse is scattered by the ground targets back to the antenna (Reddy, 2008). Figures 6 and 7 below show the antenna interaction with ground target and ground target interaction with the antenna respectively.

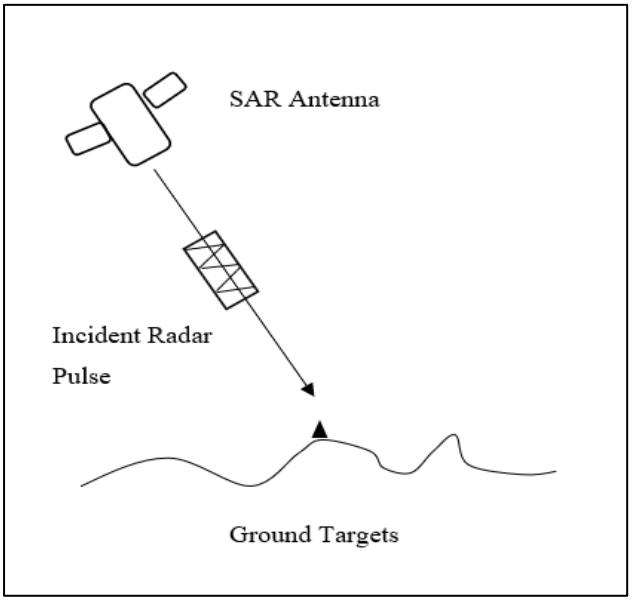

Figure 6: Antenna interaction with the ground target

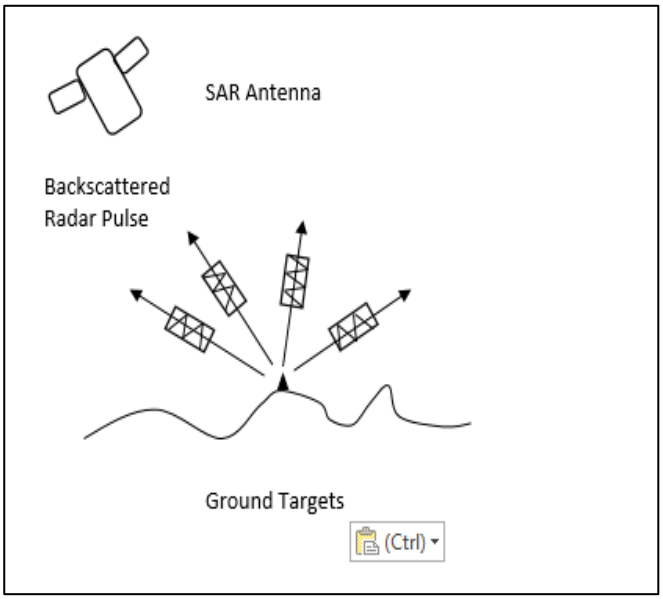

Figure 7: Ground target interaction with antenna

Adapted from: Reddy (2008)

c. Sentinel-2A

The European Space Agency (ESA) launched the Sentinal-2A mission on the 23 June 2015 (Vajsova & Astrand, 2015). This marked a new era of high-resolution earth monitoring. It has a five-day revisit time over terrestrial and aquatic areas making the data of great use for studies. Two satellites are equipped with state-of-art Multispectral Imager (MSI) instrument which provides high-resolution optical imagery. A push broom concept is use by the MSI which has a swath of 290 km (Tsapanou, et al., 2018). Table 2 below depicts the resolution for the 13 bands which is adopted from (Vajsova & Astrand, 2015).

Table 2: Resolution of Sentinal-2A bands (Adopted from Vajsova & Astrand, 2015)

Bands	Spatial resolution (m)
B2, B3, B4, B8	10
B5, B6, B7, B8a, B11, B12	20
B1, B9, B10	60

The ESA developed this mission to perform terrestrial observations such as forest monitoring, natural disaster management, risk mapping, security concerns and land cover changes (Vajsova & Astrand, 2015).

d. Digital Elevation Model

The Digital Elevation Model (DEM) is the digital representation of the land surface elevation with respect to a reference datum (Balasubramanian, 2017). A reference datum is any datum, plane or surface from which other quantities are measured (Janssen, 2009). Topography is often represented through DEMs, which are the simplest of digital representation. DEMs are commonly used to determine terrain attributes such as slope, aspect, surface roughness and elevation at any point. In the past contoured maps or stereoscopic aerial images were used to create DEMS (Balasubramanian, 2017). Today the information from radar is used to create high resolution DEMs (Balasubramanian, 2017).

A DEM only has surface elevation information whereas the Digital Surface Model (DSM) includes all objects seen from a synoptic view. The Digital Terrain Model (DTM) includes the elevation model and other information such as the slope, aspect, curvature and skeleton (ibid).

The gridded DEM is made up of regular grids (Zhou, 2017). The elevation information is provided for each grid. The use of smaller grids increases the accuracy. However, this does increase the computational time as it increases the data size. The TIN method is a more robust method for storing spatially varied information. A dense network of triangles is used in a rough terrain to capture abrupt changes (ibid).

The information required to create a DEM can be attained from field surveys, topographic contours, aerial photographs or any other sources using satellite imagery (ibid). The field surveys provide the elevation point and this is represented through topographic maps. Contours are used to connect points of equal heights. Usually, interpolation methods such as kriging, Tin and linear interpolation are used. Photogrammetry method, Radar Interferometry and Light Detection and Ranging (Lidar) altimetry are methods that are also used. Pairs of stereo photographs are used in photogrammetry to provide continuous elevation data. The radar interferometry uses a pair of images of the same location just from two different points (ibid). The Lidar altimetry uses a similar method to radar interferometry to generate the elevation data.

High resolution DEMS are available through various sources such as: FTOPO30, NOAA GLOBE project, SRTM, ASTER Global Digital Elevation Model and Lidar DEM (ibid). The United States Geological Survey (USGS) publishes the GTOPO30 global elevation data. The spatial resolution of the data is 30 arc second which is roughly 1 kilometre (ibid). The Global land One-Kilometer Base Elevation (GLOBE) generates a spatial resolution of 3 arc second which again is roughly 90 metres. This data is available from the NOAA National Geophysical Data Centre. The Shuttle Radar Topography Mission (SRTM) in conjunction with the National geospatial Intelligence Agency (NGA) and National Aeronautics and Space Administration (NASA) generated the topographic data of the majority of the surfaces $56°S\ to\ 60°N$ of the Earth. The DEM was generated by using radar interferometric techniques. The

spatial resolution is 3 arc seconds which is approximately 90 m. The Advanced Spaceborne Thermal Emission and Reflection Radiometer (ASTER) and the Reflection Radiometer instrument produced stereo pair images which were used to create the ASTER Global Digital Elevation Model. This data is available at a 30 m spatial resolution. Lastly, LIDAR uses pulses which are sent as laser on board an aircraft (ibid). The difference in time between the signal being sent and received back from the object is stored.

In 1994, two successful Shuttle Radar Lab (SRL) missions were tested using the SIR-C/X-SAR instrument (Richar & Bamler, 1999). The bands used were the United States polarimetry L-and C-band as well as the German or Italian X-band SAR. This mission was the first in many areas such as the first single-pass spaceborne Interferometric synthetic aperture radar (InSAR) system, it was the first simultaneous dual-polarization wide-swath dual frequency InSAR and it has the largest rigid structure that has flown in space (Richar & Bamler, 1999).

e. CHIRPS

The Climate Hazards Group Infrared Precipitation with Stations (CHIRPS) has been functional since 1981. CHIRPS is a quasi-global rainfall dataset with high spatial resolution (Paredes-Trejo, et al., 2020). Studies have been conducted which have proven that CHIRPS rainfall works relatively well at regional and at a global scale when compared to other state-of-the art satellite rainfall products. It was found that CHIRPS is more accurate where there is heavy rainfall rather than in dry regions (Bai, et al., 2018).

f. WorldClim

Worldclim is a set of global climate layers also referred to as climate grids which has a spatial resolution of 1 square kilometer (European Environment Agency, 2015). This has been widely used

for ecological studies, forestry and ecological modelling as it is freely available, has a high resolution and covers the globe (Marchi, et al., 2019). The European Environment Agency (2015) states that the data is used for mapping and spatial modelling in GIS or with other computer programs. A study conducted by Marchi et al. (2019) found that the version 2 of Worldclim identified that there might be a lack of reliability in the values as it is difficult to interpolate the precipitation values due to low spatial and temporal autocorrelation.

g. Tropical Rainfall Measuring Mission (TRMM)

The National Space Development Agency (NASDA) and the National Aeronautics and Space Administration (NASA) combined their effort to produce TRMM. The initial goal of this was to determine the distribution and variability of precipitation on a monthly basis to improve short term climate models, global circulation models and to assist in hydrological models. It uses a combination of high-resolution radar, passive microwave radiometer and visible-infrared radiometer measurements taken from a spacecraft at rapid precision the spatial resolution is 0.25 degrees in latitude and longitude.

h. Moderate Resolution Imaging Spectroradiometer (MODIS)

Terra and Aqua are the two sensors on board the MODIS satellite. These sensors are ideal for flood mapping and surface water measurement (Anderson & Brackenridge, 2006) and they help in the application of hydrology to detect floods, their characteristics and give out warning signs. Other applications include flood disaster response and prevention. This satellite has been operating since 2001 and it has a number of spectral bands with a spatial resolution of 500m and the nadir at 1km in addition it has two visible and near infrared spectral bands at 250 m resolution. The reason this

satellite is used to differentiate between water and land bodies is because the latter mentioned bands are of acceptable resolution. The spectral classification of band 2 allows one to successfully classify water (ibid).

2.3.5 Geographical Information Systems

GIS handle geographic data often referred to as spatial data. It can be said that it encompasses Information Systems with the element of spatial data (Reinhardt, 2000). GIS have become very popular as land use, vegetation, built environment are related to geographical positions.

The five basic elements of GIS are people, data, software, hardware and methods. People are the most important part as they develop the procedures and system that need to be followed. The data acquired is attained from various sources some which are free, and some are available at a cost (Goodchild, 1992). The quality of this data determines how well the questions presented can be solved. The software used should include tools to create databases, make drawings, perform statistical analysis and provide imagery. The hardware contributes to how fast the system can function. The methods are procedures followed to analyse and query the data (Goodchild, 1992).

GIS is divided into three categories - database view, map view and model view (Escober, et al., 1999). The database is represented spatially. The map view is a set of intelligent maps which show features and their relationship with the earth. Certain analytical functions are applied to the existing datasets so as to answer specific questions. GIS has become an essential tool for urban and natural resource planning. There are various functions within GIS that allow for data entry, data display, data management, retrieval of information and analysis (ibid).

The two types of data representations are vector and raster. The vector data set is always in the form of co-ordinates. The basic units of the data are either points, lines or polygons. Co-ordinates are a pair of numbers expressing horizontal distances along the axes (ibid). They represent the location on the earth's surface relative to other objects. A point is a zero-dimensional object represented by XY co-ordinates. A line is a collection of related points. Polygons are used to represent areas.

Vector and raster are two forms of datasets worked within GIS. Vector data can easily be edited, counted, rotated, merged into one and viewed from different angles. Raster data is where each area is divided into rows and columns which forms a grid-like structure. Each cell will have an attribute value as well as a location co-ordinate. Unlike the vector data set it does not store the co-ordinates explicitly. Raster represents the real world in a form of matrices. This is particularly useful in area calculations where it is often necessary to convert a raster to a vector and vice versa, processes which are possible and commonly used. However, converting vector to raster is often easier (ibid).

Pixels and cells are terminology that can be used interchangeably where the term pixel is commonly used in remote sensing and the term cells are used in GIS. Vector and raster datasets can represent a given area (Kainz, 2014). Polygon boundaries are often used to represent an area in vector datasets whereas raster datasets use pixels to determine area.

In order to attain an image of a large area, mosaics need to be created. Mosaics are usually composed of two or more image swaths (Palubinskas, et al., 2003). A mosaic can have a single strip of images – this is called striped mosaic (Th, et al., 2014). The other type of mosaic is when the images overlap with one another (Th, et al., 2014). The quality of the mosaic depends largely on the radiometric and geometric characteristics of these individual swaths. Illumination variation such as clouds, shadows and different atmospheric effects cause radiometric variations (Palubinskas, et al., 2003).

Commonly used data represents information on the computer whereas spatial data refers to spatial information that is stored on a computer to be used for processing and analysis (Kainz, 2014). When working with data certain characteristics needs to be known to choose the right data set. All this information is stored in the form of metadata. Metadata is data about the content, quality, condition and creator (Kainz, 2014).

There are various areas where errors can occur when working with geographic data. The processing that occurs on the data could possibly influence the quality of the data. These errors are often difficult to identify. Some of the errors include errors in data capture, inaccuracies in digitizing by the user, insufficient numerical accuracy, inappropriate class boundaries and insufficient technological knowledge (ibid). Image classification and weighted analysis in GIS are discussed in the subsequent subsections.

a. Image Classification

Image classification helps with the process of decision making as it separates the pixels or objects into various groups (Nath, et al., 2014). Supervised and unsupervised classification are the two types of image classifications that can be used. The major difference between these two forms of classification is that supervised classification needs training samples whereas unsupervised does not.

The steps followed in super classified classification are as follows: selecting training data, identifying signature identifiers and finally the classification of pixels. The advantage of using this method is that the operator can identify errors and correct them too. The disadvantage is that it is time consuming and costly and there is also space for human error as the training data selected may not acquire all conditions (ibid).

In supervised classification there are algorithms that help with identifying clusters (Nath, et al., 2014). The following steps must be followed: clustering of the data, these pixels are then classified based on the clusters, these clusters have to be labelled and then the classes are mapped. This method is effective as there is no room for human error and no previous knowledge is required (ibid). Figure 8 below shows the summary of both supervised and unsupervised classification methods.

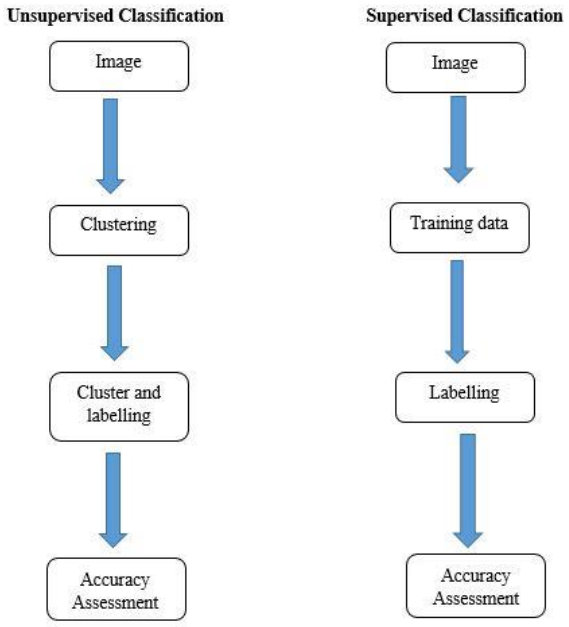

Figure 8: Supervised and Unsupervised classification methods

Adopted from ((Nath, et al., 2014)

The method mostly used in Remote Sensing is supervised classification as it produces highly accurate results, and it is user friendly. This method requires accuracy from the user as it will affect the final set of results (Stephenson, 2010).

There are parametric and non-parametric classifiers. Parametric classifiers are used when the distribution of the data is known whereas, non-parametric classification is when the distribution of the data is unknown or the number of parameters of the function is infinite (Nath, et al., 2014).

Another form of classification is hard classification and soft classification. Hard classification groups the pixels into various categories (ibid). This form of classification is good for regular or standardised data but if the area being worked with is not homogeneous the results will be very poor. The alternative to hard classification is soft classification which has an ability to deal with mixed pixels and areas that are not homogeneous (Nath, et al., 2014).

There are different classification techniques which is tabulated in table 3. The table below is adapted from (Ukrainski, 2017).

Table 3: Summary of different Remote Sensing Techniques

Methods	Examples	Characteristics
Parametric	Unsupervised and Maximum likelihood classification	The data is usually normally distributed. Before working on the area assumptions are made.
Non-parametric	Nearest-neighbour and fuzzy classification	No assumption is made on the area beforehand.
Supervised	Minimum distance, maximum likelihood, and parallelepiped	Training sites are to be identified to represent the different classes. Pixels are grouped based on statistical analysis.
Unsupervised	ISODATA and K-means	Prior ground information is not known. The pixels are grouped based on their spectral values.

Remote sensing classification is a complicated task as there are many factors that will need to be taken into account such as feature extraction, image pre-processing, selection of the appropriate classification method and post classification processing (Nath, et al., 2014). This form of classification needs training data, but this is not sufficient (Nath, et al., 2014). This problem can be overcome by semi-automated classification. This reduces computational complexity for the users. Another problem faced is the atmospheric conditions of the area that is being focused on. For instance, it is difficult to attain high-quality optical sensor data of tropical areas as there are constant cloud coverage issues and the only way to overcome this issue is to use multi sensors (ibid).

In order to perform the classification an algorithm will need to be selected. There are five main types of classification, and these are parallelepiped classification, minimum distance classification, Mahalanobis distance classification, binary enclosing classification and maximum likelihood classification (Ukrainski, 2017). If there are only two classes, then binary enclosing classification should be used. Once the number of classes have been established it overlapping between classes needs to be determined. If there is no overlapping then parallelepiped classification should be used (Wacker & Landgrebe, 1972). When the classes intersect, it is vital to analyse the shape of intersection and if there are complex shapes, then Mahalanobis distance classification should be used. Minimum distance looks at the samples and chooses whether a pixel should be part of the class based on its distance from the samples selected. Maximum likelihood is based on the distribution of the samples and looks at the highest probability of it falling it into a class.

However, in machine learning the forms of classification are found to be different. Machine learning is built on concepts such as computer science, statistics, engineering, cognitive science and many other disciplines of mathematics and science (Aized & Awan, 2017). The main application of this is in data mining. Machine learning helps mitigate errors in the analysis and in establishing relationships between features and it improves the efficiency of systems and designs of machines (Kotsiantis, 2007).

The major classification techniques include the decision tree algorithm, Bayesian Network, K-Nearest Neighbour and support vector machines (Kotsiantis, 2007). The decision tree technique is a classification technique that is often used as it is easily understandable and relatively simple. The decision tree algorithm is constructed into two phases - one being the tree growth and the second being the tree pruning. Phase one is when the training set is split continuously and recursively until partitioned into acceptable classes. The second phase involves reduction of the size of the tree

making it easier to understand (Aized & Awan, 2017). The Bayesian network is a graphical model for probability relationships among a set of variables (Kotsiantis, 2007). The K Nearest Neighbour technique is measured with respect to the value of K. This value determines how many nearest neighbours need to be examined. Lastly, the support vector machine is one of the latest supervised machine learning techniques. Support vectors are data points that lie closest to the decision surface. The classification of data vectors is executed by a hyper plane in an immense dimensional space (Aized & Awan, 2017).

The classification and regression tree (CART) methods are used for construction of prediction models (Yin-Loh, 2011). Partitions are created in the data space and a simple prediction model is fitted into each partition. The partitioning process can be represented as a decision tree. The classification trees are for dependent variables and have a finite number of unordered value whereas the regression trees are designed for dependent variables that are continuous or ordered discrete values.

Once the classification has been completed the accuracy of the classification needs to be checked (Kohavi & Provost, 1998). The first step is to compute the confusion matrix. The confusion table or the error matrix shows the quality of an algorithm. Predicted values for the class as well as the actual class are then shown as a matrix.

Table 4 below adopted from is an example of a confusion matrix where there are two classes. A confusion matrix will have dimension n x n where the predicted and actual values are shown (ibid). n In this case is equal to 2 which are the number of classes.

Table 4: Confusion Matrix (Kohavi & Provost, 1998)

	Predicted Class		**Total**
Actual Class	A	B	$\$_0$
	C	D	$\$_1$
Total	n_0	n_1	n

A and D: Show the correctly predicted values

C and B: show the incorrectly predicted values

The prediction accuracy can be calculated as follows (Kohavi & Provost, 1998):

$$Accuracy = \frac{A + D}{A + B + C + D} \tag{3}$$

Once the confusion matrix has been established the Kappa coefficient can be calculated. The kappa coefficient calculates the actual agreements compared to the observed agreement (Kohavi & Provost, 1998).

The formula used to calculate kappa coefficient is as follows (Kohavi & Provost, 1998):

$$K = \frac{(P_0 - P_e)}{(1 - P_e)} \tag{4}$$

P_o: Represents the observed agreement which can be attained from the accuracy formula mentioned above (Kohavi & Provost, 1998).

To calculate the expected agreement the following formula must be used (Kohavi & Provost, 1998):

$$P_e = \left[\left(\frac{n_0}{\mathrm{n}}\right) \times \left(\frac{s_0}{\mathrm{n}}\right)\right] + \left[\left(\frac{n_1}{\mathrm{n}}\right) \times \left(\frac{s_1}{\mathrm{n}}\right)\right] \tag{5}$$

Table 5 below shows how the Kappa values can be interpreted once computed.

Table 5: Interpretation of Kappa Values (Anothony Viera, 2005)

Kappa Values	Interpretation
< 0	Less than observed agreement
0.01-0.20	Slight agreement
0.21-0.40	Fair agreement
0.41-0.60	Moderate agreement
0.61-0.80	Substantial agreement
0.81-0.99	Almost perfect agreement

b. Weighted Overlay

Multicriteria Evaluation is used to compare alternative courses of action based on multiple factors and this helps identify the solution with the best performance (Vázquez-Quintero, et al., 2020). Multicriteria Evaluation is extremely useful in solving issues which have large sets of variables that cover widespread areas. GIS based Multicriteria evaluation is used to help in decision making of land use. Weighted Overlay analysis is a component of spatial modelling which incorporates Multicriteria Evaluation by including different weights in the multicriteria spatial analysis (ibid).

An example of a multi-criteria approach is the analytical hierarchy process (AHP) which was developed in 1980 by (Saaty, 1980) . There are four steps in this process. The initial step is to structure the problem into an order of importance or hierarchy. The second step is to determine or calculate the priority for each criterion. When doing so the goal and other criterion must be taken into account (Wu & Abdul-Nour, 2020). A 1-9 scale is used which helps obtain pairwise comparison. Table 6 below depicts the fundamental scale of AHP. This first step ensures consistency and finally, overall priorities are assigned (Wu & Abdul-Nour, 2020).

Table 6: Scale of AHP (adopted from Wu & Abdul-Nour, 2020; Hoque, et al., 2019)

Degree of Importance	Definition
1	Equal Importance
3	Moderate Importance
5	Strong Importance
7	Very strong Importance
9	Extreme Importance
2,4,6 and 8	Intermediate values

AHP is frequently used around the world due to its simplicity and because it caters for a variety of applications (Wu & Abdul-Nour, 2020).

Weighted Overlay is a technique that is both simple and straightforward which can be used in understanding multiple multi-class maps (Carvalho, et al., 2007). The weights in the model help in the analysis as weights are given to each variable as well as classes of each variable. This kind of model allows the participation of experts and changes of or adjustments to characteristics of each variable. The drawback, however, is that the weights are considered constant for the entire study area which is not always the case in reality (ibid).

Weighted Overlay analysis overlays rasters based on a common scale and weight. This is assigned to the variables and classes according to their importance (Chrysaida-Aliki & Hatzichristos, 2019). The data has to be represented as integer rasters which implies this model does not include ranges of values for the classes. Therefore, the floating-point rasters should be reclassified before used in the Weighted Overlay tool. The drawback of this method is that it has sharp boundaries between classes which means there is a possibility of ignoring certain areas. According to Chrysaid-Aliki and Hatzichristos the results tend to be more abrupt and sharper.

2.4 Study Area

Kerala is a State in the south-western region of India (Figure 1). This State roughly occupies 1 percent of the total area of the country (Noble, 2019) . The State was formed in 1956 by combining the various Malayalam speaking regions as per the States Reorganisation Act. Kerala is made up of 14 districts. The capital city is Thiruvananthapuram. Other major cities include Kochi, Calicut, Thrissur and Kollam (Padmanabhan, 2011).

The Portuguese gained power over the people of Kerala in the year 1498 (Ramerini, 2016) . It was in the 14th and 15th century that the coastal towns developed infrastructure for overseas trade . The main trade with the Portuguese was pepper in exchange for copper and as the demand for pepper increased, the wealth of Kerala increased too (ibid).

After the rule of the Portuguese, the Dutch East India Company (VOC) became the new rulers in the year 1663 (ibid). Of the 11 military outposts that the Dutch established, Kochi became one of the most important ones. The city was chosen as the headquarters for the VOC . The Dutch established their position as rulers by destroying everything that the Portuguese had established in their 130-year rule . The Dutch then enforced an autocratic rule over the local people and took over the trade of pepper. They also made a few changes to the city itself by diminishing the Portuguese fort and establishing a harbour by building piers. Many houses and warehouses were also built in Kochi by the Dutch (ibid).

The Dutch rule was then taken over by the English East India Company in 1791 (Joseph, 2014). Western institutions such as banking, public administration, western education, modern medicine and law were all introduced to Kerala. It was also during this period that modern

systems such as busses, railways and other forms of transport were established and developed. Education was also introduced into the State by the British which contributed to the high literacy rate of the State. Local jobs used to be offered to people based on ethnicity, but once the British rule came into place jobs were being offered based on educational qualification (ibid).

Colonisation in Kerala imposed a new economic structure and large-scale commercialisation (Kurien, 1994). As a result there was a fundamental change in the social structure. There were also attempts to impose major changes on indigenous religious beliefs. The indigenous Christians had been hostile towards Portuguese oppressors as they tried to remove the Christian dogma which had taken on some of the Hindu practices. The choice of the Portuguese rulers was to adopt a Christianity that was in line with Christian beliefs adopted by the Pope of Rome. The Portuguese were successful in converting large groups but the people of Kerala identified them as low caste, using the term “Latin” Christians to describe them (ibid).

The caste system embraced ideals of polygamy and slavery which was experienced many changes under the Christian ruler as these rulers considered such ideals immoral (ibid). Much of the land was in the hand of the Brahmins and Nayars, those who were part of the upper caste Hindus, but this was dismantled by the British who changed the law of the land. Previously the rule of law was that families could only portion off land to family members under British rule, land could be owned by individuals which allowed partitioning of joint family land to individual land (ibid). Under the new dispensation, Christians could own individual tracts of land, and this gave them status and power.

Under colonisation, those who belonged to lower castes also retaliated and protested in an attempt to improve their lifestyle (ibid). Many rules had changed, for instance those from the lower castes could now attend government schools and enter into employment in government jobs.

2.4.1 Geography of Kerala

As described in the introduction, Kerala is on the south west of India. The State can be split into three categories: high land (Western Ghats), low land (coastal plain of the west) and the mid-land (rich in agriculture). The lowlands and midlands are densely populated and considerably cultivated (Thomas, 2000).

The Western Ghats is internationally recognised for its biological diversity. It also brings with it geological, cultural and aesthetic values (Kandiannan, 2018). The forests found in the Western Ghats are examples of non-equatorial tropical evergreen forests. The area can be described as an unbroken hill chain or escarpment which runs parallel to the Arabian seacoast for about 1,500 km in a north-south direction. This escarpment helps in the security of water

The State has a coastline of 590 km, a territorial sea area of 13,000 km^2 and a continental shelf area of 39,140 km^2. The Exclusive Economic Zone occupies 147,740 km^2 and there are 44 rivers which constitute 85,000 ha of area and 53 reservoirs which constitute 42,890 ha of area. The brackish water takes up 65,213 ha of the area and the backwaters roughly 46,129 ha (Boopendranath, 2006).

Forty-one (41) of the 44 rivers are west flowing and 3 are east flowing. The main rivers are Nila, Periyar and Pampa. The rivers provide transport across the State and are part of the backwaters and ports. These rivers have benefited inland trade (Padmanabhan, 2011).

The riverbanks are important to Kerala as they have cultural and historical importance. In modern times hydro-electric and irrigation systems were put in place playing a significant role in the industrialization of the State (ibid). The Nila River was the cradle of civilisation in Kerala. The riverbanks were where many of the first tribal settlements occurred.

Kerala is known for its lagoons and backwaters. The backwaters run parallel to the seacoast. This allows travel to occur between different parts of the State. The important lakes of Kerala are Vembanad, Ashtamudi, Bakel and Kumbla (Padmanabhan, 2011). The Vembanand Lake is the largest which extends from the South all the way to Kochi.

These physical features have all played a role in the settlement of the people of Kerala. The settlement of Kerala is a continuous one - the different settlements border on one another (ibid). The forest area, water reservoirs, stream and wastelands all form part of the settlements. It is common to see a house being built in the centre of a plot with an agricultural area surrounding the house. This feature of fields around houses makes it possible to identify villages in Kerala (ibid).

2.4.2 Climatic Conditions

Kerala's climate is highly influenced by chemical weathering and the occurrence of landslides. Climatic conditions in Kerala State can be divided in to three: hot and wet coastal areas (along the west), temperate central midlands and cool eastern highlands (Madhusoodanan, 2018) . There are four seasons in Kerala: southwest monsoon, north east monsoon, summer and winter. The south- west monsoon occurs towards the end of May or the beginning of June. When the southwest monsoon retards the north–east monsoon kicks in. Winter is the period

from December to February. Summer starts in the beginning of March. It has been found that Kerala experiences more rain than the weighted average rain across India as a whole (ibid) .

As there is an uneven distribution of rainfall, large reservoirs are needed to redistribute the natural flow of water (D, et al., 2015). The State experiences rain around 120-140 days in a year. The summer is more prone to cyclones, droughts, gale force winds and increase in sea level.

A study conducted by the Kerala Agriculture University shows that the average annual rainfall in the State from 1871 to 2005 was 2,817 mm (Krishnakumar, et al., 2008). Rainfall in June is the highest and contributes 24.3 % of annual rainfall, followed by July (22.4%). August and September contribute 13.2% and 8.0% to the annual rainfall respectively (ibid). The lowest amount of rainfall is found in January which contributes 0.4%. An excess amount of rainfall was found during the period between 1900 to 1980 following on from which the rainfall has been relatively low to normal till 2005. In August 2018, Kerala received an extended period of heavy rainfall caused by low-pressure and the monsoon period (Hunt & Menon, 2020).

A report submitted to the Government of Kerala by Dr Madhusoodanan in the year 2018, States that 75% of annual rainfall is received from the South-west monsoon and North-east monsoon. The Western Ghats play a crucial role in triggering heavy rainfall as it lies almost perpendicularly to monsoonal airflow. An increase or decrease in the rainfall can cause flooding or drought draught in the State and because it is a highly populated area, this impact on livelihoods and properties (Madhusoodanan, 2018).

2.4.3 Land use/ land cover

The changes in land use and land cover explain the human relationship with the environment which impacts on the ecosystem and human livelihoods (Fox, et al., 2017). Before managing the changes in land use and land cover the changes must be accurately measured both quantitively and qualitatively. There are various methods which do so, including classification of remotely sensed imagery, physical field measurements, consulting government records and interviewing land users' or occupants (ibid).

Paddy and coconuts are the prominent crops in the State (Bureau of Economics and Statistics Trivandrum, 1977). Paddy is grown during winter, summer and autumn. The annual crops are banana, plantains, sugar cane and pineapple. The seasonal crops include tapioca, groundnuts, pulse sand ginger. Other crops that can be harvested for long periods of time from the same tree are cashews, peppers, coffee, tea, rubber and cardamom.

The plantations are grouped into two categories which are food crops and non-food crops. The food crops include pulses, sugarcane, pepper, chillies, ginger, turmeric, cardamom, mangoes, banana, tea, coffee, rubber, cashew and tapioca. The non-food crops include groundnut, sesamum, coconut (ibid). Crops such as tea, coffee, black pepper and cardamom are produced in the districts of the Western Ghats. These crops are found in rainfed areas which are usually along the Western Ghats (Kandiannan, 2018).

Kerala, traditionally, is known for home gardens which is a combination of various trees and crops. The agriculture land in in these home gardens were mainly agroforests. Agroforests promote productivity and sustainability (Kumar, 2005). The home gardens in Kerala were quite small, but other plantations and paddy lands also existed. Since 1970 there has been a

shift in farming from the traditional agriculture to monoculture. The paddy fields have also shifted to other agricultural crops and agroforests (Fox, et al., 2017). A study conducted in Kerala, found that the home gardens toward the coast were smaller than those in the mountainous areas. It was also found that 75 percent of those who participated in this study had reduced production or abandoned cultivation in cashew, pepper and rice. Rubber, rice and curry trees did not see many changes in production but there was a also decline in stock ownership (ibid).

The change in agriculture has caused a decline in the forest land cover of the State and the remaining of the forests structural integrity is questionable (Kumar, 2005). Figure 9 below shows the forest percentage area in the State for the years 1905, 1965, 1973 and 1983. *

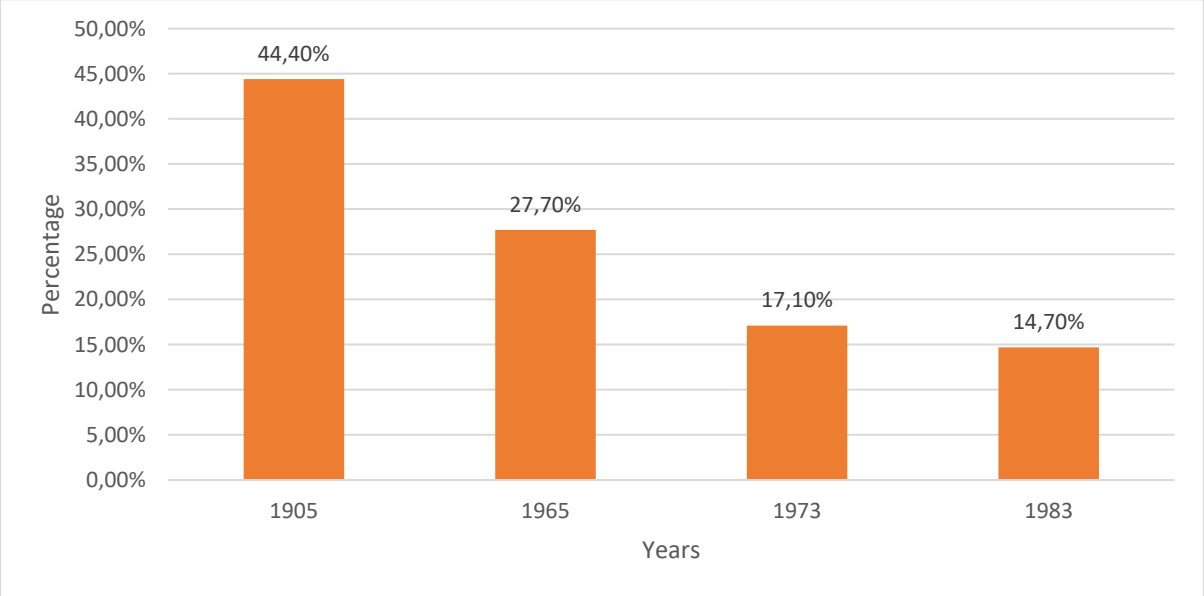

Figure 9: Percentage of Forest Land cover in Kerala

Source: (Kumar, 2005)

Figure 10 depicts a definite decrease in forest area in the State. Four phases of deforestation have been identified: The one being conversion of forest land to plantations in the late 19th

century, whilst in the mid-1940s forest areas were opened for the cultivation of food crops. Deforestation was caused during colonisation which created new settlements and lastly, infrastructure developments post-independence were set up in forest areas. The official statistics of the State show that from 1980 onwards the forest cover under public management has remained constant (Kumar, 2005). The Kerala State of Environment and Related Issues claims that from 2006 to 2018 the forest area has stayed constant at 28 percent of land coverage (Kerala State of Environment and Related Issues, 2020). However, the study conducted by Kumar States that per capita forestland availability declined from 0,060 in 1961 to 0,034 ha in 2001 (Kumar, 2005). Even though forestland was cleared out for agriculture the cultivated land per capita decreased from 0.14 to 0.08 ha between the years 1961 and 2001 (Kumar, 2005). This information was attained from satellite data. Figure 10 below depicts the land use percentage of the State.

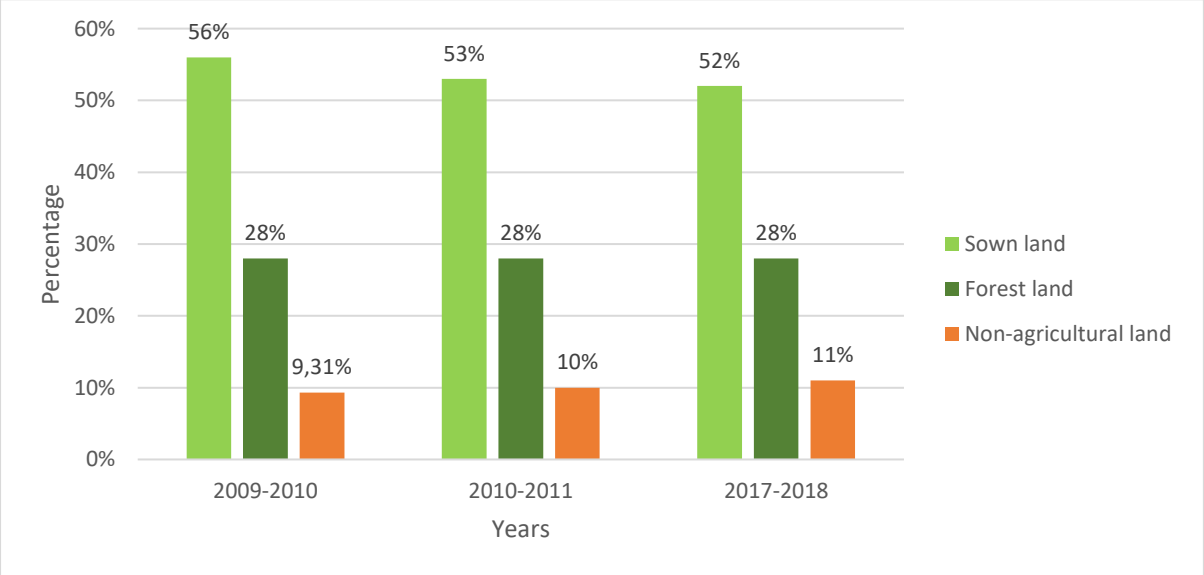

Figure 10: Land Use Percentage (adopted from Kerala State of Environment and Related Issues, 2020)

The above figure was compiled from the information provided by the Kerala Government. It shows a decrease in sown land, consistency in forest land and an increase in non-agricultural land (Kerala State of Environment and Related Issues, 2020). The reasons for the decrease in agriculture in Kerala are multiple: the change in weather, decrease in access to labour, declining profit margins, lack of access to pesticides and fertilizers, an increase in pests and diseases, the stigma against agriculture and the increased need for infrastructure development (Fox, et al., 2017).

A water body is defined as a structure where water from ice-melt, streams, springs, rain or drainage of water from residential areas is accumulated or stored (Standing Committee of Water Resources, 2016). When cities and towns expand, the planners and policy makers see water bodies as a constraint. These developers ignore the conservation of water bodies and transform them into other developments (Bindu & Mohamed, 2016). Encroachment is defined as the illegal entry into a defined boundary of the water body for various human activities like construction and agriculture (Standing Committee of Water Resources, 2016).

A study conducted in a district called Idukki in Kerala shows an increase in water bodies between the years 1975 to 1990s and again between the years 1990 to 2001 (Ramachandran & Reddy, 2016). The initial reason for the increase in water bodies is because plantation and forest areas were submerged under water. Some plantation areas were converted to water bodies. The second increase can be attributed to the construction of the Iddukki Dam (ibid) . This paper goes on to further State that the district showed a significant increase in vegetation and water bodies between 1990 and 2001.

Krishnakumar states that the rapid urbanisation and the poor waste disposal system has left the water bodies in Ernakulam, a city in Kerala, in a bad State. The Periyar river is the sole

drinking source for many people (Krishnakumar, 2019). The condition of this river at many parts both upstream and downstream seems to be negatively affected due to urbanisation and pollution. The Indian Government identified reasons for each State encroachment. Kerala's encroachments were initially due to agriculture which then changed when people started constructing houses and other commercial establishments along the banks of the water bodies (Standing Committee of Water Resources, 2016).

The Indian Express wrote in an article that several ponds were turned into dump yards for waste which has led to water scarcity and seasonal flooding (Simon, 2018). The major cities in Kerala – Thiruvananthapuram and Kochi - are in low lying areas which are adjacent to rivers and lakes. These areas are experience flooding (Standing Committee of Water Resources, 2016). The Government of Kerala States that human activities such as filling up ponds and wetlands in cities for development is the major reason for flooding in the cities. The natural drains which carry water and discharge to large water bodies have also been encroached on and some are found without any flow of water (Standing Committee of Water Resources, 2016). The Hindu released an article stating that inorganic and organic waste is seen in many upstream regions of rivers (Krishnakumar, 2019).

2.4.4 Growth of Kerala

Urbanisation is the movement of people from rural areas to modern industrial towns and cities. There are three phases of urbanisation (Jaysawal & Bharati, 2014). Urban towns in India are classified into three categories: statuary towns, census town and urban agglomeration. Statutory towns are governed by the Municipality Corporation. Census towns have a minimum population of 5000 with at least 75% of males working. In this category, the

population density should be at least 400 persons per sq.km. Urban agglomeration is the spread of a town into other towns (ibid).

The rate of urbanisation in India varies from State to State. The States South of India experience high levels of urbanisation (Jaysawal & Bharati, 2014). It is believed that urbanisation is often seen as more of a 'push' from the rural area than a 'pull' from the cities. The reasons people leave the rural areas are because of the poverty and lack of jobs as, when moving to the city, it is believed that one will be able to attain a job of some sort. There are many issues with urbanisation and India experiences poor city planning and also urbanisation with poor economic planning (ibid).

The cities are growing both vertically and horizontally. When the city expands horizontally it takes up agricultural land which reduces land available for agriculture (Jaysawal & Bharati, 2014). Vertical expansion is building upwards to house more people instead of building horizontally. There are many challenges when urbanisation occurs at a fast pace such as increasing demand for housing and property, increasing pressure on sewage, transport etc. Due to poor maintenance of water supply systems and sewage the contamination of water increases as existing systems are overburdened because of leakages in the pipes (ibid). The authorities are aware of such issues but cannot do much to control migration and movement towards the cities as India is a liberal democracy where people are able to move freely from one place to another.

Kerala is unique in the way that it has achieved high social development and quality of life despite having a relatively low level of economic development (Tharamangalam, 1998). The State has a low per capita income, but when it comes to social development it is far ahead of

all the other States taking into account the social development criteria such as adult literacy, life expectancy, infant mortality and birth rates (ibid).

It was in the mid-1980s that India underwent economic reform (Kannan, 2005). Kerala saw an increase in economic growth in the 1990s. In an article written in 1995, Kochi was one of the four cities to be identified as becoming the future metropole of India (Sharma, 2018). The growth between the years 1981 and 1991 were taken into consideration and this study included population growth, increase in investment and the intensified industrial action. However, Kerala has a week industrial sector, and it appears that the money that keeps this sector going is from abroad (Kannan, 2005). Kerala became rich as money from the Gulf was sent back to Kerala.

One of the main reasons for the growth between the 19th to 20th centuries was that transport facilities increased, and the roads were built to connect the east side and west side of the State (Kuruvilla, 2018). There is a high concentration of many of the towns in the lowland coastal areas. The number of towns found per 1000 square km was very high. The urban population increased from 6.5 percent in 1881 to 7, 5 percent in 1901. Kochi is the most urbanised city in Kerala as the urban population of Kochi in 1881 was 10.6 percent and is 1901 was 10.8 percent (Kuruvilla, 2018).

Kerala is the third highest average population density State in India with 859 people per square km, this is three times the national average. In 2011, the growth for the decade was + 4.85% (Kerala State of Environment and Related issues, 2020). Kerala's female population has always outnumbered the male population (National Academy of Sciences, 2001).

A major reason for the decrease in agriculture is that Kerala shifted from being an economy driven by agriculture to an economy driven by consumption. The male workforce has shifted from agricultural industries to providing services and trade (Kuruvilla, 2018).

The main factor that distinguishes Kerala from the rest of India is that it hard to distinguish between urban and rural areas as villages are often found within an urban area. The services available in rural small towns are nearly at par with what is available in the cities (S & C, 2016). However, despite the blur with many cities having 'villages' within them, a city can be distinguished due to a higher population and more concentrated settlements. As is clear from the discussion above, one of the reasons that Kerala is different from the rest of India is that the State has many micro towns (Kuruvilla, 2018). Once again, the development of a complex transport system has played a vital role in the development of these towns.

Chapter Three

3 RESEARCH DESIGN AND METHODOLOGY

3.1 General methods

This chapter covers a description of the data, resources and the techniques employed in this study. The results of the applied method were later tested to check for accuracy. This study was guided and based on a desktop review and pertinent literature. The three main research papers that guided and informed flood susceptibility and vulnerability modelling in this study were conducted in Tunisia (Hammami, et al., 2019), Pune (Mundhe, 2018) and Bangladesh (Hoque, et al., 2019). Flood susceptibility must be conducted before flood vulnerability can be effectively modelled. Figure 11 depicts the methodology used to attain the flood susceptibility while Figure 12 depicts the process which was conducted to obtain the final results for flood vulnerability.

To attain the flood susceptibility model (Figure 11), the datasets were processed to attain land use/cover, elevation, slope, drainage density, rainfall, lithology and soil. Once this was attained the variables were reclassified according to their susceptibility (1-9). The multi-criteria approach was conducted where weights were given to each variable. This was then checked by other literature to ensure it was correct. The software used in this study was ArcGIS.

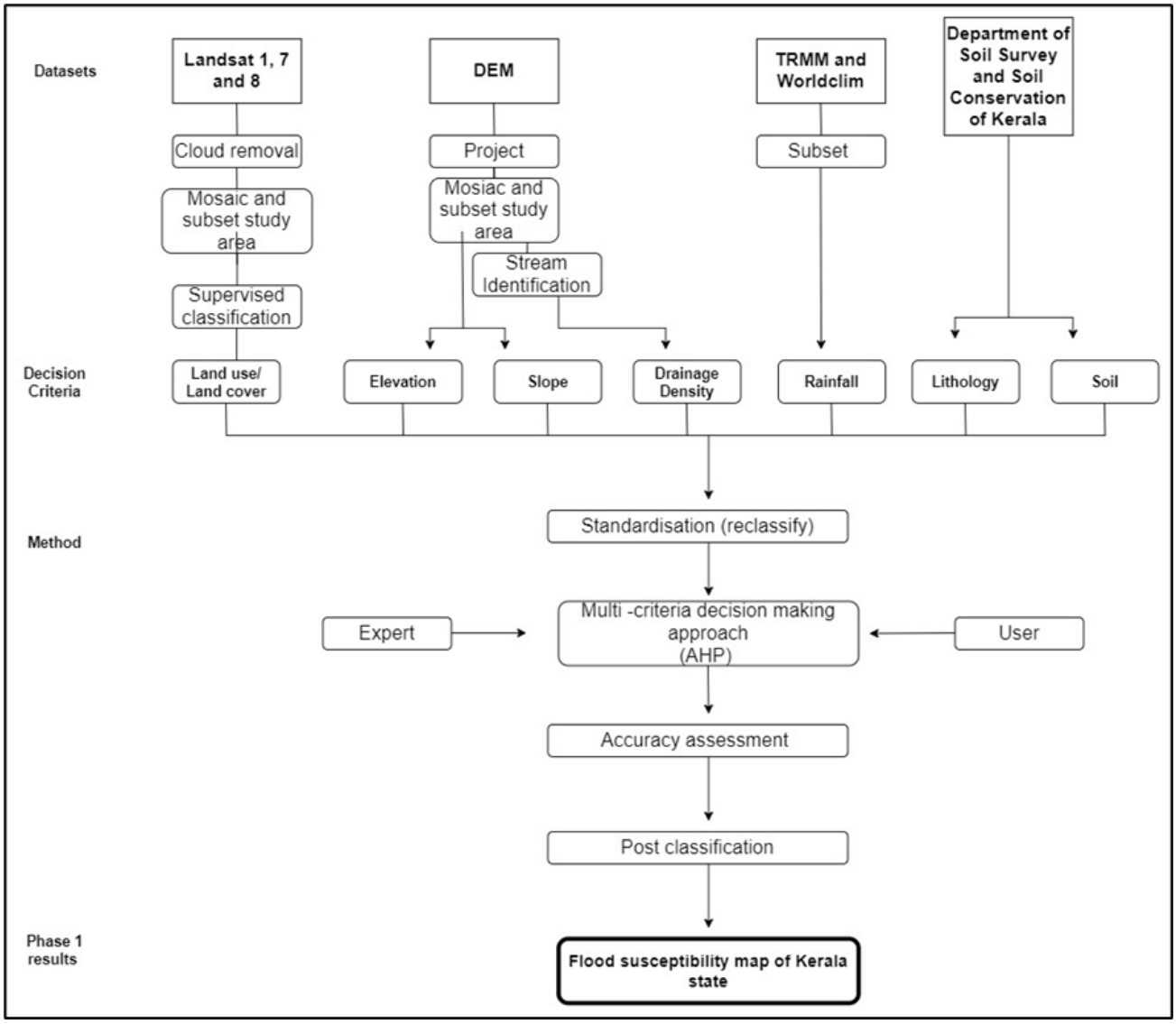

Figure 11: Flood Susceptibility modelling process

Flood vulnerability for the year 2018 (figure 12) was attained by attaining multiple variables for copying vulnerability, physical vulnerability, social vulnerability and infrastructure vulnerability. These variables can be seen in table 19 below. These individual variables were reclassified to values between 1-9 and then given weights. Each vulnerability was attained (copying, social and infrastructure). They were then processed again by giving them weights to attain the overall flood vulnerability of the state.

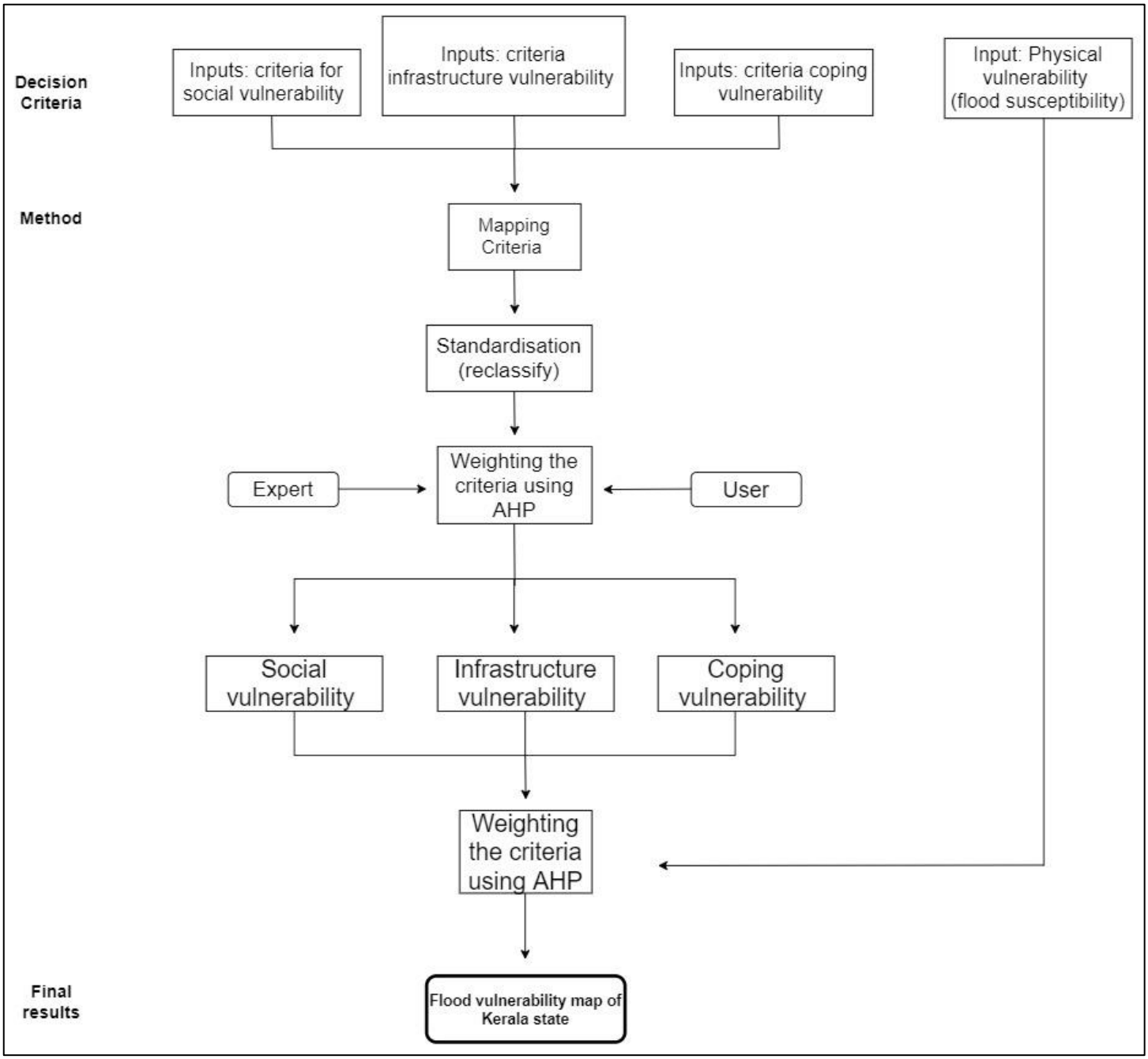

Figure 12: Flood Vulnerability modelling process

3.2 Spatial Data Preparation for Flood Susceptibility Modelling

Spatial data used in this study are presented in Table 7. To attain land use/cover Landsat data was processed which was attained from the United States Geological Survey website.

Different versions of the Landsat data were used for the years as they upgraded their imagery and satellites. DTM which was attained from the same website above was processed to attain the elevation, drainage density and slope. Worldclim and Chirps data sets were processed to attain the average annual rainfall for the years 1973, 2001 and 2018 respectively. The lithology, soil and water bodies were attained by the department of Soil Survey and Soil Conservation of Kerala. The major roads, road network and railways were attained from OpenStreetMap. The health centre shapefile was attained from healthsites.io which was processed to attain only the hospitals. The census data was attained from the National Centre of Earth Science Studies which required projection and processing. Lastly, Sentinel -2A data was attained from the United States Geological Survey which was used to identify the built environment.

Table 7: Data, source, date scale and usage of data

DATA	Source	DATE	Scale or resolution	USAGE
Landsat OMI	United States Geological Survey	2018	30m	Land Use/ land Cover information
Landsat 7 ETM+	United States geological Survey	2001	30m	Land Use/Land Cover information
Landsat 1-5 MSS C1	United States geological Survey	1973	60m	Land Use/Land Cover information
Digital Elevation Model (SRTM)	United States geological Survey	2014	30m	Elevation, Drainage Density and Slope
Worldclim	Worlclim	1973	2.5 minutes	Annual Rainfall
CHIRPS	CHIRPS	2001 and 2018	0.05 degrees	Annual Rainfall
Lithology	The department of Soil Survey and Soil Conservation of Kerala	2016	0.01 degrees	Lithology structure
Soil	The department of Soil Survey and Soil Conservation of Kerala	2016	0.01 degrees	Soil types
Sentinal-2A	United States Geological Survey	2018	10m	Infrastructure
OpenStreetMap	OpenStreet	2020	Varies	Major Roads and road networks
OpenStreetMap	OpenStreet	2020	Varies	Railways
Census data	National Centre of Earth Science Studies	2011		Non-working population
Census Data	ESRI	2018	Varies	Population and Female population
Health centres/hospitals	Healthsites.io	2020		Health centres
Water bodies	The department of Soil Survey and Soil Conservation of Kerala	2020	30m	Mapping of water bodies

3.2.1 Land use/cover

ArcGIS was used to import and process Landsat satellite images. The bands used for Landsat 8 were 2, 3, 4, 5, 6 and 7. Landsat 7 used bands 1, 2, 3, 4, 5 and 7. Lastly, Landsat 1-5 used bands 4, 5, 6 and 7. These bands were brought to create a multiband layer. After which, the boundary of Kerala was used to clip the multiband layer. Figure 13 below depicts the boundary of Kerala.

Different bands were selected based on the Landsat images which were then restricted to the boundary of Kerala.

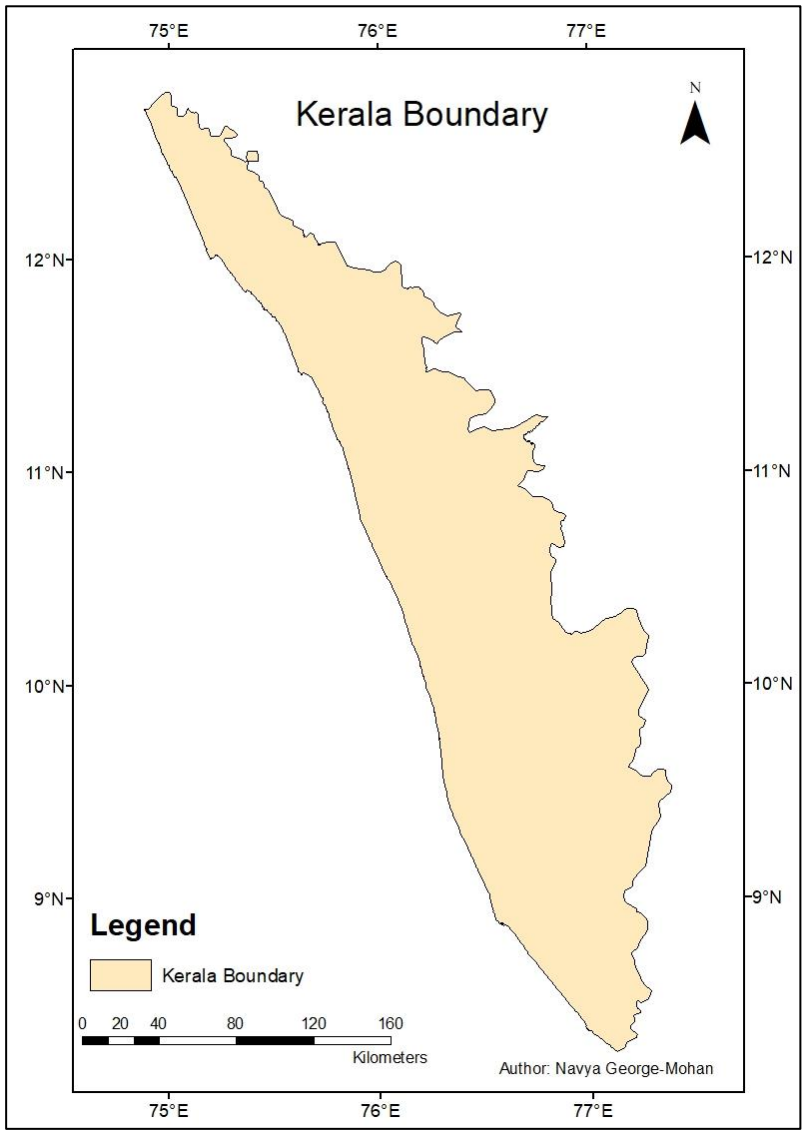

Figure 13: Kerala Boundary

The Kerala State boundary shapefile was attained from ESRI India Technologies Ltd, which was accessible from the ArcGIS data hub. The clip tool was used to remove the black border by assigning a pixel value of 0. Figures 14 and 15 below show the black border around the satellite image and the clipped version of the image to restrict it to Kerala boundary respectively.

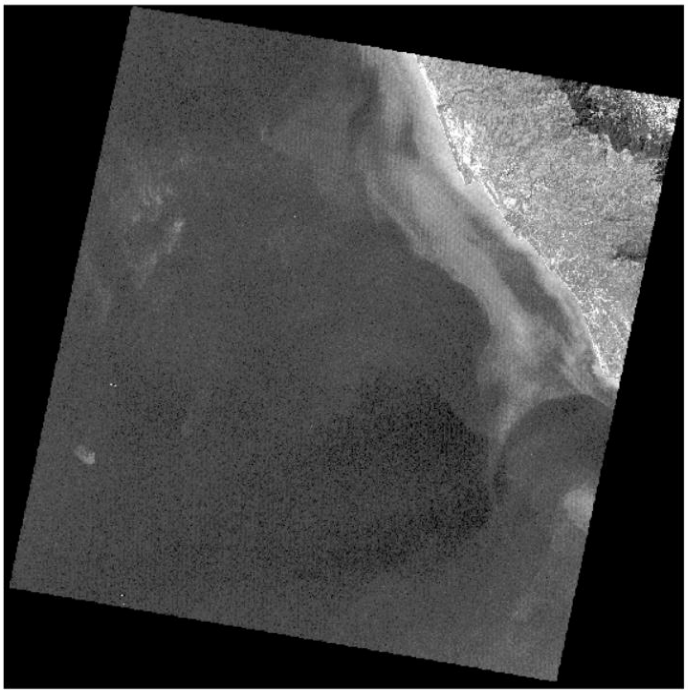

Figure 14: Black border around image

Figure 15: Clipped image

Those images that had cloud visibility underwent a different process. Two shapefiles of the same region were created - one to determine the clouds and the second to create a boundary of the entire image. Once the cloud shapefile was created the polygon tool was used to identify and remove the clouds. The clip tool was then used to extract the clouds from the boundary shapefile created. Figure 16 and 17 below is an example of the process followed to identify and remove cloud cover.

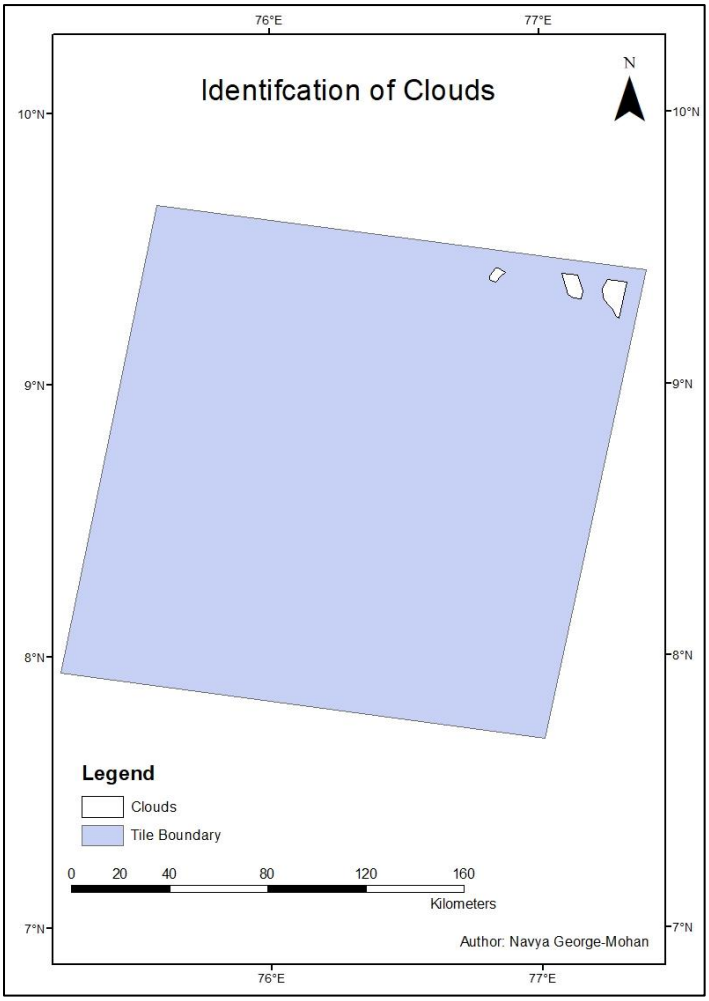

Figure 16: Cloud and Tile boundary shapefile

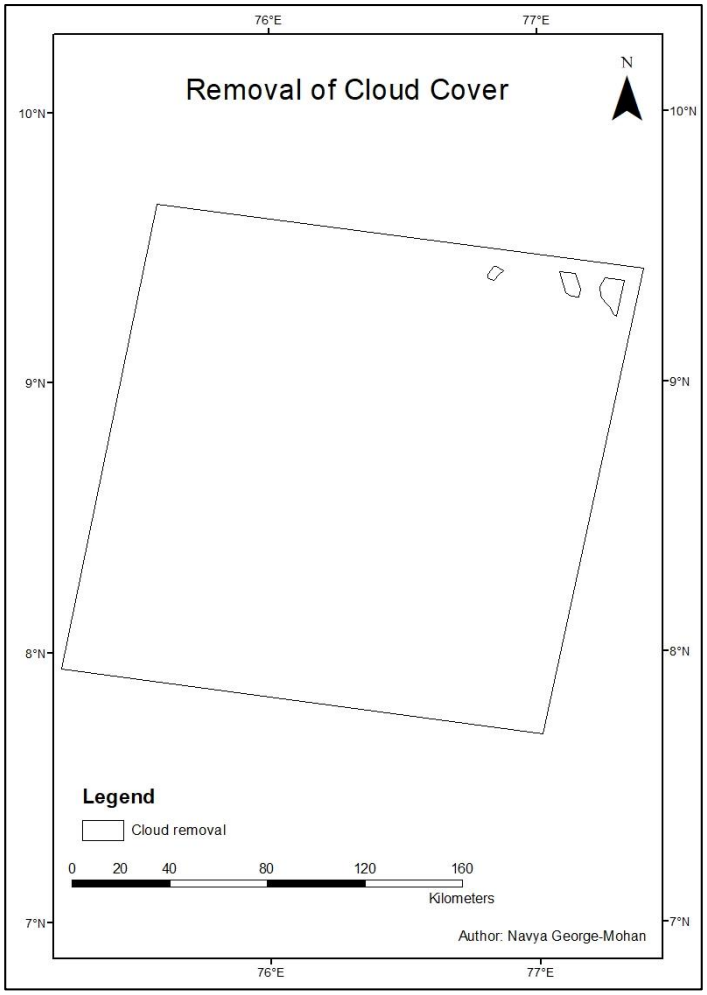

Figure 17: Tile shapefile with the removal of cloud cover

The shapefile in Figure 27 was used to remove cloud cover in each band of the satellite image with the Erase tool. This caused gaps in the band as cloud cover was removed. To overcome this issue, another satellite image from that year of the same area was used as tabulated in Tables 7, 8, 9 and 10. This was done via the Raster Calculator. The formula used: Con (IsNull (band, substitute band, band). This translates as follows: if the band layer has no value it is substituted with the band layer of the second image. This process was conducted for every band of the satellite image. Once this process for each band was completed a multiband image was created. After which, the Clip tool was used to limit the boundary to the State of Kerala.

To create one image of these multiple tiles the Mosaic to New Raster Tool was used. The images (Figures 18, 19 and 20) below illustrate the 2018, 2001 and 1973 mosaicked images. Epochs of uniform intervals were not possible as the years between 1980 and 1995 had extreme cloud cover.

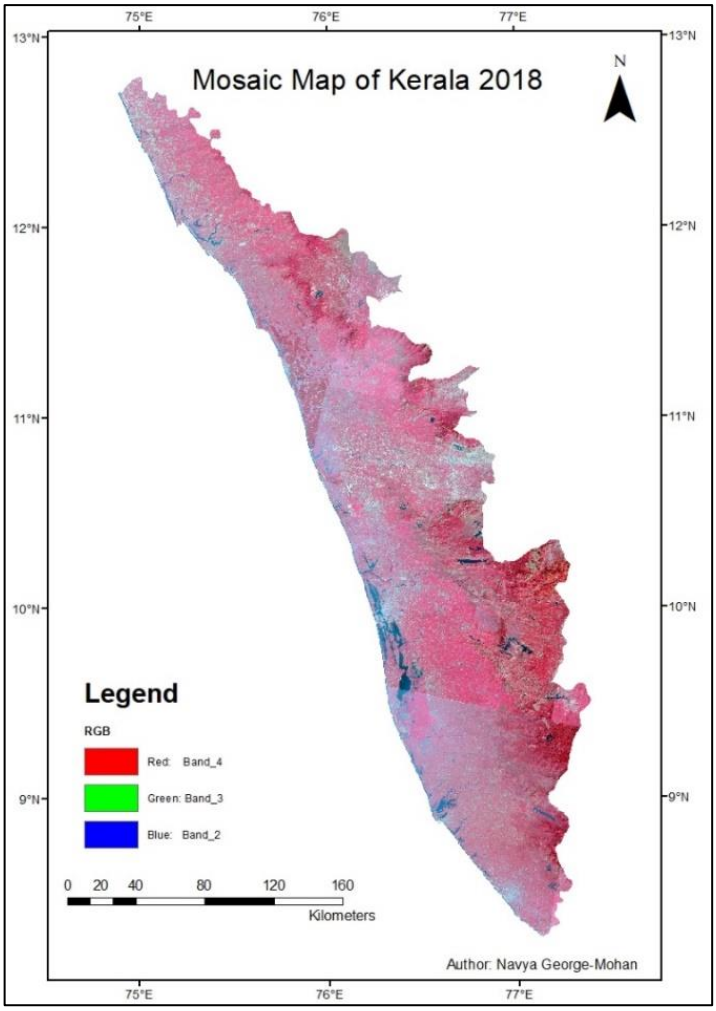

Figure 18: Kerala 2018 Mosaic Image

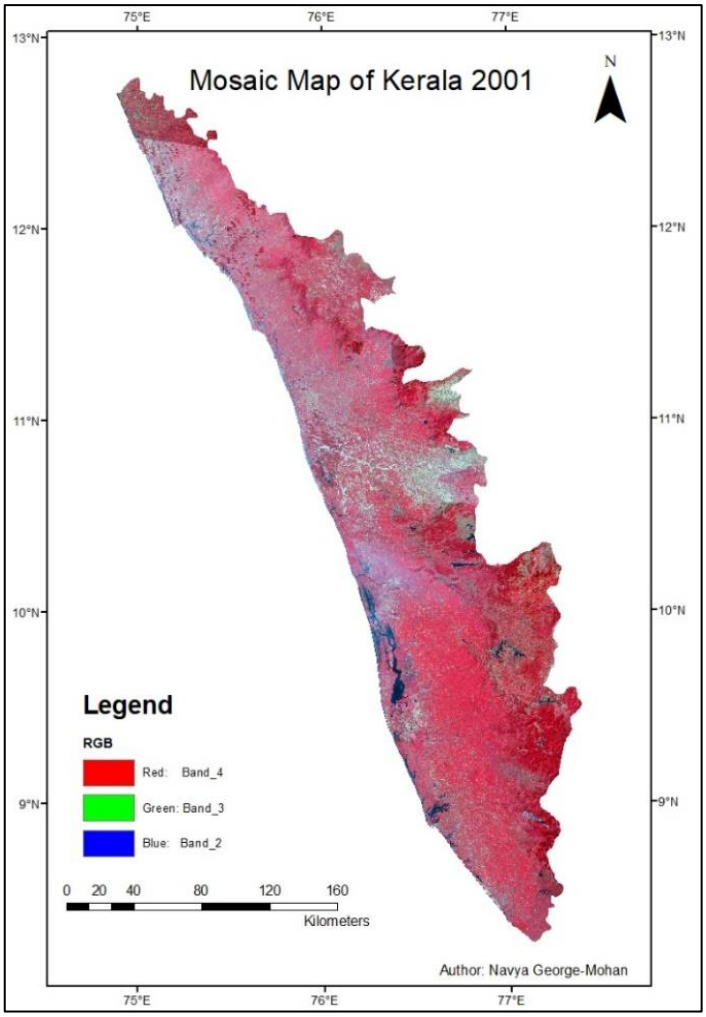

Figure 19: Kerala 2001 Mosaic Image

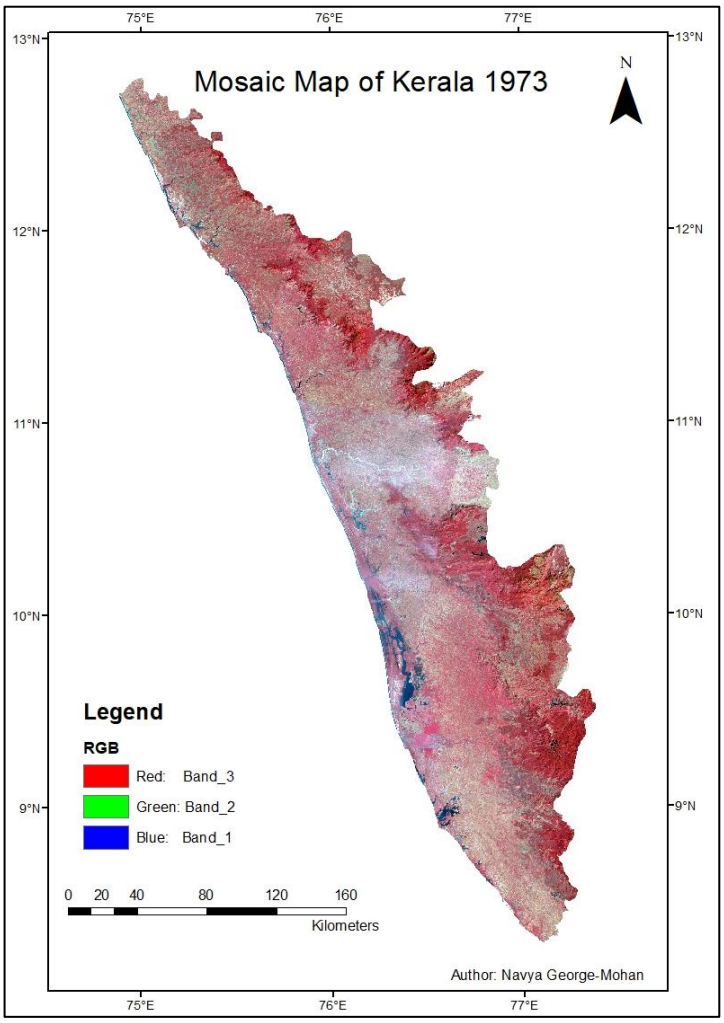

Figure 20: Kerala 1973 Mosaic Image

Once the images had been mosaicked - the classification tool was used to select training samples for the following classes – water bodies, built-up areas, crops, forest/trees and bare land. These classes were selected as they are the dominant land use/cover classes. These classes were identified visually and were based on the study by Hammami, et al. (2019). The training data for each class was equal – 250 each. Different band combinations were used to better identify each class. The different combination highlights the different classes. This was then saved as a signature file. Tables 8, 9 and 10 tabulate the satellite images used for the years 2018, 2001 and 1973, respectively.

Table 8: 2018 Satellite Images

Tiles	Original date	Substitute date
Nagercoil	3 March 2018	
Kasargod	1 March 2018	
Kollam	21 January 2018	
Ooty	22 February 2018	6 February 2018
Thrissur	6 February 2018	21 January 2018
Kozhikode	1 March 2018	28 March 2018

Table 9: 2001 Satellite Images

Tiles	Original date	Substitute date
Nagercoil	7 January 2001	
Kasargod	20 December 2000	
Kollam	3 March 2001	27 November 2001
Ooty	14 January 2001	3 March 2001
Thrissur	27 November 2000	3 March 2001
Kozhikode	26 March 2001	20 December 2000

Table 10: 1973 Satellite Images

Tiles	Original date	Substitute date
Bekal	11 February 1973	
Kannur	9 February 1973	
Kollam	9 February 1973	
Ooty	23 January 1973	28 February 1973
Thrissur	10 February 1973	23 January 1973
Vagamon	10 February 1973	

The signature file was used to perform maximum likelihood classification which is explained in section 2.3.5.a Clouds were removed by removing those sections on the images and these areas were filled with images from other date ranges.

3.2.2 Elevation and Slope

The digital elevation model (DEM) was downloaded from the United States Geological Survey website. The DEM downloaded was the SRTM 1-arc second Global for the year 2014. There

were several tiles that were downloaded which were then mosaicked in ArcMap. The mosaicked DEM was clipped to fit the boundary of Kerala. This was done using the shapefile of Kerala. DEM was then projected to WGS_1984_UTM_Zone_43N. Figure 21 below depicts the projected DEM. The elevation was then reclassified.

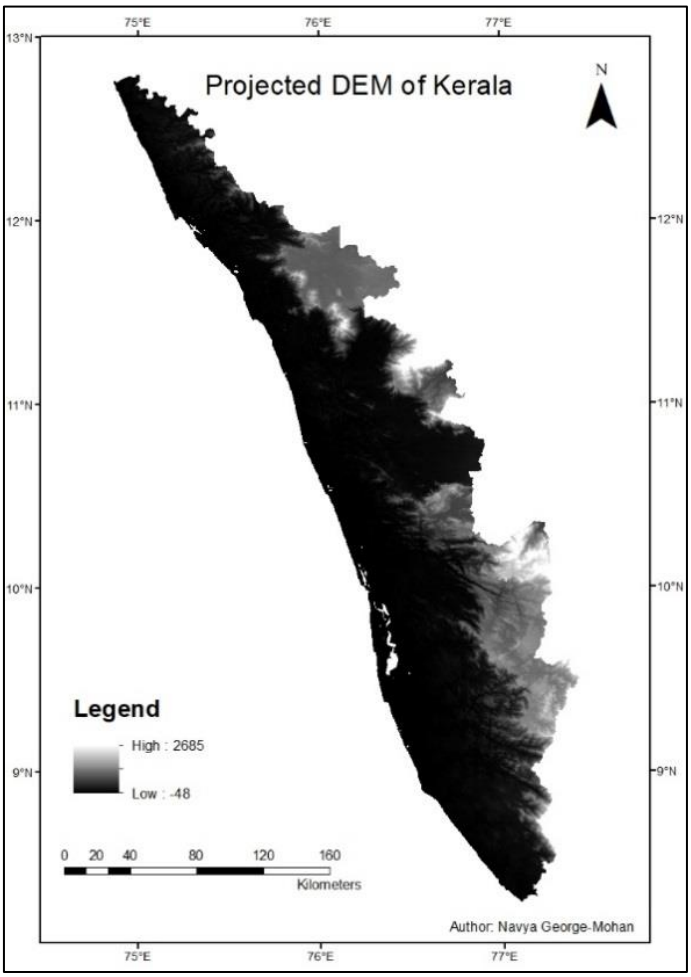

Figure 21: Clipped and Projected DEM for Kerala (units are in m)

The slope of Kerala was attained by using the clipped and projected DEM, Figure 21. The spatial analyst tool -Slope- ensuring that the output is in degrees was used. Figure 22 below depicts the slope of Kerala there is low, mid and high range areas. The raster was then resampled.

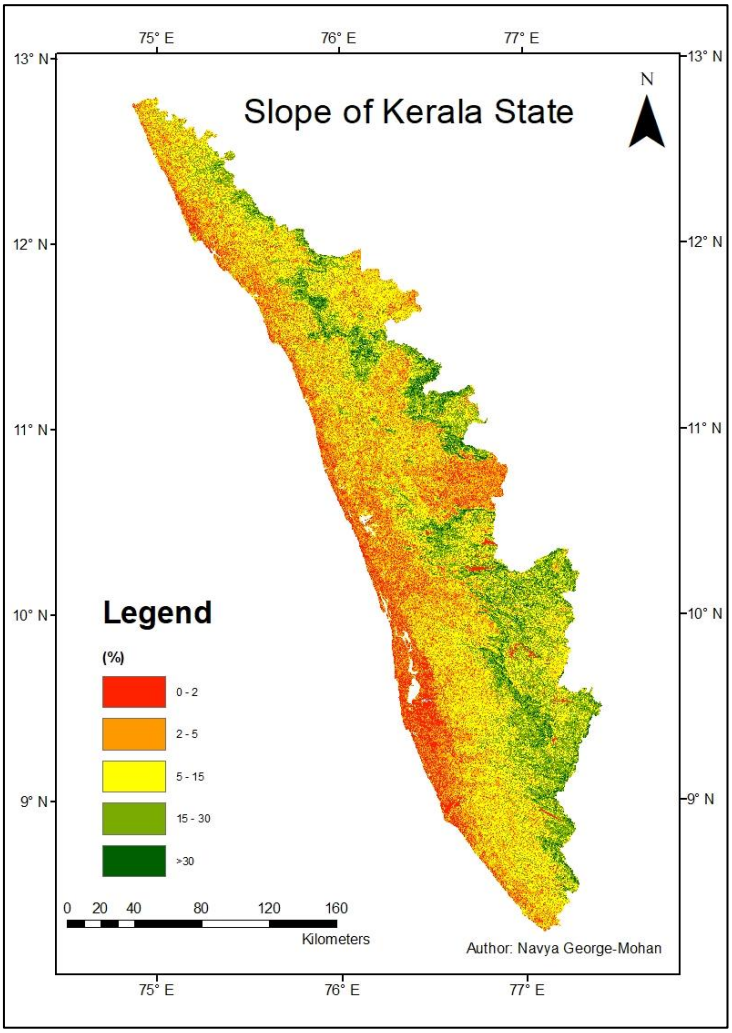

Figure 22: Slope of Kerala

3.2.3 Precipitation

Monthly data for the years 1973 was downloaded from the WorldClim website. Figure 23 below is an example of a TIFF file that was brought into ArcMap which was then clipped to be limited to Kerala. Figure 13 was used to extract the region of interest. Once the images for all 12 months were processed the raster calculator was used to add all the raster layers together.

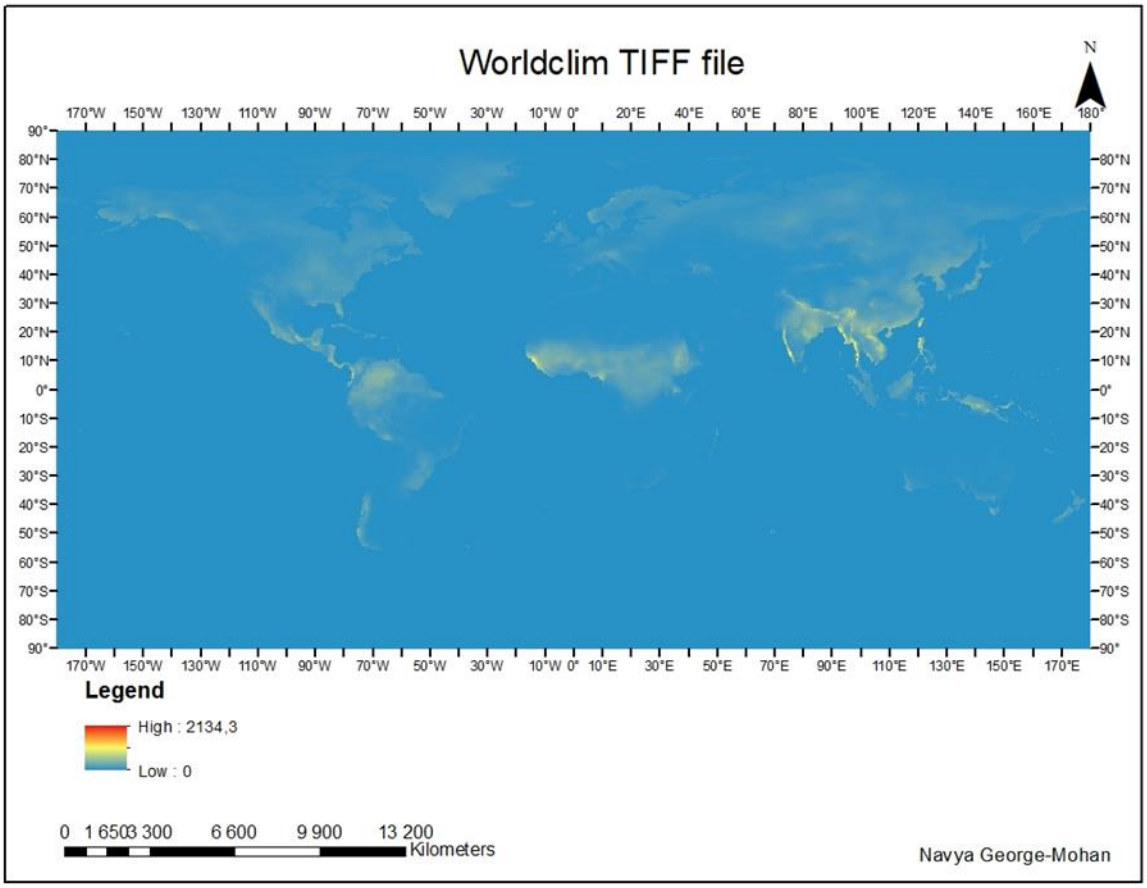

Figure 23: Worlclim TIFF file

The sum of these layers was then divided by 12. This helped attain the average annual rainfall for the year 1973. This raster file was then resampled.

The monthly rainfall data for the years 2001 and 2018 were attained from the United Stated Geological Survey website. The raster layer for each month was restricted to Figure 16. Once the region of interest was achieved the raster calculator as mentioned above was used to attain the average annual rainfall for the respectful years. Figure 24 depicts the TIFF file used to extract the region of interest.

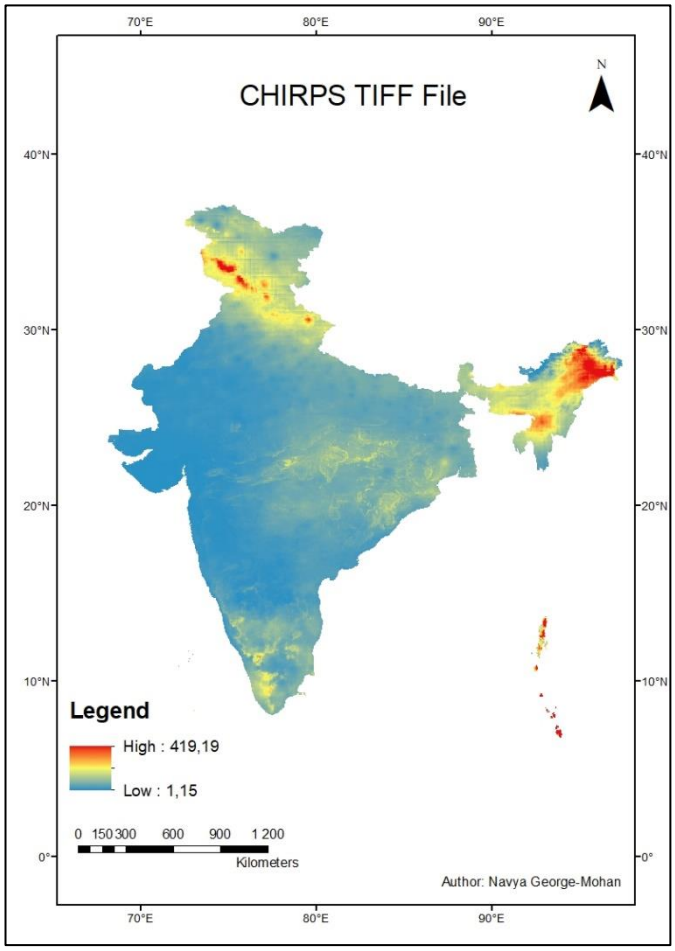

Figure 24: CHIRPS TIFF file

There is a significant difference between WorldClim and CHIRPS data. CHIRPS data coincides more with the data published by the State. CHIRPS data Is not available for the year 1973 that is why Worlclim was used. These datasets were then reclassified to between 1-9, 1 being very low rainfall and 9 being very high amounts of rainfall. Any data received from a 3rd party site was restricted to the boundary of Kerala and the average annual rain fall was calculated.

3.2.4 Lithology

The lithology data for each district was attained from the Department of Soil Survey and Soil Conservation in Kerala. The Merge tool was used to bring all the datasets together. The further classification of this data was guided by the University of Cape Town's Geology lecturers. This vector file was converted to a raster file which was later resampled. Figure 25 depicts the lithology of Kerala State.

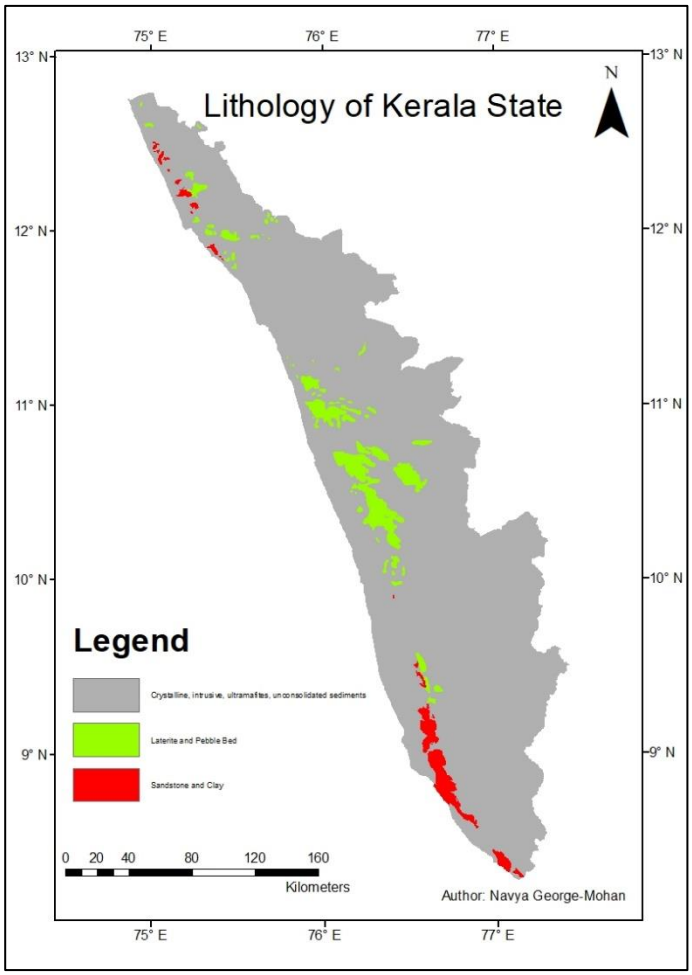

Figure 25: Lithology of Kerala

The lithology was grouped according to permeability. Table 11 below tabulates how the lithology was grouped. The data obtained were based on districts which was then brought together to form the state.

Table 11: Grouping of Lithology

Lithology	Permeability
Crystaline, Intrusive, Ultramafites, unconsolidated sediments	Impermeable
Laterite and Pebble beds	Semi-permeable
Sandstone and Clay	permeable

3.2.5 Drainage Density

The clipped and projected DEM, Figure 24, was used to attain the drainage density. All the tools used belonged to the hydrology toolbox. To remove all imperfections from the DEM the Fill tool was used to fill the sinks in the surface. The result was then used to find the flow direction. Figure 26 shows the Flow Direction in Kerala State.

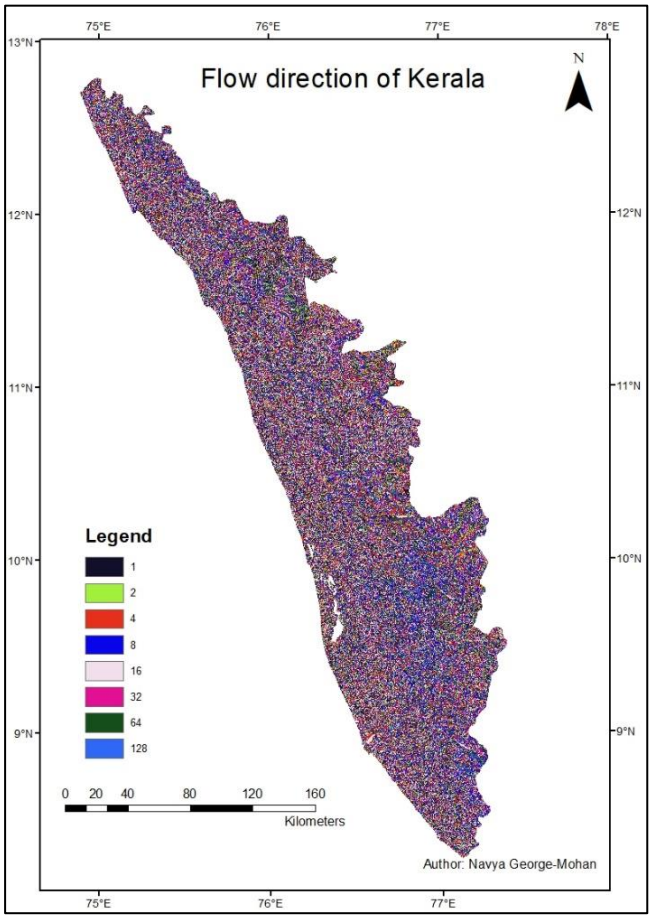

Figure 26: Flow Direction of Kerala

Table 12 below depicts what direction the values in Figure 30 depict.

Table 12: Flow direction of values

Legend	Direction
1	East
2	South- East
4	South
8	South-West
16	West
32	North-West
64	North
128	North-East

Once the Flow Direction had been computed this data was used to calculate the flow accumulation. The Flow Accumulation tool was used to do so. After this, the Greater Than tool was used where any pixel value above 1000 would be identified as a stream. The image produced values 0 and 1. The 0 represents a null value whereas the 1 represents the streams (Figure 31). Once the streams had been identified, unique values were assigned to sections of the raster linear network between intersections using the Stream Link tool. This was then converted to a vector using the Stream to Feature tool. Figure 27 below depicts the linear network in a feature format rather than a raster format (Figure 26)

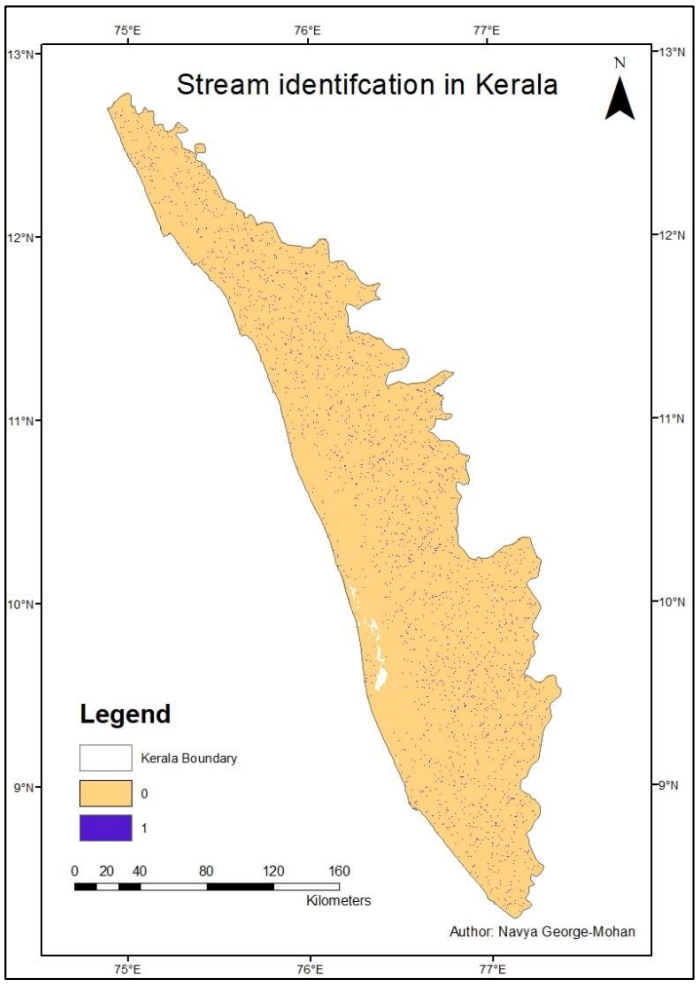

Figure 26: Stream identification of Kerala

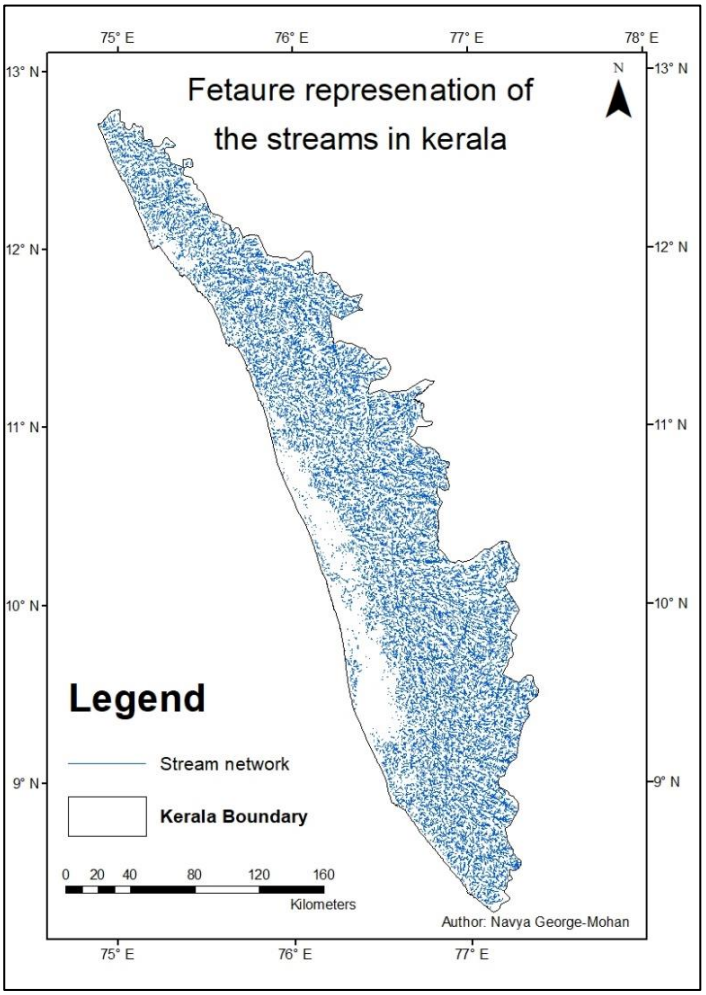

Figure 27: feature representation of streams in Kerala

To attain the stream density the grid-code from the attribute table from Figure 27 was used as an input in the Line Density tool to attain drainage density. Figure 28 below depicts the drainage density of Kerala. Drainage Density is the measure of stream spacing which expresses the length of river per unit of area (Hammami, et al., 2019)

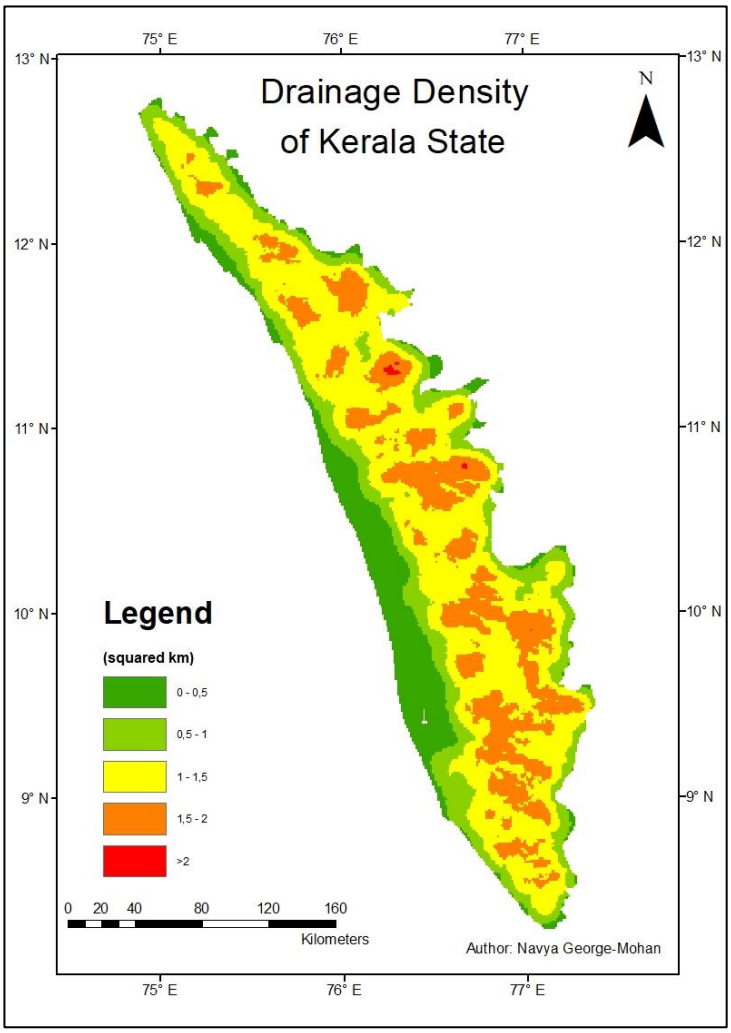

Figure 28: Drainage Density of Kerala

3.2.6 Soil

Each district in Kerala has its own shapefile which was attained from the Department of Soil Survey and Soil Conservation in Kerala. To have one dataset the Merge tool was used. The classification of this data set was guided by the University of Cape Town's Geology lecturers. The raster file was attained by converting the vector file. This file was then resampled. Figure 29 depicts the soil categories of Kerala State. Each district had its own dataset, this was brought together to form the state of Kerala.

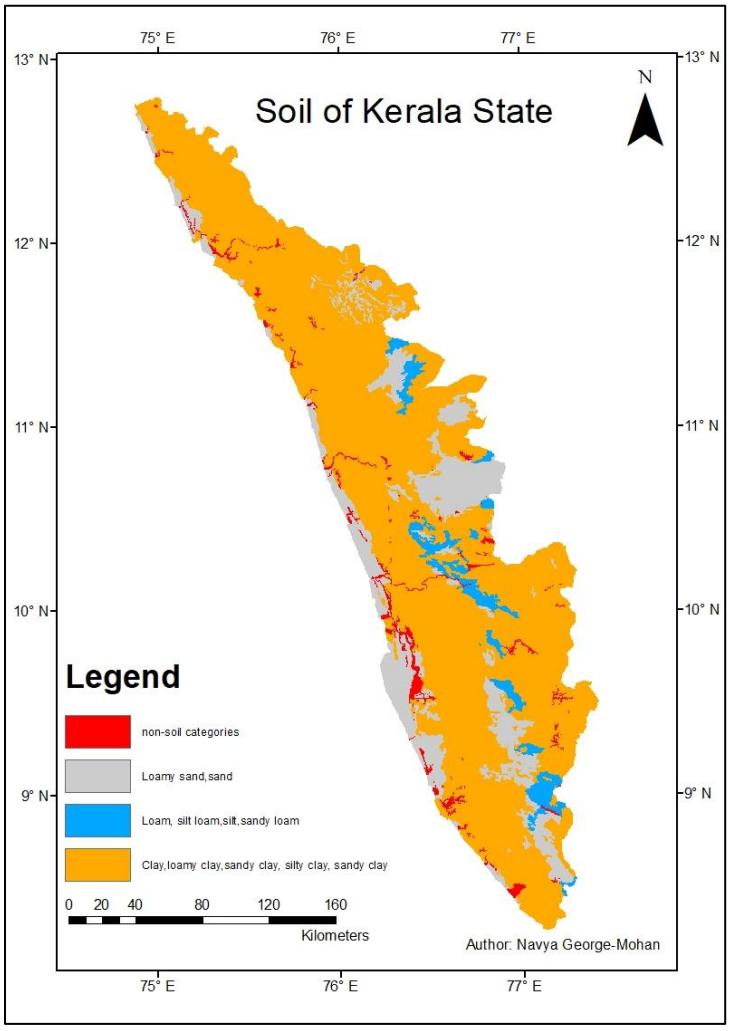

Figure 29: Soil of Kerala

The soil types were categorised according to levels of permeability. This was made possible through the guidance of the University of Cape Town's Geology Department and reference to the literature presented in chapter 2.4.2 Table 13 below depicts the grouping of the soil types according to their permeability levels.

Table 13: Soil permeability

Soil Type	Permeability
Clay, Loamy, clay, sandy clay, silty clay	Semi -Permeable
Loam, silt loam, silt, sandy loam	Permeable
Loamy sand, sand	Very permeable
Rock(other)	impermeable

3.3 Flood Susceptibility Modelling

All the raster files were resampled to be in the WGS_1984_UTM_Zone_43N projection and the cell size for the years 2018 and 2001 were set to 30m, whereas for the year 1973 the cell size was set to 60m as the satellite imagery followed this resolution. The processes followed was the analytical hierarchy process and the weighted overlay analysis which is explained in chapter 2.3.5.b.

The Weighted Overlay tool was used to determine the areas which are susceptible to flooding. This was made possible by ensuring that all inputs were raster datasets which were in the same projection and had the same cell size. The scaling of this study was based on the studies mentioned in chapter 3.1. However, this study used a scale of 1-9 where those studies used a scale of 1-4 (Mundhe, 2018) and 1-10 (Hammami, et al., 2019) . In order to adapt it to this study it was rescaled accordingly. The assigning of the scales was guided by table 4 in chapter 2.3.3.2.2.

Once this was established the Weighted Overlay tool was used, and each dataset was uploaded individually and given their respective weights. The research papers that were consulted were Hammami, et al. (2019) and Mundhe (2018). These guided the weight assigning process. Tables 14 show scale and weights given to the variables for the years 2018, 2001 and 1973. The variables, classes, scale and weights used are stipulated.

Table 14: Variable contributing to flood susceptibility for the years 1973, 2001 and 2018

Variables	Classes	Scale	Weight
Land use/Land cover	Built-up area	9	32
	Bareland	7	
	Water bodies	5	
	Crops	2	
	Forest	1	
Elevation	0-100	9	20
	100-250	7	
	250-500	6	
	500-1000	5	
	1000-1500	4	
	1500-2000	2	
	>2000	1	
Drainage Density	>2	9	9
	1,5-2	7	
	1-1,5	5	
	0,5-1	4	
	0-0,5	1	
Slope	0-2	9	5
	2-5	7	
	5-15	4	
	15-30	2	
	>30	1	
Soil	non-soil categories	9	4
	Clay, Loamy, clay, sandy clay, silty clay	7	
	Loam, silt loam, silt, sandy loam	4	
	Loamy sand and sand	1	
	Crystalline, Intrusive, ultramafites,	9	16

Lithology	unconsolidated sediments		
	Sandstone and clay	7	
	Laterite and Pebble Bed	4	
Rainfall	1100-1200	9	14
	1000-1100	7	
	500-1000	4	
	350-500	2	
	<350	1	

Once the weighted overlay tool completed the processing it produced a map with numbers in the range of 1-9. Table 15 below depicts the reclassification of susceptibility level.

Table 15: Reclassification of weighted overlay

Original Class	Class Name
1	Very Low
2	
3	Low
4	
5	Medium
6	
7	High
8	
9	Very High

The water and river shapefile provided from the Kerala Land Use Board was used to remove the water bodies of the maps produced from Table 7.

3.4 Spatial Data Preparation for Flood Vulnerability Modelling

This section looks at the different types of flood vulnerability – Social, Copying and Infrastructural. Flood Susceptibility has already been covered in section 3.3. Table 16 depicts the components used to determine flood vulnerability in consideration of flood susceptibility.

Table 16: Criteria for deciding flood vulnerability

Types of Vulnerbility	**Variables**
Infrastructural Vulnerability	Road network density
	Railway network density
	Building density
	Distance to rivers
Social Vulnerability	Population density
	Percentage of female population
	Percentage of non- working population
Copying Vulnerability	Distance to health centres
	Literacy rate

3.4.1 Infrastructural Vulnerability factors

The Infrastructural vulnerability factors considered in this study were road network, railway network and building density. Road and railway networks were obtained from OpenStreet portal in a shapefile format. Figures 30 and 31 below depict the road network and railway network of Kerala for the year 2018. The maps show the boundary of Kerala and their respective networks.

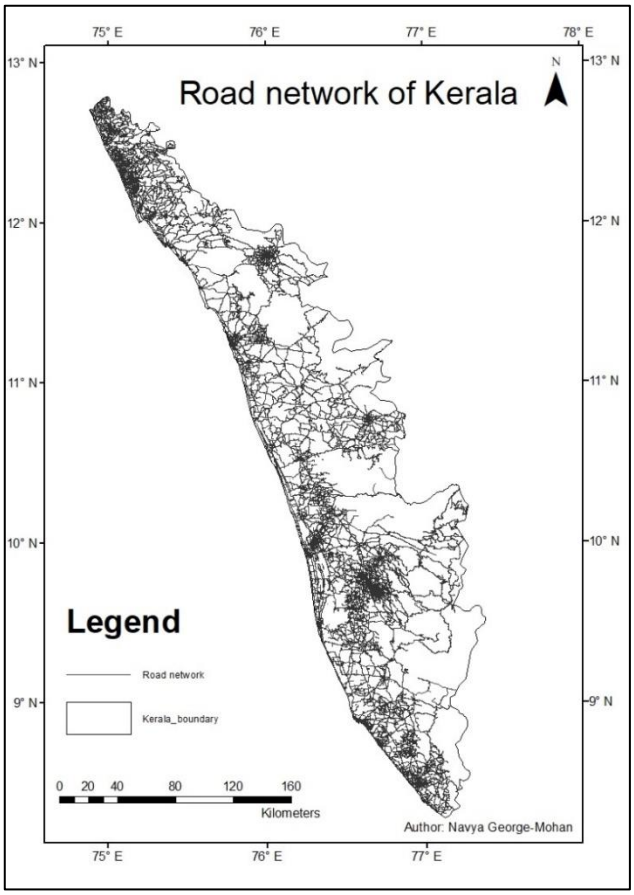

Figure 30: Road Network of Kerala

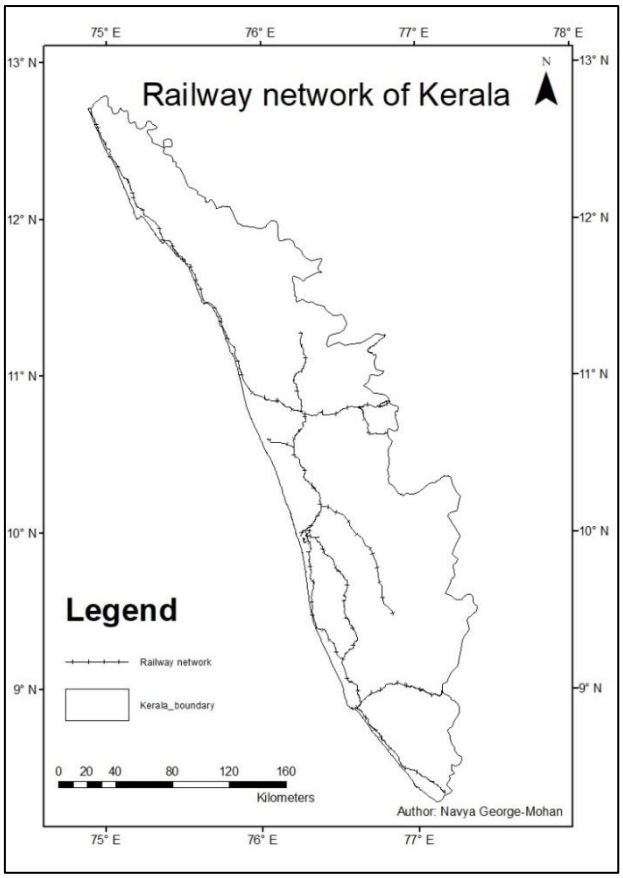

Figure 31: Railway network of Kerala

Google Earth Engine was used to classify Sentinal-2A to achieve the built-up area for the year 2018. The image was filtered according to the date required (2018-01-01, 2018-03-03) and the cloud pixel percentage below 1 percent. Minimum spectral values were used on the image. Once the pre-processing was achieved. The image was added as a layer using bands 4, 3 and 2. This achieved a true colour image.

The training data was achieved by using the geometry tool to visually identify vegetation, water bodies, bare land and built-up area. Feature Collection tool was used as the import type for all training data. The merge function was used to combine the individual feature collections. After which, the bands 2, 3, 4 and 8 were used to extract the training data. The classification was then trained using the smileCart classifier which uses classification and

regression trees (CART) methods. This is explained in chapter 2.3.5.a. Once the classification was completed the classification layer was displayed. The image was then exported as a TIFF file to the cloud and processed further in ArcMap.

The TIFF file was reclassified further to attain only the infrastructure. This was attained by using the Reclassify tool. Once the buildings were produced this was converted to a point feature class. The Point Density tool was then used to determine the building density. Figure 32 below depicts the built-up area of Kerala. The boundary of Kerala and the built environment is shown in the figure.

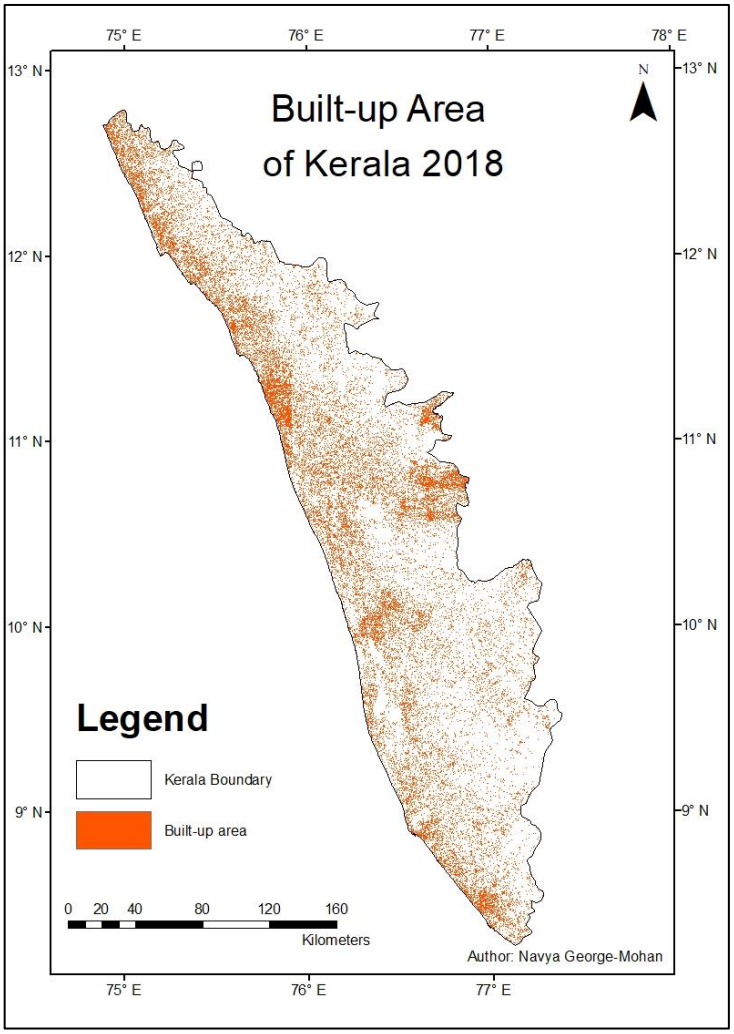

Figure 32: Built- up area of Kerala

Sentinal-2A was used to easily identify built up areas. Once samples of the classes were identified Google Engine was used to classify the image. This image was then taken over to ArcGIS and the built-up area was extracted.

The water body data mentioned in table 8, chapter 3.1 was used to calculate the distance to the rivers. This was calculated using the Euclidean distance tool. Figure 33 below depicts the distance to water bodies in Kerala.

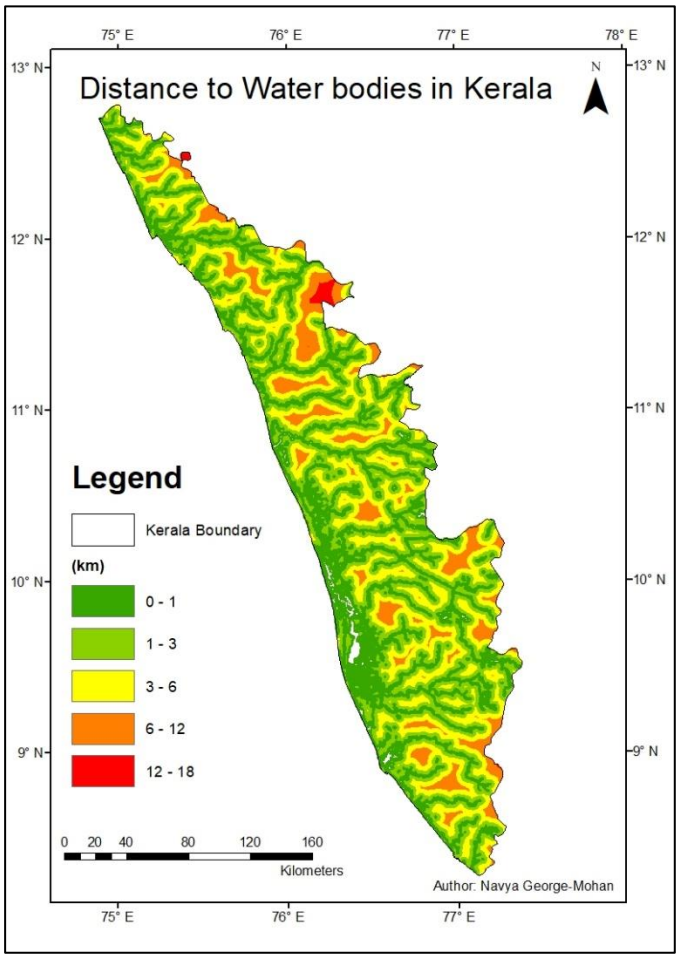

Figure 33: Distance to water bodies in Kerala

3.4.2 Social Vulnerability factors

The social vulnerability factors considered in this study were; population density, percentage of non-working population and population of Women. Population Density was derived from district population.

Even though census data was attained from Kerala, it was only for the year 2011 which is not sufficient to project population for the 2018. Therefore, The Data Enrichment function was used on ArcGIS PRO to determine the 2018 population. This data is gathered from a variety of sources – ESRI's own data development and other third part sources (ESRI, 2016). The region of interest was uploaded on ArcGIS PRO, this function was called and the required data was filtered.

Once the 2018 population was attained this was joined to the shapefile with the districts. After this, the population density was calculated in the attribute table using the calculator. The total population of each district was divided by the total area per district. Figure 34 below illustrates the population projection of Kerala in the year 2018. The states 14 districts population is depicted. The population density of the state can be found in chapter 4.3.2.

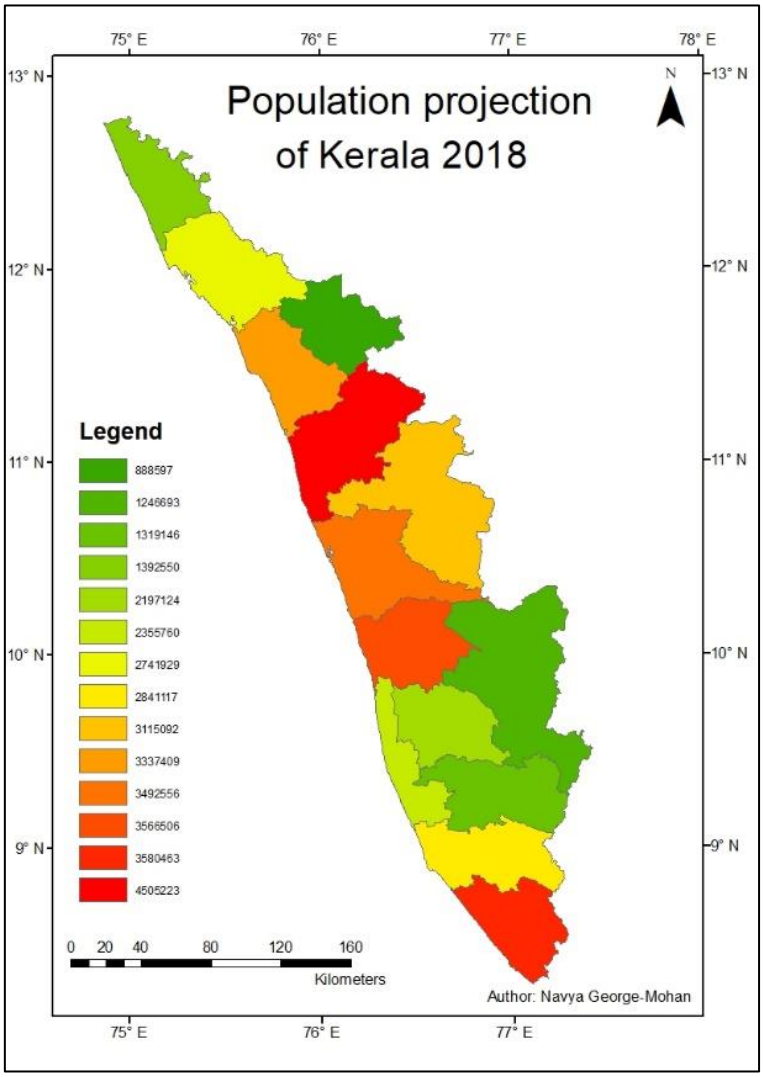

Figure 34: Population projection of Kerala for the year 2018

The percentage of non-working population was derived from 2011 census data. Each district total number of non-workers was divided by the total population per district and then multiplied by a hundred. This table was then joined to the Kerala district shapefile. Figure 35 below portrays the non-working population of Kerala in the year 2011.

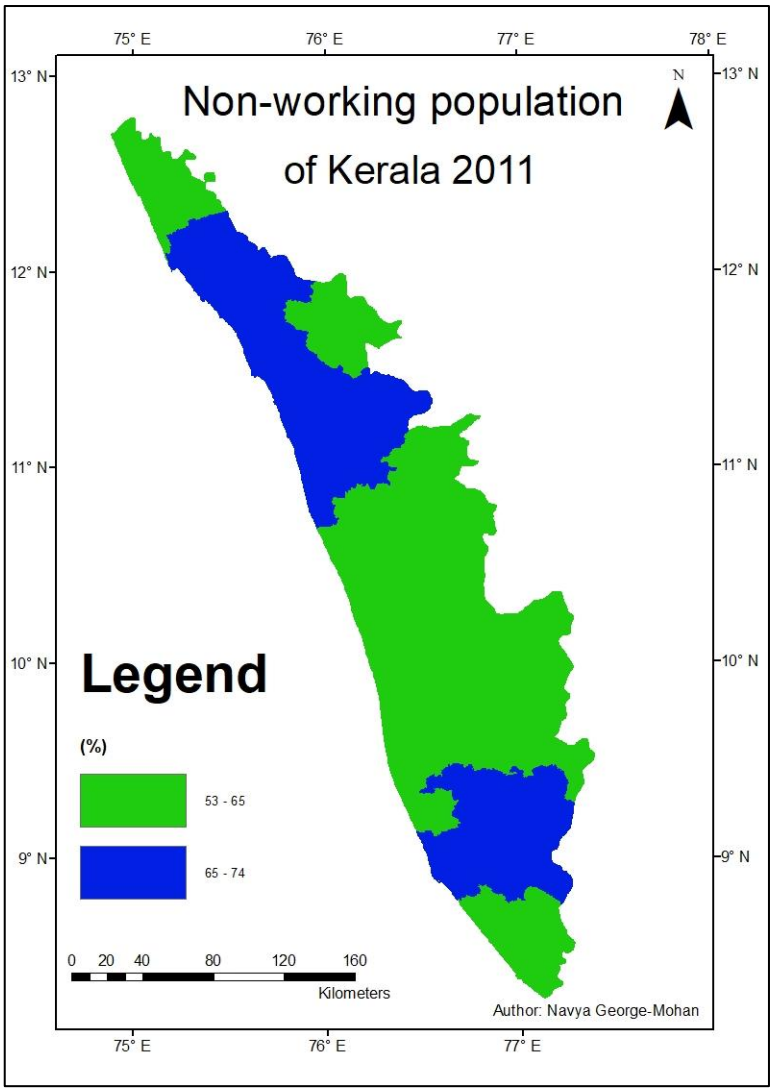

Figure 35: Percentage Non-working population of Kerala in the year 2011 (units are in %)

The female population for the year 2018 was attained the same way the population of Kerala in the year 2018 was determined. The Data Enrichment function was used in ArcGIS pro as stated earlier in in this section. Figure 36 below depicts the projected percentage of the female population in Kerala in 2018.

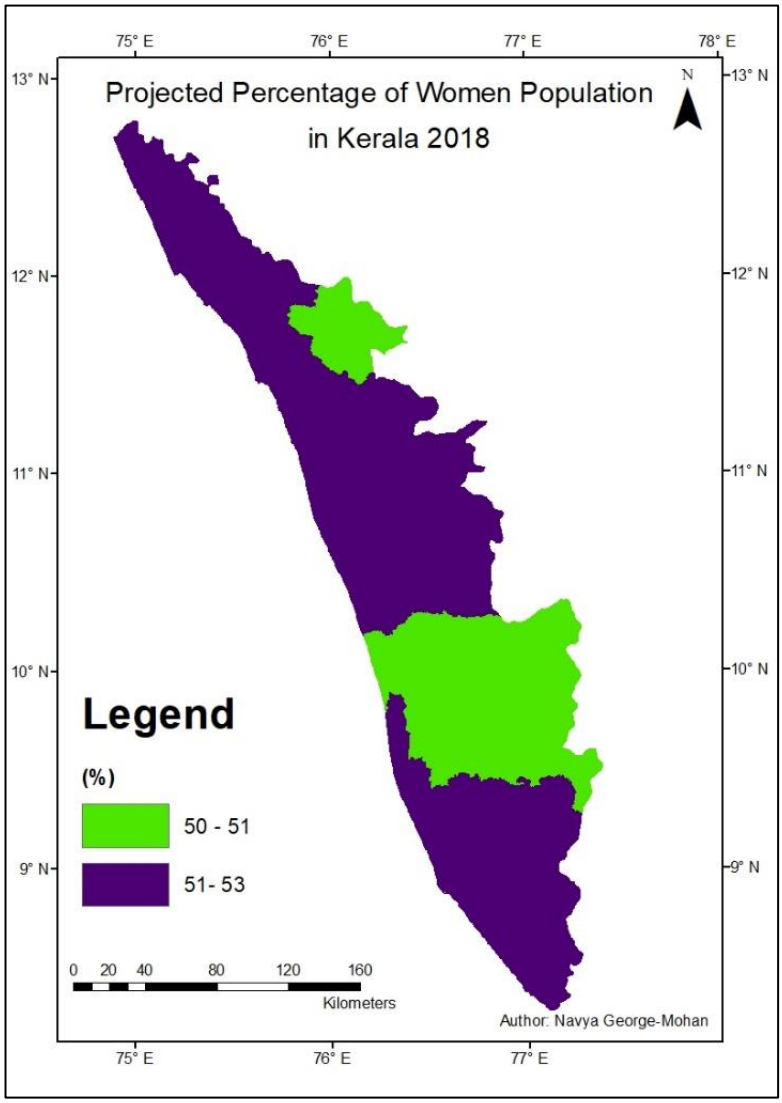

Figure 36: Projected women population of Kerala in the year 2018

3.4.3 Copying Vulnerability factors

The copying vulnerability factors considered in this study were; distance to health centres and literacy rate. The health centre data was downloaded from the website be https://www.healthsites.io/.he shapefile has all types of health care centres such as rehabilitation centres, clinics, dentists, hospitals, pharmacies and the same data for alternative medicine. Clinics, hospitals, doctors, pharmacies as well as the alternative medical

centres were chosen for processing. The data was projected to WGS_1984_UTM_Zone_43N. The Euclidean Distance tool was used to attain the distance to health centres in km. Figure 37 below depicts the distance to health centres in Kerala.

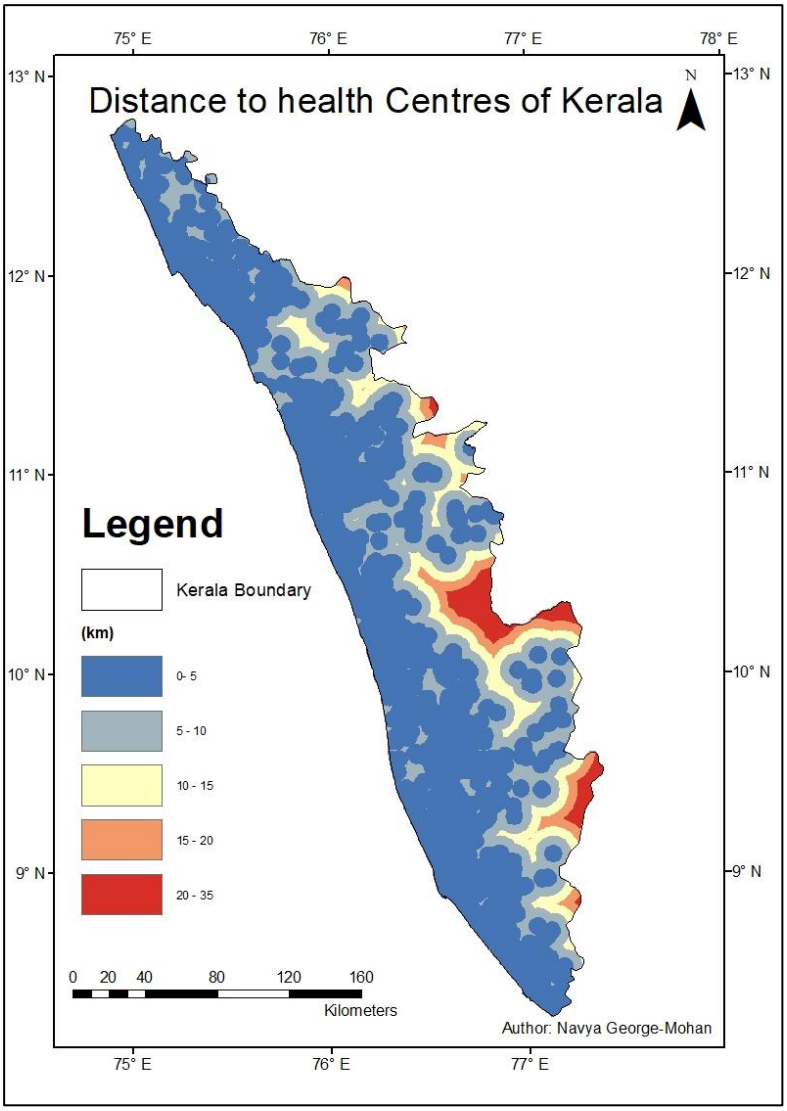

Figure 37: Distance to Health Centres in Kerala

The literacy rate was based on the data set of 2011. This was calculated by taking the literate population per district and dividing it by the total population per district and multiplying it by a hundred. This table was used and joined to the Kerala district shapefile. The literacy rate for

the entire State is between 78- 88 percent which is depicted in figure 38 below. The state has an overall high literacy rate.

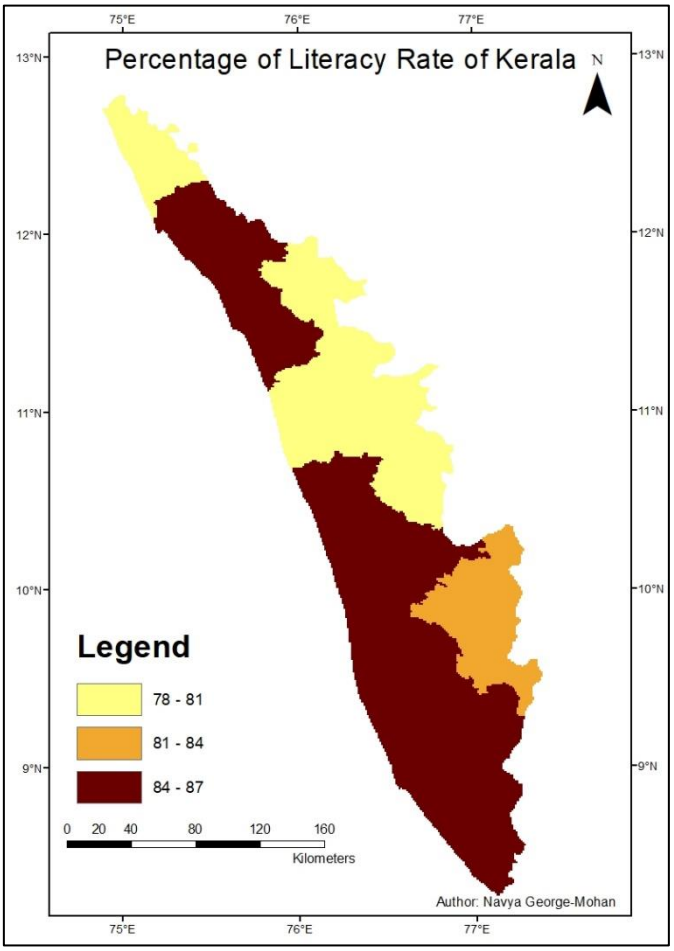

Figure 38: Literacy Rate of Kerala

3.5 Flood Vulnerability Modelling

The vulnerability components mentioned in chapter 3.4, table 16 were reclassified, given weights and assigned a CR (consistency ratio). AHP technique was followed as Stated in chapter 2.3.3.1.8. Table 18 below stipulates the scale factor given to each component. The study in Bangladesh used a scale of 1-5 and this was rescaled to follow the AHP scaling system 1-9 and Hoque et al. (2019). Table 17 below depicts the flood vulnerability variables classes assigned with scales.

Table 17: Flood Vulnerability variables assigned classes and scales

Variables	Classes	Scale
Road density (km^2)	0-2	1
	2-4	3
	4-6	5
	6-8	7
	8-10	9
Railway density (km^2)	0-0,4	9
	0,4-1,02	7
Building density (km^2)	0-100	1
	100-250	3
	250-400	5
	400-550	7
	550-723	9
Distance to river (km)	0-1	9
	1-3	7
	3-6	5
	6-12	3
	12-18	1
Population density (km^2)	250-450	1
	450-650	3
	650-850	5
	850-1050	7
	1050-1650	9
Female percentage	50-51	7
	51-53	9
Non-working population percentage	53-65	7
	65-74	9
Literacy rate	78-88	1
Distance to health centres (km)	0-5	1
	5-10	3
	10-15	5
	15-20	7
	20-35	9

Table 18 below depicts the weights and CR given to the variables to attain the flood vulnerability map. The weights and CR were adopted from a study conducted in Bangladesh (Hoque, et al., 2019).

Table 18: Weights and CR assigned to variables

Variables	Classes	Weight	CR
Flood susceptibility	Low	0,10	0,20
	Medium	0,30	
	High	0,60	
Infrastructure vulnerability	Road density	0,30	0,35
	Railway density	0,15	
	Building density	0,35	
	Distance to river	0,20	
Social vulnerability	Population density	0,35	0,20
	Female percentage	0,45	
	Non-working population	0,20	
Coping vulnerability	Literacy rate	0,35	0,25
	Distance to health centres	0,65	

The results were then reclassified into no vulnerability, very low vulnerability, low vulnerability, medium vulnerability, high vulnerability and very high vulnerability.

Chapter Four

4 RESULTS AND DISCUSSION

This chapter presents the results attained from the methods used. The results depict various characteristics of the State. There are also quantitative results that have been computed to allow for statistical analysis. There were three studies that were taken into account when making a decision regarding the variables required and the weighting and scaling of these variables. These include land use/cover distribution and changes, flood susceptibility and flood vulnerability in Kerala State. Results for these components are discussed in the subsequent sections.

4.1 Land use/cover Changes over Kerala from 1973 to 2018

This study looks at the change in land use/cover through the years 1973, 2001 and 2018. Initially the plan was to include a fourth classified image between 1985 and 1991, however, this was not possible as the Landsat satellite images of that period of time either had a high percentage of cloud cover or no data was available. The classes chosen were Bareland, Built-up area, Crops, Forest/Trees and Water bodies. Forest area and trees are grouped as one criterion as it is very difficult to differentiate the two from an aerial perspective in the area of study.

Figures 39, 40 and 41 present the land use/cover for the years 1973, 2001 and 2018 respectively.

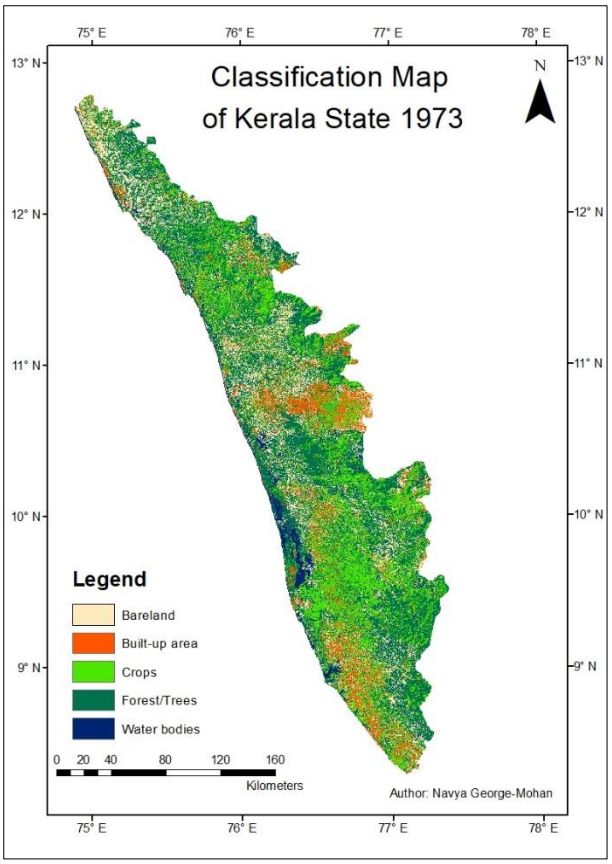

Figure 39: Land use/ land cover map of Kerala 1973

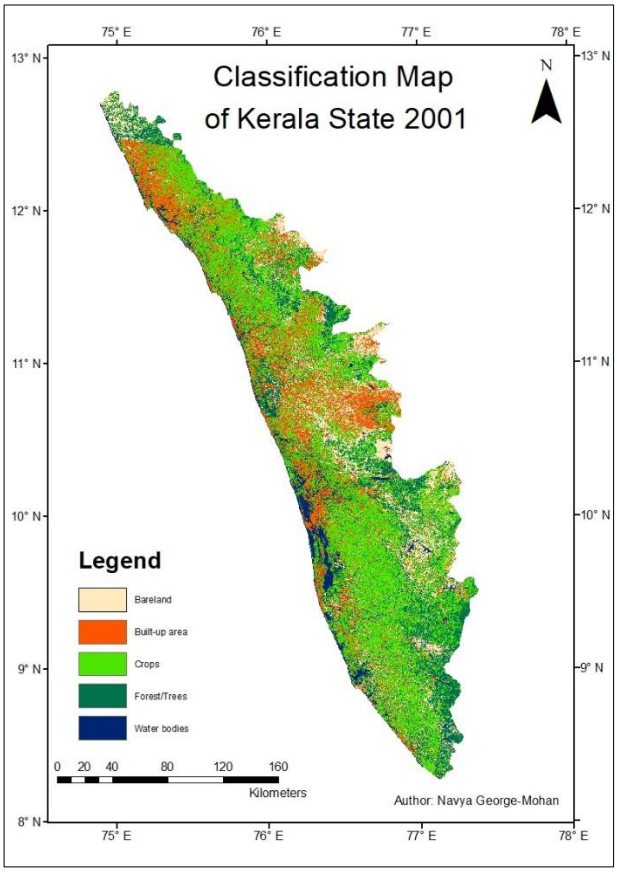

Figure 40: Land use/ land cover map of Kerala 2001

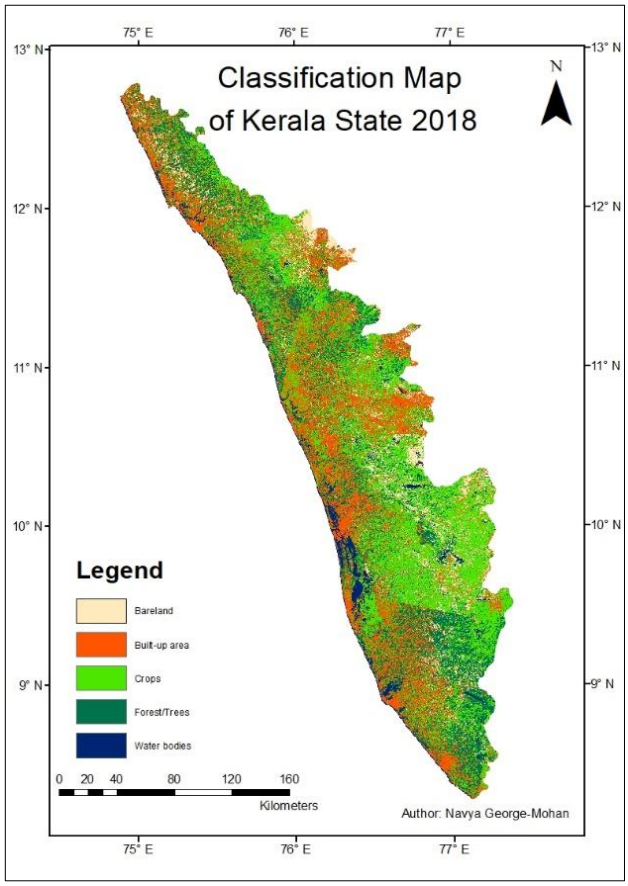

Figure 41: Land use/ land cover map of Kerala 2018

Visually it is clear that the bare land has decreased especially through the centre of the State. In 2001 there were more clusters of buildings than in 1973 whereas in 2018 the built-up area has grown and has spread widely across the State. 2001 and 2018 show greater crop land than Forest/Tree area. Unfortunately, visually, the change in water bodies cannot be identified.

Table 19 and 20 below depict the land use/land cover in hectares and the percentage of land use/cover respectively. Figure 42 below depicts the percentage of land use/land cover.

Table 19: Land use/land cover in hectares

Classes	1973	2001	2018
Water bodies in hectares	122,845.74	162,368.82	133,595.73
Bare land in hectares	641,478.60	558,518.48	336,010.91
Crops in hectares	956,804.58	1,558,687.48	1,406,592.13
Forest/Trees in hectares	1,674,461.99	786,323.50	843,493.20
Built-up area in hectares	349,402.40	711,067.01	1,053,552.15
Other in hectares	133,356.68	101,384.71	105,105.88
Total	3,878,350.00	3,878,350.00	3,878,350.00

Table 20: Land use/land cover percentage

Classes	1973	2001	2018
Bare land	16.54%	14.40%	8.66%
Built-up area	9.01%	18.33%	27.16%
Crops	24.67%	40.19%	36.27%
Forest/Trees	43.17%	20.27%	21.75%
Water bodies	3.17%	4.19%	3.44%
Other	3.44%	2.61%	2.71%
Total	100%	100%	100%

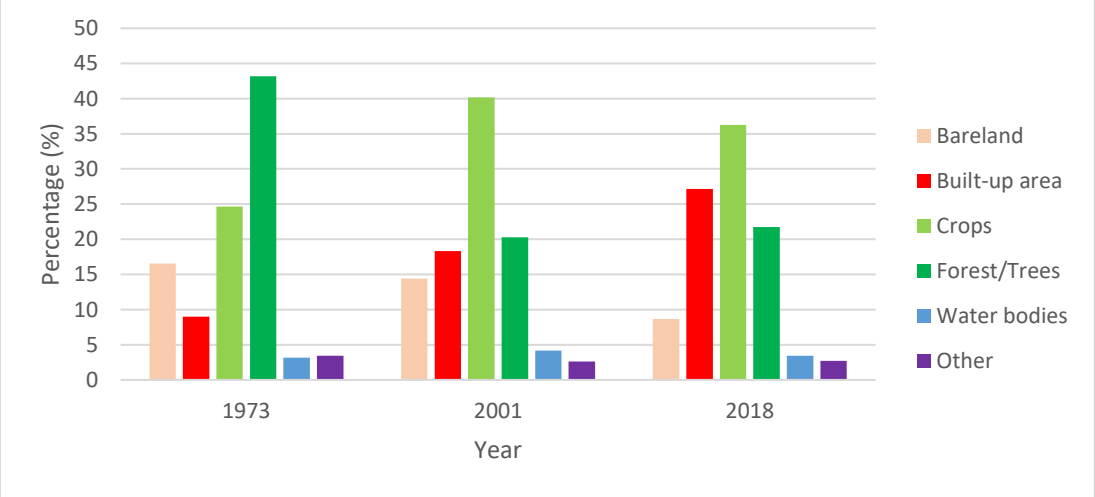

Figure 42: Percentage of land use/cover from 1973 to 2018 in Kerala State

Tables 19 and 20 and Figure 42 above show a class called “other”. These pixels have not been allocated a class as their spectral index values do not fall in the range of the 5 classes - water bodies, forest/trees, crops, built-up area and bareland. It is expected that the class ‘other’ would decrease over the years as the resolution of Landsat datasets improved. This is stated in chapter 2.3.3.1.1 and explained by Wulder, et al. (2015). Figure 57 illustrates that there is a decrease of the class “other” between the years 1973 and 2001 at the rate of -24.13% which is expected. However, an increase in the class ‘’other’ has been noted between 2001 and 2018 at a rate of 3.83% which is an unexpected result. The year 2018 satellite imagery had a high percentage of cloud cover and considerable pre-processing (chapter 3.1) was required which could explain the slight increase in non-classified pixels.

Tables 19 and 20 and Figure 42 show an increase in built-up area over the years 1973, 2001 and 2018. The percentage of built-up area is found to be 9.01, 18.33 and 27. 16 percent for the years 1973, 2001 and 2018, respectively. The percentage change in built-up area between 2001 and 1973 is 103.51% (3.70% per year), between 2018 and 2001 is 48.17 % (2.83% per year) and between 1973 and 2018 is 201.53% (4.48 per year). Jaysawal & Bharati (2014) state that there is an increase in urbanisation in India, especially in South India which is where Kerala is situated. This explains the general increase in built-up area. Further explanations of this phenomenon can be found in section 2.4.5 where it is noted that the drastic increase in built-up area between the years 1973 to 2001 is because of economic reform that took place in the 1990s. Section 2.4.5. 2001 was the first post-independence era where Kerala had a higher urban growth than a rural one. Many of the rural villages were reclassified to census towns during this period as there was an increase in densification of houses and settlements (Kuruvilla, 2018). Another reason for this growth can be attributed to the fact that the

transport facilities increase connecting the east to the west of the State. The statements above are further explained in chapter 2.6.2.

As presented in chapter 2.2.2, forestry and agriculture play a vital role in preventing floods as it more prone to infiltration. This study shows that there has been a general decrease in forest/tree areas since 1973. Forest/tree area covered 43.17% (1674461.99 ha) percent in 1973 which declined to 20.27% (786,324 ha) in 2001. This represents a negative change of -53.05% (-1.89% per year). A slight increase of forest/tree area was seen between the years 2001 to 2018 from 20.27% to 21.75%. The percentage rate of change for the year 2001 to 2018 is 0.26 percent. Kumar (2005) states that there was a decline in forestry between the year 1965-1983 in Kerala, due to the conversation of forest land to plantations. Figure 11 in chapter 2.4.3 visually depicts the decrease in forest area between those years. Chapter 2.6.3 explains that the cultivation of crops decreased whereas the tree crops stayed the same. This could possibly explain the slight increase in forest/tree areas in the year 2018. The Kerala State has claimed that the forest area between the years 2016 to 2018 has remained constant at 28 percent. This statement does not agree with the findings of this thesis as well as that of Mohan Kumar who states that the forests structural integrity is questionable.

This study shows an increase in crops from the year 1973 to 2001 at the rate of 62.9 percent and a slight decrease between 2001 and 2018 at a rate of -9.75 percent. The difference in hectares are 601 882.9 and -152 095 hectares respectively. Chapter 2.6.4 explains in detail the varied crops found in the State from non-food crops to food crops and seasonal crops. Even though Egregious Thomas (2000) states that the mid lying areas are rich (chapter 2.6.1.) in agriculture Kandiannnan (2018) explains that the Western Ghats are rich in rainfall which

helps certain crops grow (chapter 2.6.4). Visually one can see this in the images presented in chapter 4.1.

An increase of more than double in area is seen between the years 1973 to 2001 due to deforestation in the 1990's, making way for plantation (Kumar, 2005). Section 2.4.4 goes on to further explain that Kerala was known for its agroforest but there was a shift to monoculture (Fox, et al., 2017). A study conducted in Idukki, which is explained in section 2.4.4., found that there was a drastic increase in vegetation between the years 1990 to 2001 which supports the findings of this study. One can assume that this increase occurred across the State (Ramachandran & Reddy, 2016). The decrease in crop land between the years 2001 to 2018 can be explained by the change in culture of the State. A stigma was attached to agriculture and, as is clear from the discussion in 2.4.5 there was the need to develop land. The article "Agricultural land-use change in Kerala, India: Perspectives from above and below the canopy" by Fox, et al., explains that there has also been a decrease in access to labour, the profit margins have decreased, there has been an increase in lack of access to pesticide and fertilizers and lastly an increase in pests and diseases has been seen (Fox, et al., 2017). Figure 11 in chapter 2.4.4. shows a percentage decrease in sown land which was published by the Kerala State of Environment and Related Issues, supporting the findings in this study.

As explained in chapter 2.6.1 Kerala has a variety of water bodies from rivers to reservoirs. These water bodies played a vital role in the development of the State (Padmanabhan, 2011). The backwaters found in the State form part of the transport system, confirming that water bodies play a vital role in the development of the State.

The percentage rate of change in water bodies between the years 2001 an1973 is 1.15% and between 2018 and 2001 is -1.05 %. Table 21 shows that there has been an increase in water

bodies by 395 23,08 ha between 1973 and 2001. There is a decrease in 2018 of 336011 ha. The increase in water bodies was found in Idduki in the years 1990 to 2001 by Ramachandran and Reddy (2016). These authors explained that the increase in water bodies is because of the construction of the Idduki Arch Dam. They also saw an increase in waterbodies between the years 1975 to 1990 because plantation and forest areas were submerged in water bodies and many plantations were converted to water bodies. Further explanation of this can be found in section 2.4.4. One can assume that the findings of this district are true for the entire State during this time period. The Standing Committee of Water Resources (2016) presents evidence of a decrease in water bodies between the years 2001 and 2018 which could possibly be linked to illegal encroachment for construction and agriculture as stated in section 2.6.4. The same report found that the initial encroachment of water bodies in Kerala was for agriculture which then later became for construction of houses and other commercial establishments. Section 2.4.4. explains how various authors have found that many water bodies in cities are filled with waste leaving these bodies barren and dry. This could explain why there was a decrease in water bodies over time.

The bare land for the years 1973, 2001 and 2018 are 641479 ha (16,54%), 558518 (14,405) and 336011 (8,66%) respectively. One can see a decrease in this bare land in Figure 42, the percentage rate of change is -0.86 and 0,23% for the years 1973 to 2001 and 2001 to 2018 respectively. The decrease in bare land is linked to the increased need for agriculture and non-agriculture activities which has been explained in detail above.

4.2 Flood Susceptibility in Kerala

This section presents the reclassified data tabulated in chapter 3.2 - drainage density, slope, soil, lithology, average annual rainfall and land use/land cover with their scaling 1-9. The statistical analysis is also conducted.

4.2.1 Reclassified Drainage Density

Figure 43 below is the reclassified drainage density of Kerala.

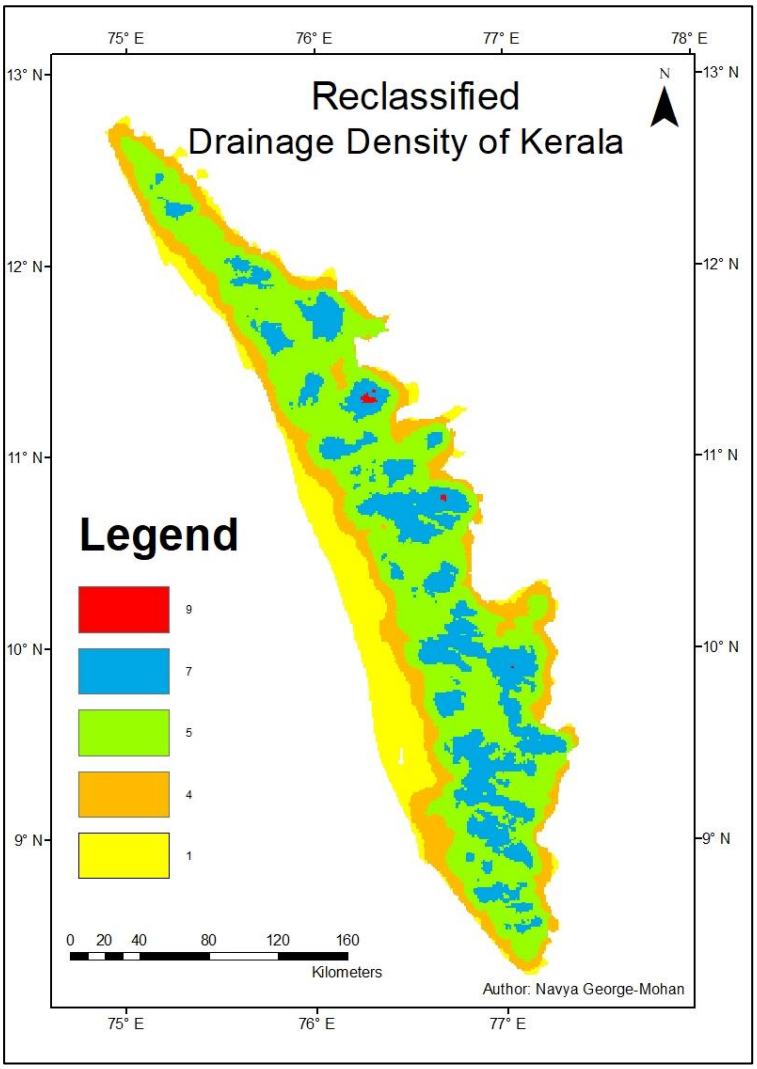

Figure 43: Drainage Density of Kerala

As discussed in section 2.2.3 drainage density is the measure of stream spacing which represents the length of river per unit of area. Visually, most of the area of the State is found in the medium to lower region with drainage density values (1-5). There are very few high drainage values (9).

Only 21 percent of the area has high to very high drainage density values. As stated in section 2.2.3 the reason that the majority of the drainage density values (72.4 %) are found in the medium-lower region could be related to the humid weather in Kerala. Table 21 below stipulates the area and percentage of each class.

Table 21: Drainage Density of Kerala

Drainage Density	Values	Area (ha)	Percentage (%)
0-0,5	Low	540120,59	13.93
0,5-1	Low	489440,78	12.62
1-1,5	Medium	1778809,20	45.87
1,5-2	Medium	813639,96	20.98
>2	High	4928,40	0.13
Other	N/A	251411,06	6.48
Total		3878350,00	100

This classification of Kerala's slope is divided into lowlands, midlands and highlands which is Stated and explained in section 2.4.1. As seen from the table above 28.85 % are lowland areas, 57.51% are midland and 13.64 % are highland areas. Section 2.4.1. States that the mid lands are rich in agriculture which is visually supported by the maps in section 4.1 as the majority of crops are found there. The midlands cover more than half the State which could explain why Kerala is known for its agriculture (section 2.4.4)

4.2.2 Reclassified Slope

Slope can be described as the elevation difference between two points or as a gradient as mentioned as mentioned in chapter 2.2.3 (Balasubramanian, 2007). Figure 44 below depicts the reclassified slope of Kerala.

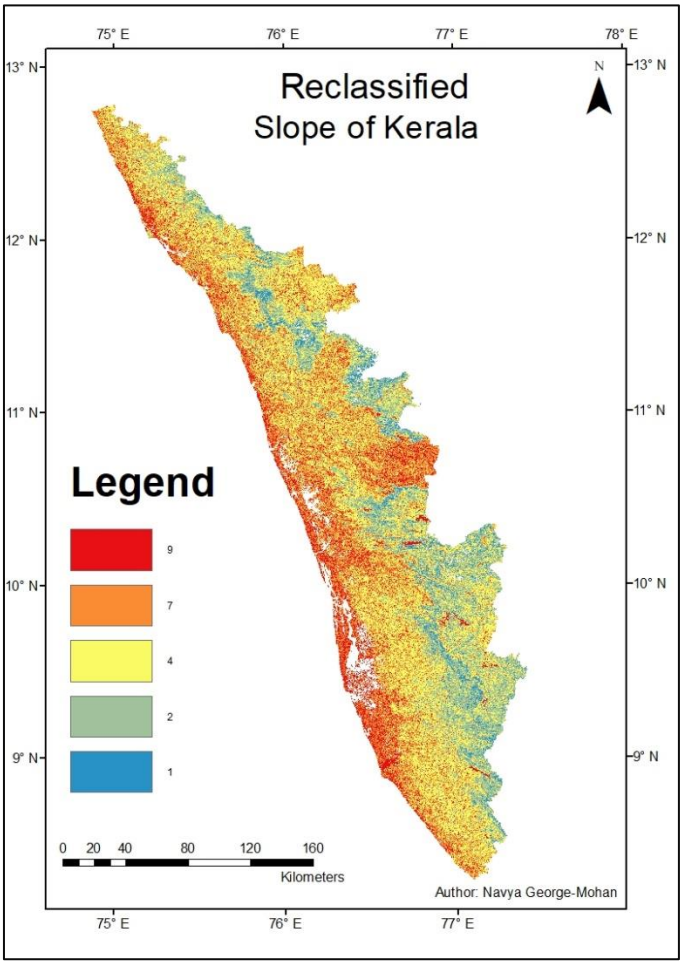

Figure 44: Reclassified slope of Kerala

One can clearly see that the State has low lying (1 and 2), mid (4) and high ranges (7 and 9) which is supported by literature in section 2.4.1 which states Kerala has highland (Western Ghats), lowland (coastal plain of the west) and the midland (rich in agriculture) (Thomas, 2000). Most of the area lies within the midland area. A significant amount of land is in the

low-lying area which is more flood prone than the other land ranges as stated in section 2.2.3 The areas in blue are high range areas which are not flood prone (Lappas & Kallioras, 2019).

This classification of Kerala's slope divided into lowlands, midlands and highlands which is stated and explained in chapter 2.6.1. As seen from the table 25 below 28.85 % are lowland areas, 57.51% are midland and 13.64 % are highland areas. Section 2.4.1 states that the mid lands are rich in agriculture which is visually supported by the maps in section 4.1 as the majority of crops are found there. Table 22 below presents the slope statistics of Kerala.

Table 22: Slope statistics of Kerala

Slope	Area	Area (ha)	Percentage (%)
0-2	Low	375267.53	9.68
2-5	Low	743512.30	19.17
5-15	Mid	1486950.93	38.34
15-30	Mid	743512.30	19.17
>30	High	153092.47	3.95
Other	N/A	376014.47	9.70
Total		3878350.00	100

4.2.3 Reclassified Soil

As Hammami et al. (2019) claim, soil plays a role in water storage capacity and the permeability of water as stated in chapter 2.2.2. Impermeable soil causes flooding as it has low infiltration. Looking at the soil of Kerala, the majority of the soil is very impermeable (7) and a significant amount is semi permeable (1). Figure 45 below depicts the reclassified soil of Kerala.

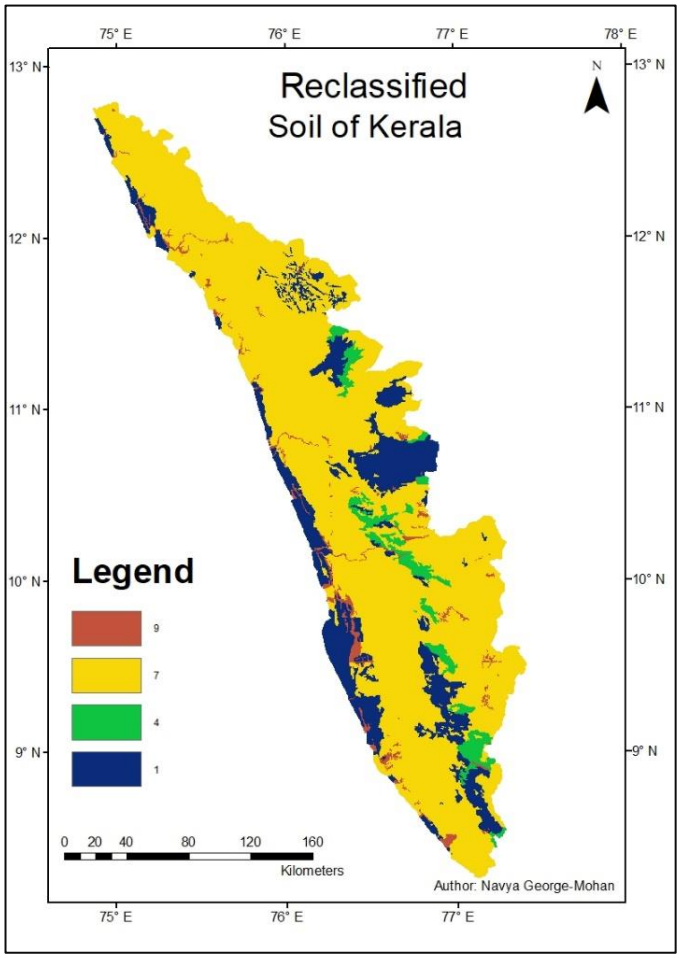

Figure 45: Reclassified soil of Kerala

Soils play a vital role in agriculture which is explained in section 2.4.2 (Baxter & Williamson, 2001). Section 2.4.2 further explains the key role soil plays in water and nutrient holding capacity which is highly dependent on the rate and amount of water and air that moves through the soil. The number, size and shape of the pores as well as structure of soil plays a role in the permeability (Hammami, et al., 2019). Most of the soil type found in Kerala is semi-permeable (77.60%) followed by very permeable soil types (15.44%). This is further supported by the State of Kerala position that the general soil type is low water holding (section 2.4.2). Table 23 below tabulates the permeability and percentage of the different soil types.

Table 23: Soil permeability and statistics

Soil	Permeability	Area(ha)	Percentage (%)
Loamy sand and sand	Very Permeable	598775,39	15,44
Loam, silt loam, silt, sandy loam	Permeable	164993,97	4,25
Clay, Loamy, clay, sandy clay, silty clay	Semi-Permeable	3009530,75	77,60
non-soil categories	Impermeable	105017,97	2,71
Other	N/A	31,92	0,00
Total		3878350,00	100,00

4.2.4 Reclassified Lithology

Section 2.2.3 explains why lithology plays a vital role in flooding. It further states that flooding can be caused by infiltration in impermeable rocks (Hammami, et al., 2019). Most of the area is impermeable (9). As seen in Figure 53 there is no data for below 'very permeable'(1). Very few permeable rocks can be identified (4). Lithology plays a vital role to help define flooding as different rock types vary in water storage and permeability as explained in section 2.2.3 (Hammami, et al., 2019). This chapter presents evidence that shows impermeable rocks cause water runoff. Figure 46 below depicts the reclassified lithology of Kerala.

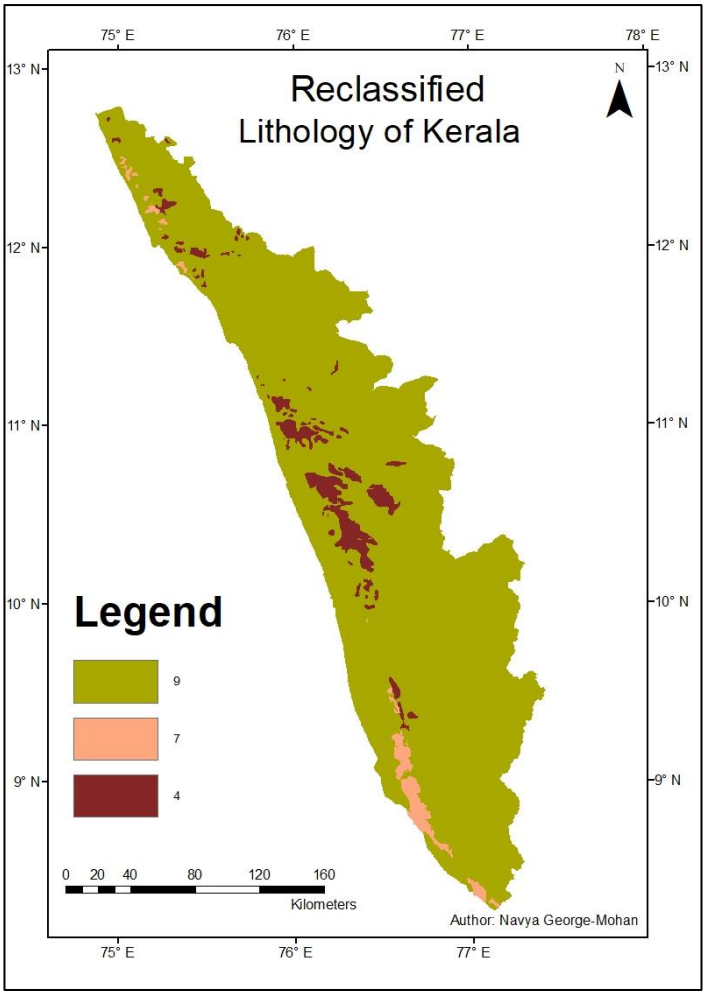

Figure 46: Reclassified lithology of Kerala

Table 24 below tabulates the permeability and percentage area of each class. The percentage of impermeable rocks occupies most of the State. One can conclude that there is high water runoff caused by the rocks.

Table 24: Permeability and statistics of the lithology

Lithology	Permeability	Area(ha)	Percentage (%)
Laterite and Pebble Bed	Permeable	195920.85	5.05
Sandstone and clay	Semi-permeable	82767.72	2.13
Crystalline, Intrusive, ultramafites, unconsolidated sediments	Impermeable	3599654.30	92.81
Other		7.12	0.00
Total		3878350	100.00

4.2.5 Reclassified Rainfall

As explained in section 2.2.3 extreme rainfall can trigger flooding. The types of flooding it can cause are pluvial and riverine which is further expanded on in sections 2.1.1 and 2.1.2. Figure 47, 48 and 49 depict the average annual rainfall of Kerala for the years 2018, 2001 and 1973 respectively.

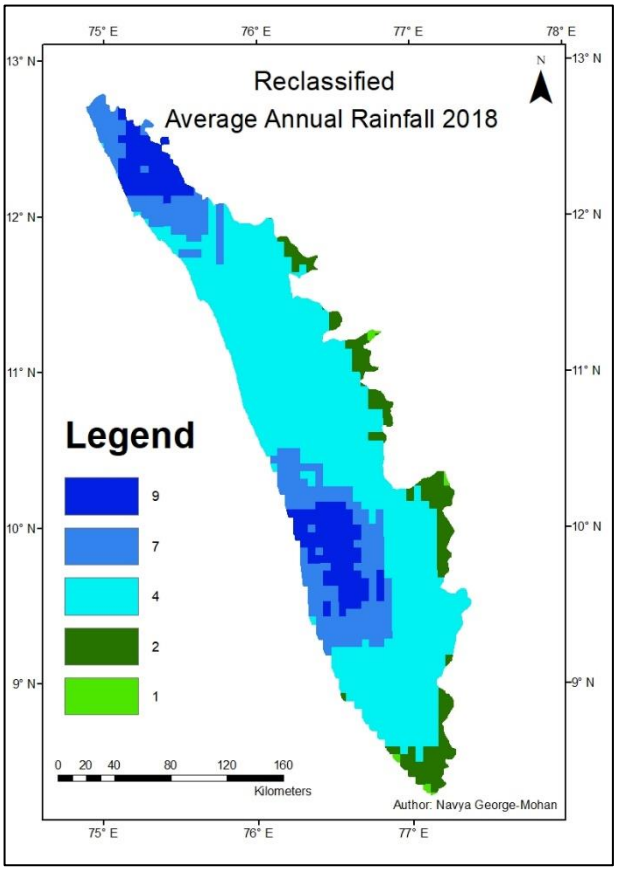

Figure 47: Reclassified average annual rainfall 2018

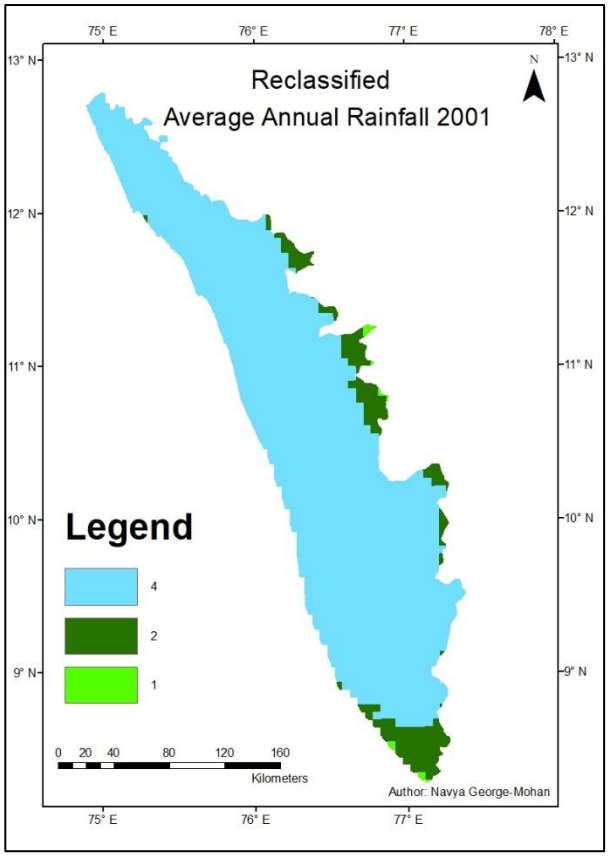

Figure 48: Reclassified average annual rainfall 2001

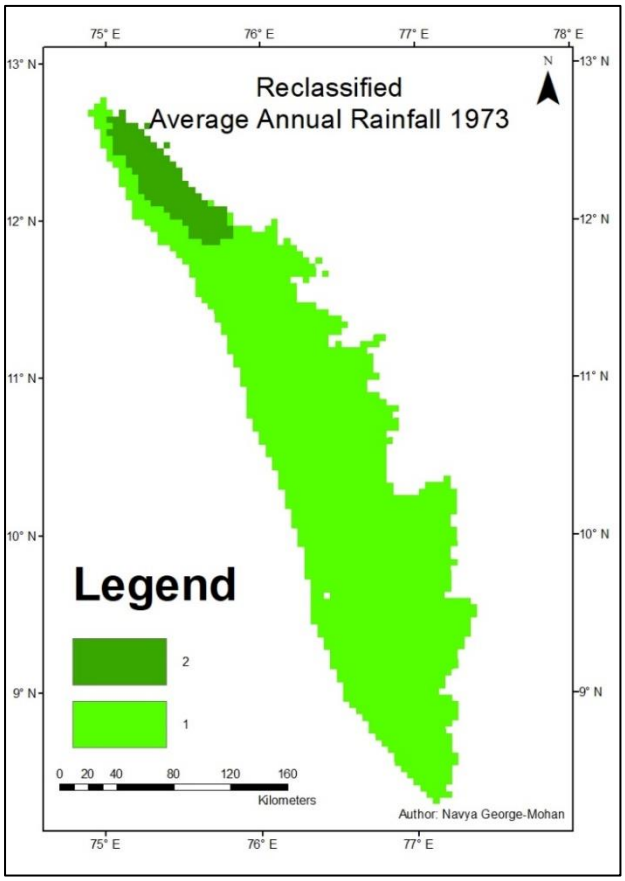

Figure 49: Reclassified average annual rainfall 1973

The year 2018 had the most amount of rainfall when compared to the years 2001 and 1973. Most of the rainfall in 2018 ranges from medium (4) to very high (9) amounts, whereas 2001 is mostly medium (4) rainfall and 1973 is mostly very low rainfall (1) with no amounts of medium to high rainfall. The map of 2018 clearly shows there is an uneven distribution of rainfall which is stated by D, et al. (2015) in section 2.4.3. Table 25 below stipulate the rainfall for the years 2018, 2001 and 1973.

Table 25: Amount of Rainfall in 2018, 2001 and 1973

Amount of Rainfall (mm)	Levels of Rainfall	2018	2001	1973
1100-1200	Very High	✓		
1000-1100	High	✓	✓	
500-1000	Medium	✓	✓	
350-500	Low	✓	✓	✓
<350	Ver Low	✓	✓	✓

Statistically one can note that 2018 had the highest rainfall if compared to the years 2001 and 1973. Even though 1973 has a level of rainfall fall as “Very High” the volume of rainfall reported in 2018 differs because the data types used are not the same. Rainfall statistics are confirmed in the literature in chapter 2.6.3 that states that until the year 2005 there was fairly low rainfall in Kerala (Krishnakumar, et al., 2008). The high amounts of rainfall in 2018 are explained by Hunt & Menon (2020) who confirm that Kerala has experienced a long duration of rainfall during that year (Chapter 2.6.3.)

4.2.6 Reclassified Land use/cover

Figures 50, 51 and 52 below depict the reclassified land use/land cover of Kerala for the years 2018, 2001 and 1973 respectively.

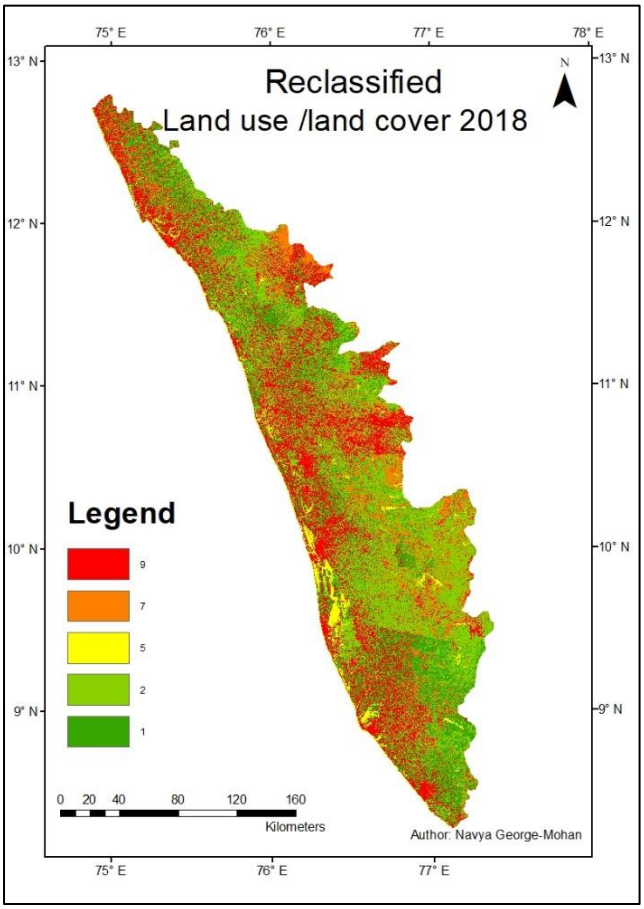

Figure 50: reclassified land use/land cover 2018

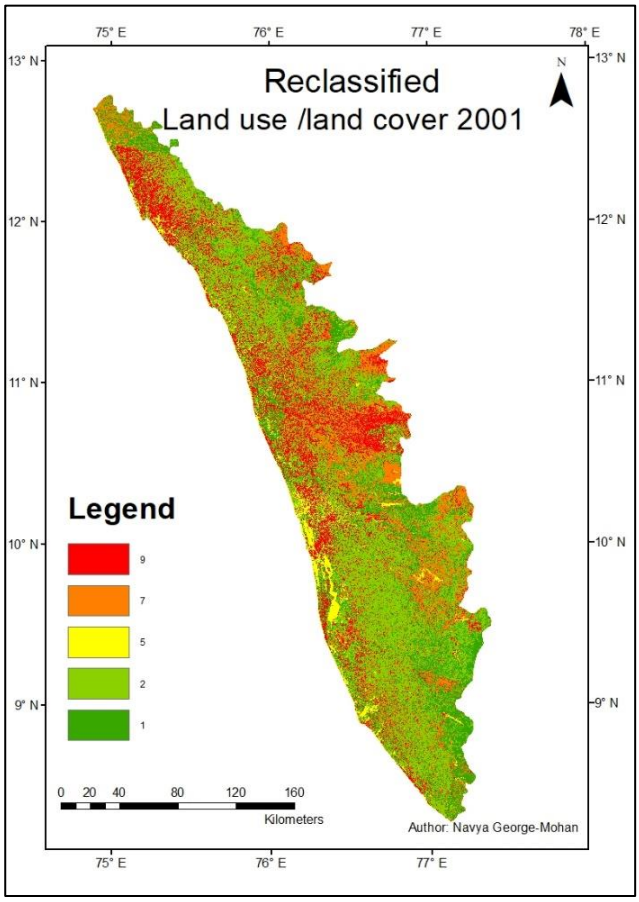

Figure 51: reclassified land use/land cover 2018

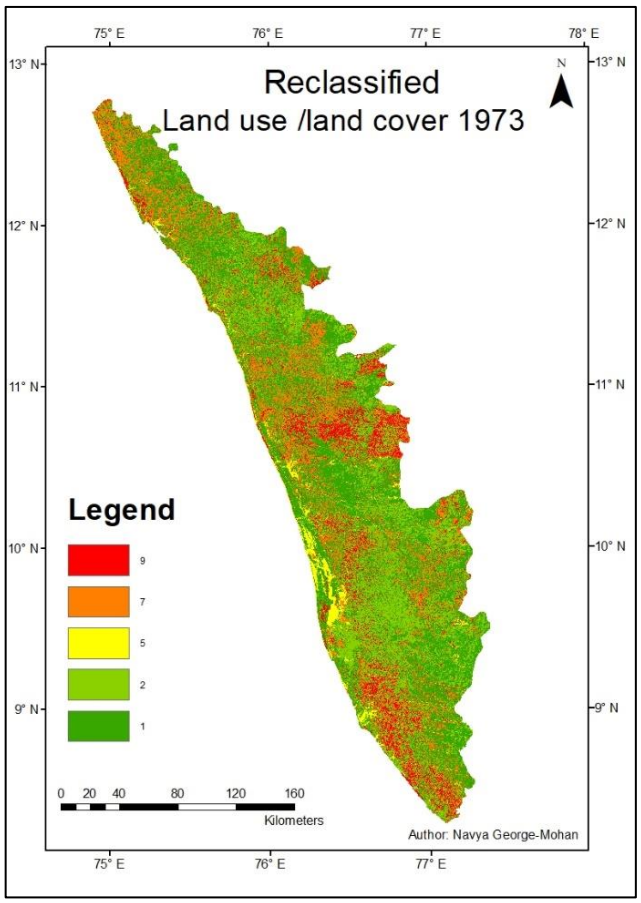

Figure 52: reclassified land use/land cover 2018

The year 1973 depicts that most of the area is falling under very low (1) to low susceptibility (2), very minimal medium susceptible regions (5) and, patches of high (7) and very high (9) susceptibility. 2001 shows a decrease in very low (1) to low susceptibility (2) which is caused by an increase in high (7) and very susceptibility (9). 2018 is the year one can see a drastic increase when compared to the previous two years. This in turn causes an extreme decrease in low (2) and very low (1) susceptibility.

The maps shown in section 4.1 show an increase in built up area and a decrease in vegetation, bareland and forest areas. Visually the high susceptibility regions coincide with the areas which have a high concentration of built-up area. These findings are supported by literature

written by Lappas & Kallioras (2019) who claim that urban areas are more likely to be prone to flooding.

4.2.7 Composite Flood Susceptibility

Section 2.2 presents flood susceptibility and looks at the physical characteristics of the area. Figures 53, 54 and 55 depict the flood susceptibility areas for the years 1973, 2001 and 2018.

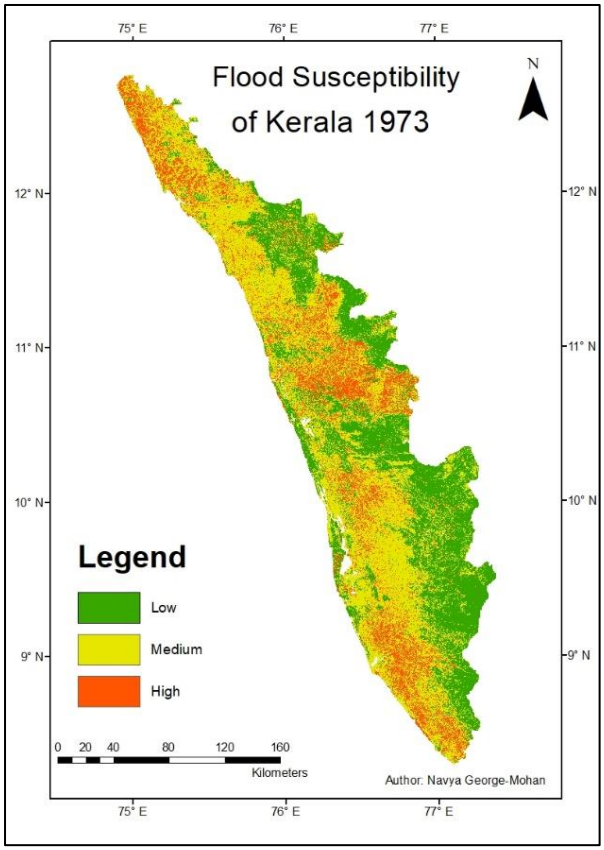

Figure 53: Flood Susceptibility of Kerala for the year 1973

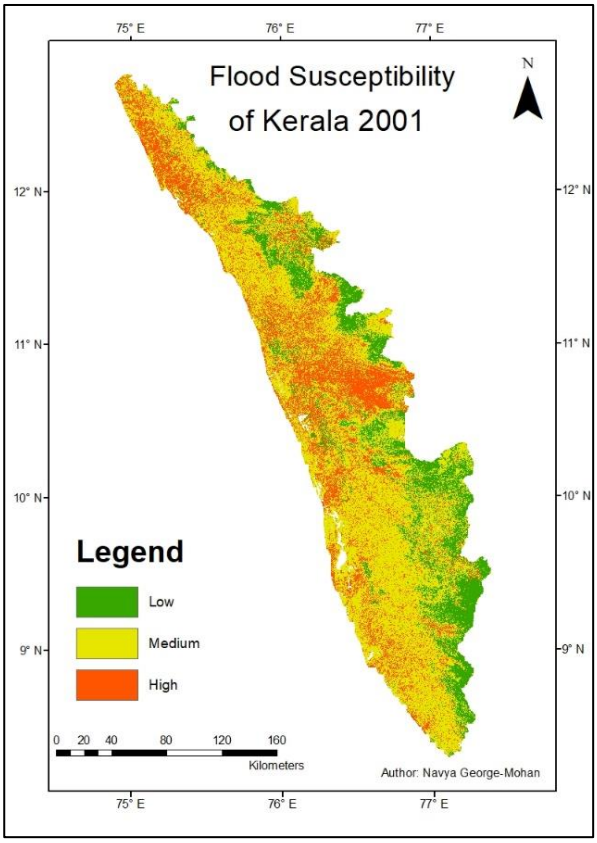

Figure 54: Flood Susceptibility of Kerala for the year 2001

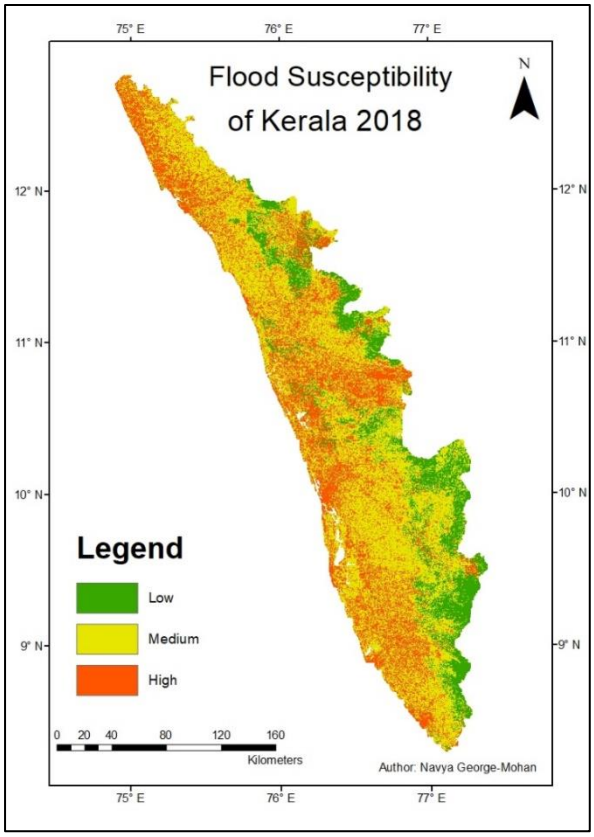

Figure 55: Flood Susceptibility of Kerala for the year 2018

Visually one can see that in the year 1973 the majority of land is in low susceptibility areas which is mainly found on the Western Ghats. Areas of medium susceptibility are predominantly visible in the midlands and highly susceptible zones are concentrated within a few areas. 2001 shows a shift from the majority of the area being low susceptibility to medium susceptibility with high susceptibility regions spread across the State unlike the year 1973. The year 2018 shows a further decrease in low susceptibility areas and a further increase in medium and high susceptibility regions. The major factors that contribute to the increase in flood susceptibility is the change in rainfall and the built environment. The other variables do not vary as much.

4.2.8 Flood Susceptibility Statistics

This chapter presents the flood susceptibility statistics and goes on to further analyse these results with land use/land cover statistics. Tables 26 depicts the susceptibility levels in hectares and Table 287 depicts the percentage of susceptibility levels. Figure 56 depicts the percentage of flood susceptibility levels.

Table 26: Flood susceptibility areas in Hectares

Year	Low (ha)	Medium (ha)	High (ha)	Other (ha)	Total (ha)
1973	1220814.10	1673438.72	618932.05	365165.13	3878350
2001	639860.19	2032178.22	867481.18	338830.41	3878350
2018	562652.88	1895323.57	1082687.10	337686.45	3878350

Table 27: Percentages of flood susceptibility

Year	Low (%)	Medium (%)	High (%)	Other (%)	Total (%)
1973	32.41	44.42	16.43	6.74	100
2001	16.98	53.94	23.03	6.05	100
2018	14.94	50.31	28.74	6.01	100

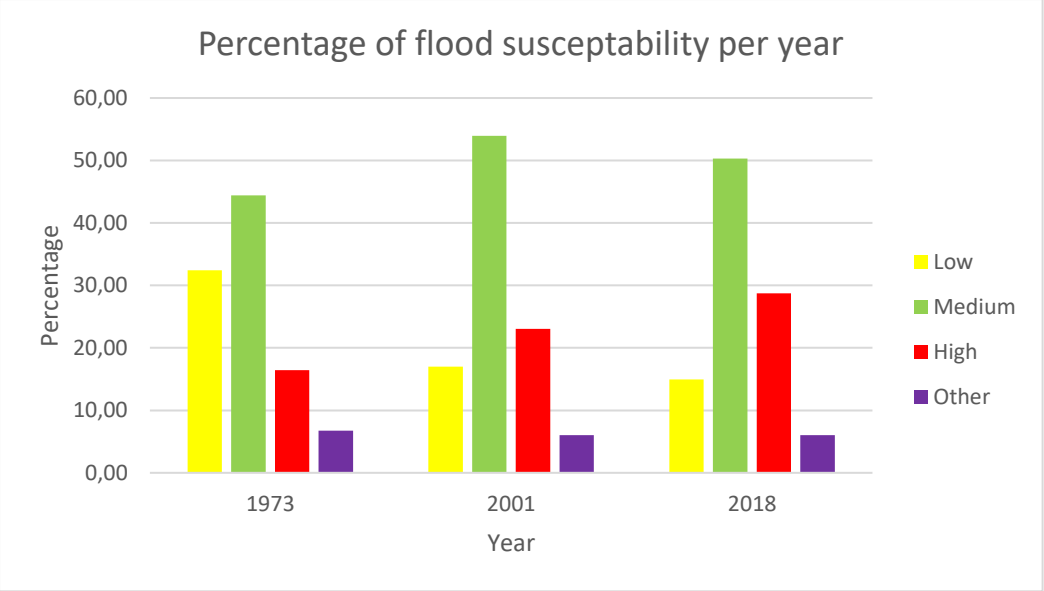

Figure 56: Percentage of flood susceptibility

The class “other’ is represented by the unclassified pixels that have not been allocated a class. Their spectral index does not fall within the range of low, medium or high. The years 1973, 2001 and 2018 has the class low susceptibility which covers 1220814.10 ha (32.41%), 639860.19 ha (16.98%) and 562652.88 ha (14.94%) of land. The percentage rate of change between the years are -47.61 % and -12.01%. One can visually see that the ‘low’ class has decreased over the years.

The medium susceptibility areas for the years 1973, 2001 and 2018 cover 1673438.72 ha (44.42%), 2032178.22 ha (53.94%) and 1895323.57 ha (50.31%) of land. The percentage rate of change between the years is 1.7% and -0.40% for 2001-1973 and 2018-2001. A significant increase in the medium susceptibility regions can be seen between the years 1973 to 2001. A decrease in in this area is seen between the years 2001 to 2018.

The high susceptibility areas for the years 1973, 2001 and 2018 are 618932.05 ha (16,43%), 867481.18 ha (23.03%) and 1082687.10 ha (28.74%). The percentage rate of change for the years 2001 and 2018 are 1.43 and 146 percent. An increase can be seen over the years.

Medium susceptibility percentage of land cover was fairly high since the year 1973 at 44,42 percent. A decrease in low susceptibility regions were seen as the regions of medium and high increased. In 2018 a decrease in medium susceptibility regions was noted from 2001. However, an increase in high susceptibility regions is also noted and there is a shift in susceptibility areas. The lower susceptibility regions get smaller and the medium to higher susceptibility regions increase accordingly.

Table 28 below combines the land cover/ use findings with flood susceptibility findings. Figure 57 below shows the relationship between land cover and flood susceptibility.

Table 28: Land cover/land use and flood susceptibility in hectares

Land use/cover						**Flood Susceptibility**		
	Bare land	Built-up area	Crop	Forest/Trees	Water bodies	Low	Medium	High
1973	641478,60	349402,40	956804,58	1674461,99	122845,74	1220814,10	1673438,72	618932,05
2001	558518,48	711067,01	1558687,48	786323,50	162368,82	639860,19	2032178,22	867481,18
2018	336010,91	1053552,15	1406592,13	843493,20	133595,73	562652,88	1895323,57	1082687,10

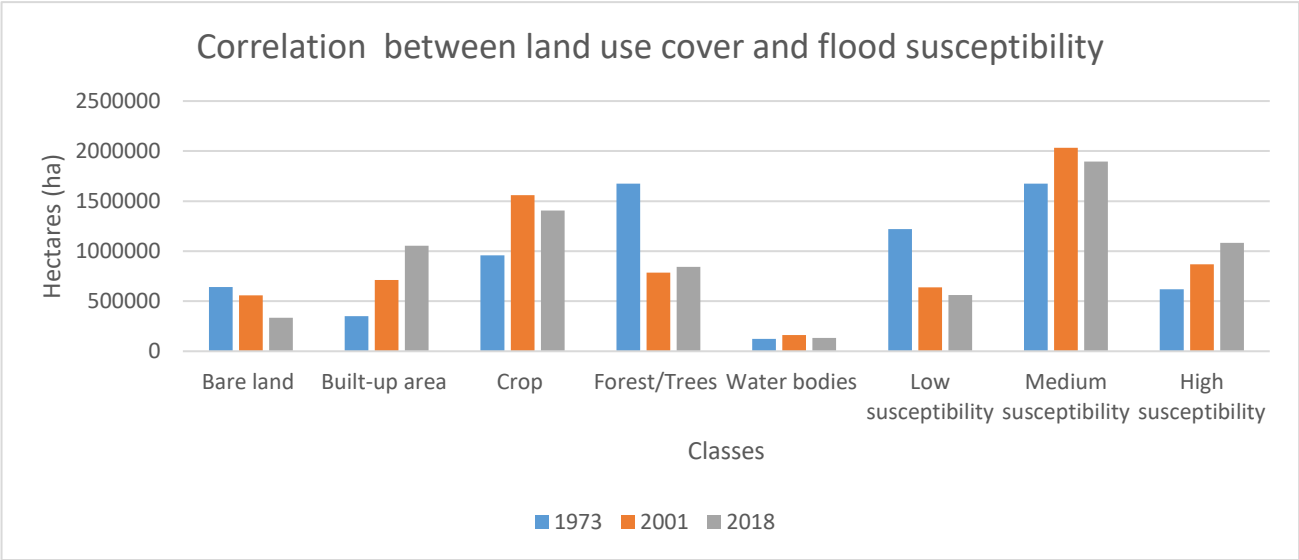

Figure 57: Correlation between land use cover and flood susceptibility

Table 29: Difference in land use/cover and flood susceptibility regions

Land use/cover						Flood susceptibility		
	Bare land (Ha)	Built-up area (Ha)	Crop (Ha)	Forest/Trees (Ha)	Water bodies (Ha)	Low (Ha)	Medium (Ha)	High (Ha)
1973								
2001	-82960,12	361664,60	601882,90	-888138,49	39523,08	-580953,91	358739,50	248549,13
2018	-305467,69	704149,75	449787,55	-830968,79	10749,99	-658161,22	221884,84	463755,05

Figures 58 and 59 depict the difference in land use/cover and difference in flood susceptibility since 1973.

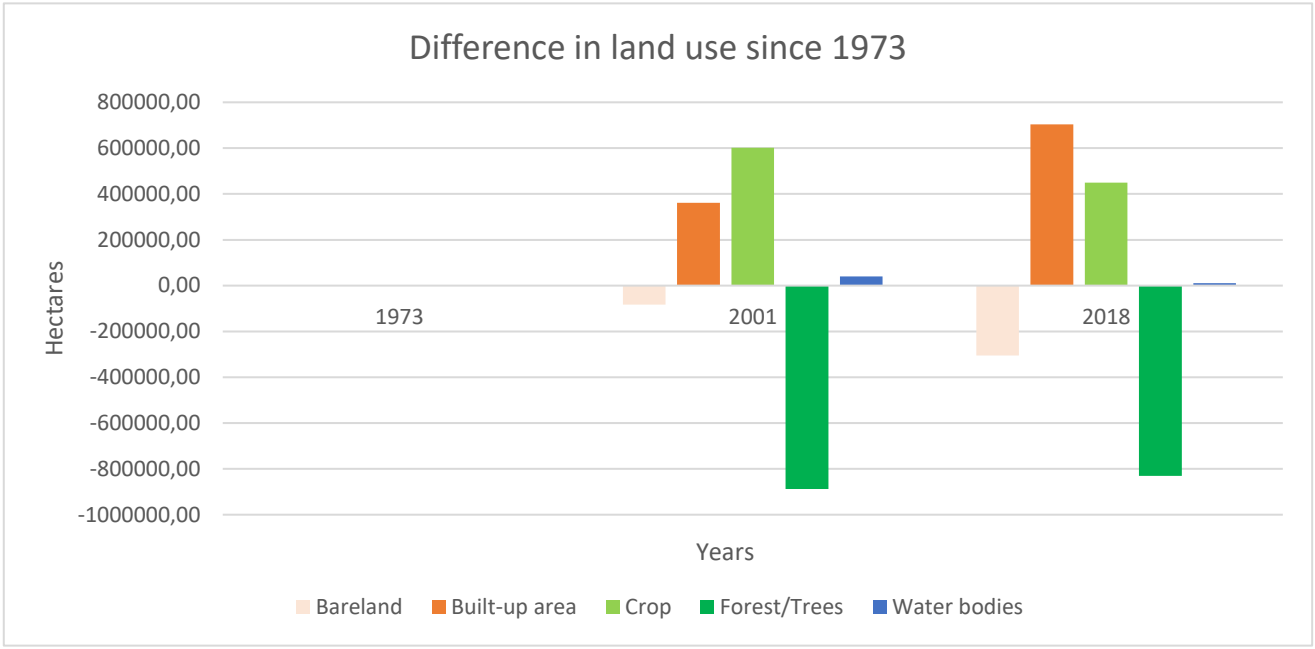

Figure 58: Difference in Land use/cover

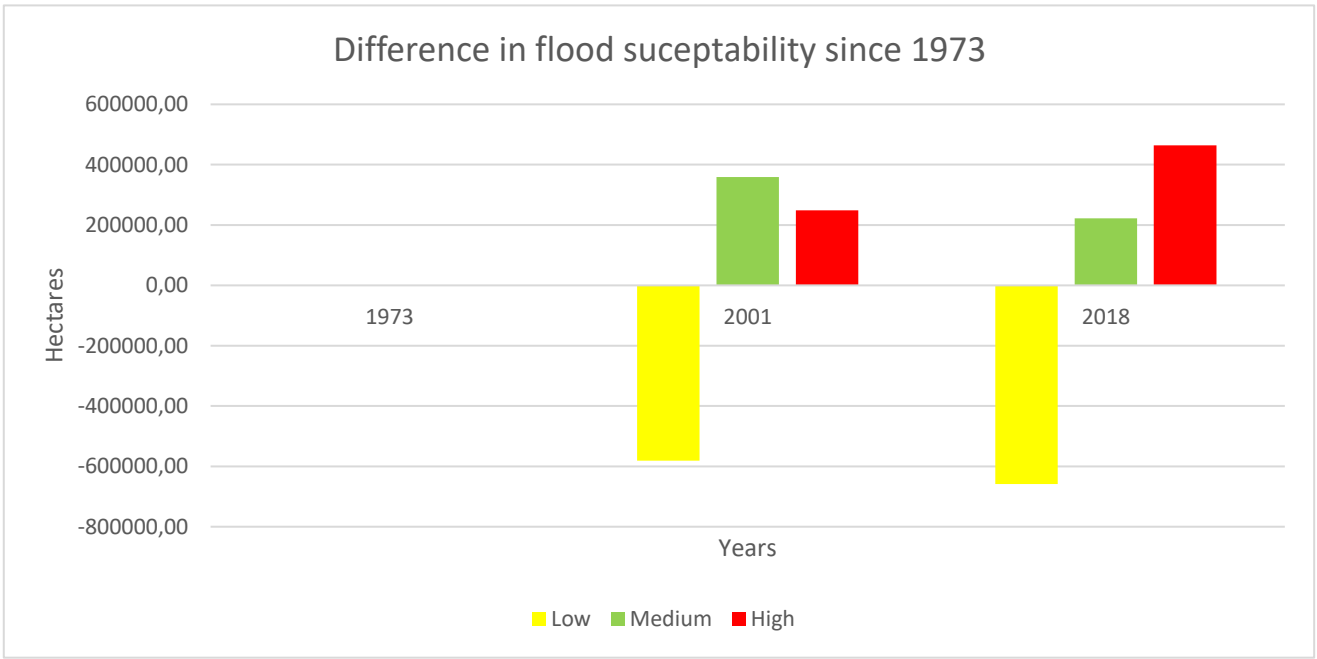

Figure 59: Difference in flood susceptibility areas

It can be seen from Figure 57 and Table 29 that the bare land has decreased from 1973 by 82960.12 ha in 2001 and a further decrease of 305467.69 ha was seen in the year 2018. Another decrease can be seen in forest/trees by 888138.49 ha in 2001 and 830968.79 ha in 2018. The water bodies have increased since the year 1973 by 39523.08 ha in 2001 and 10749.99 ha in 2018. The built-up area had increased since 1973 to 361664,60 ha in 2001 and a further increase in 2018 by 704149,75 ha. The crop area ha also increased by 601882,90 ha in 2001 and 449787,55 ha in 2018.

Table 29 and figure 57 show that there has been an overall decrease in low susceptibility regions since the year 1973. Since 1973 there has been a decrease of 580953,91 ha and 658161,22 ha for the years 2001 and 2018. The medium flood susceptibility zones have increased since 1973 by 358739,50 in 2001 and 221884,84 ha in 2018. A slight decrease in medium susceptibility regions can be noted in 2018 from 2001 as the increase since 1973 was less than that of 2001. The increase in high susceptibility regions since the year 1973 is 248549,13 ha in 2001 and 463755,05 ha in 2018. The high susceptibility zones have kept on growing over the years.

The pressure put on the land for built-up areas and crops could explain why the low susceptibility regions decreased over the years whilst in turn increasing the areas of medium and high susceptibility. A decrease in the medium susceptibility regions in the year 2018 and an increase in high susceptibility regions should be noted. As one would expect a constant increase in these categories, this is not the case for the medium susceptibility regions for the year 2018. A shift has occurred from areas in the medium susceptibility regions to the high susceptibility regions. This could be explained by the increased need in built-up areas which has, in turn, increased the high susceptibility regions. An increase in built up area reduces

infiltration of rainwater into the ground, hence increase in runoff and flooding. Flood Vulnerability in Kerala

This section presents the infrastructure vulnerability, social vulnerability, coping vulnerability and the composite vulnerability. The results will then be statistically analysed. Flood susceptibility is included in the composite vulnerability result as flood susceptibility looks at the physical aspects of the region which in this study is taken as physical vulnerability.

4.2.9 Accuracy Assessment of Flood Susceptibility

This section of the study looks at the confusion matrix and the kappa coefficient. The results of these calculations will be presented in this section. The results of the classification were checked to see if it was in an acceptable range or not. If the accuracy of the classification was not in an acceptable range, then the classification was redone. Table 30, 31 and 32 below show the confusion matrix for the years 1973, 2001 and 2018.

Table 30: 1973 Confusion Matrix

CLASS	Truth 1	Truth 2	Truth 3	Total
1	79	22	9	110
2	15	88	9	112
3	2	19	65	86
Total	96	129	83	308

Table 31: 2001 Confusion Matrix

CLASS	Truth 1	Truth 2	Truth 3	Total
1	89	14	7	110
2	21	87	4	112
3	2	16	68	86

Table 32: 2018 Confusion Matrix

CLASS	Truth 1	Truth 2	Truth 3	Total
1	89	15	6	110
2	15	93	4	112
3	5	13	68	86

The year with the highest misclassification is 1973 and the most accurate is 2018. This can be explained by the resolution of Landsat 8(2018) is better than that of Landsat MSS (1973) and Landsat ETM + (2001).

Once the confusion matrix was computed the kappa Coefficient was determined. Table 33 below shows the final results for the confusion matrix and Kappa Coefficient.

Table 33: Kappa Coefficient

Year	**Accuracy**	**Kappa Coefficient**	**Interpretation**
1973	0.75	0.61	Substantial Agreement
2001	0.79	0.69	Substantial Agreement
2018	0.81	0.74	Substantial Agreement

From the above table it can be seen there is an increase in accuracy between 1973 to 2018. 1973 produced an accuracy that could be questioned. However, Landsat MSS (1973) image was coarser and had very few bands. It is also acceptable as the area of classification is quite big. The image had a resolution of 60m X 60m. Whereas, the other images had a resolution of 30m X 30m. An expected trend is that the accuracy would increase with the change of satellite which can be seen in this study. However, an exponential increase in accuracy can not be seen as the classification covered a large area.

4.3 Flood Vulnerability in Kerala

This section of the study presents the results for infrastructural, social, copying, the composite vulnerability and flood vulnerability statistics. The classes low to very high are present in the state. It is to be noted that the class very low is not present in the state. Majority of the state is lies in the regions medium (60.59%) followed by high (28.48%) vulnerability. The medium and high vulnerability regions are mostly found on the west coast which are the low-lying regions of the state.

4.3.1 Infrastructure vulnerability

This section looks at the reclassified road, railways and building density. The overall infrastructure vulnerability is also presented. Figures 60 and 61 below depict the reclassified road density and railway density of Kerala.

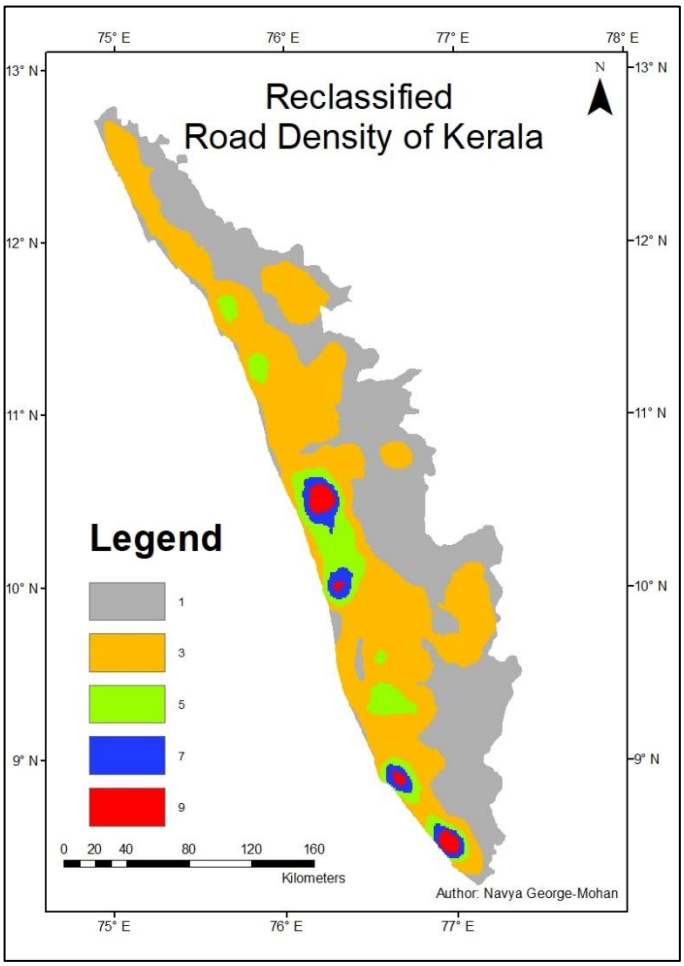

Figure 60: Reclassified Road density of Kerala

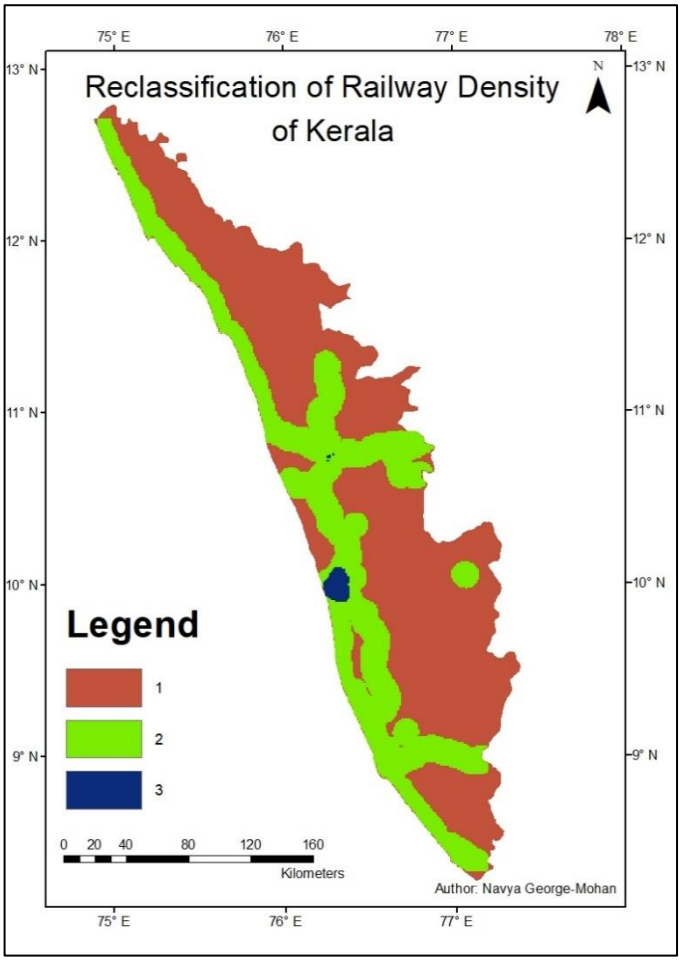

Figure 61: Reclassified railway density of Kerala

With regards to the road density there are pockets of very high vulnerability regions (9). The majority of the area lies in the very low to low vulnerability areas. The railways density ranges between very low vulnerability to medium vulnerability. The majority of the area has very low vulnerability. Yacoub Kuruvilla (2018) states that the transport system helped connect the east to west which shows how the east coast connects to the west.

Figure 62 below depicts the building density of Kerala. The majority of the area lies in the low vulnerability regions followed by very low and medium vulnerability regions. Four pockets of very high vulnerability areas are noted and here one would expect a much higher density of building. However, Yacoub Kuruvilla (2018) states that Kerala is different to the rest of India

as there are scattered micro towns which could explain why there are not many areas of very high building density. According to Kuruvilla (2018), most of the high concentration high building density is found in the coastal areas and, according to the same author, high concentrations of town are found in the low land coastal area.

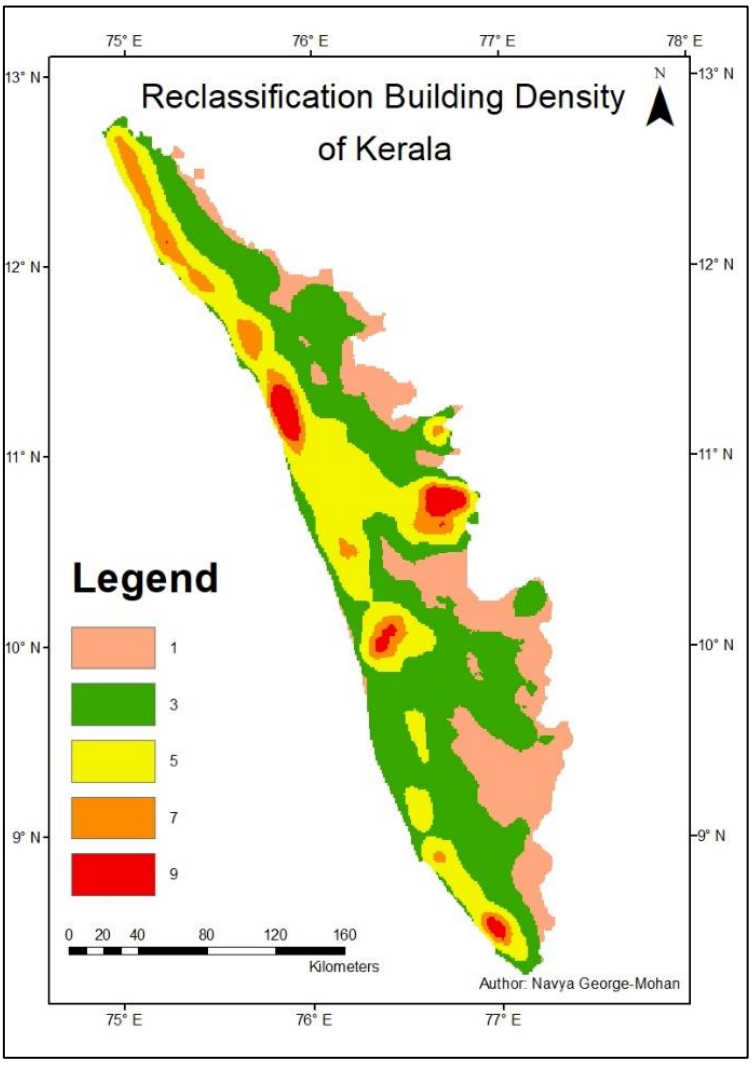

Figure 62: Reclassified Building density of Kerala

Figure 63 below shows the infrastructure vulnerability of Kerala. Most of the area lies in the low vulnerability regions. Pockets of high vulnerability areas can be seen too. Medium vulnerability regions are also prominent.

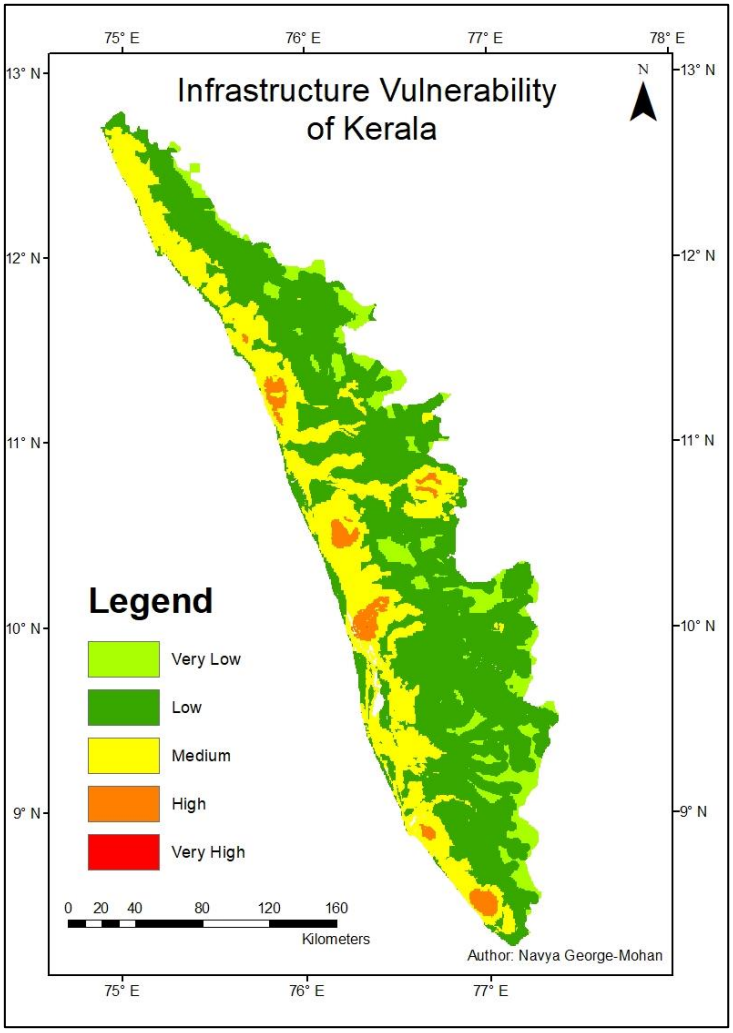

Figure 63: Infrastructure vulnerability of Kerala

4.3.2 Social Vulnerability

This section presents the reclassified total population and female population density as well as the percentage of the non-working population. The total social vulnerability map is also shown.

Figure 64 below depicts the reclassification of the population density. Most of the State has a very high population density (9). Low to high population density is prominent throughout the State (3-7). The high population density is explained in chapter 2.6.5 - the State has the third highest population density in the country which is three times the national average (Kerala State of Environment and Related Issues, 2020).

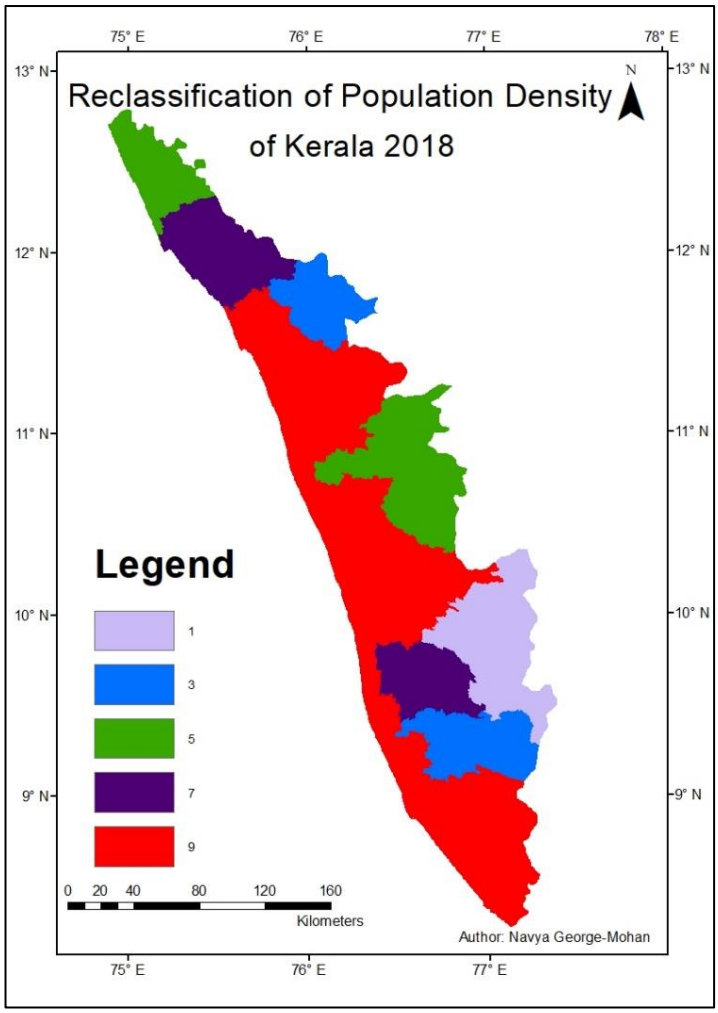

Figure 64: Reclassification of Kerala's population density of the year 2018

Figure 65 below depicts the reclassification of the female population in the State. One can deduce that the State has a high to very high percentage of women (7 & 9). In fact, most of

the State has as very high percentage of women. The National Academy of Sciences acknowledge that Kerala's female population has always surpassed the male population (National Academy of Sciences, 2001).

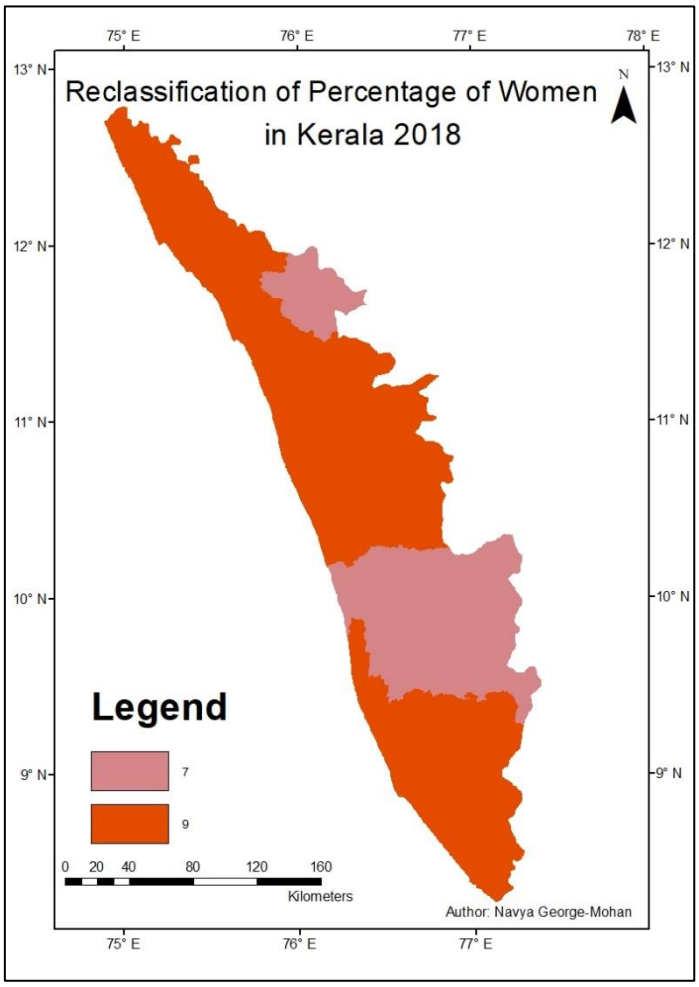

Figure 65: Reclassification of Kerala's percentage of women in the year 2018

Figure 66 below shows the non-working population of the State. The non-working population ranges from high to very high. Most of the State has a high non-working population. The high percentage of non-working class can be supported by the literature presented in chapter 2.6.5. Joseph Tharamangalam (1998) states that Kerala has a relatively low economic development. Kannan (2005) explains that despite the week industrial sector, money flows in

from the Gulf which has made the State rich. The Kerala government has attributed the high unemployment to the high population density which can be seen in Figure 69 above and this is backed up by various other reasons discussed in chapter 2.4.5.

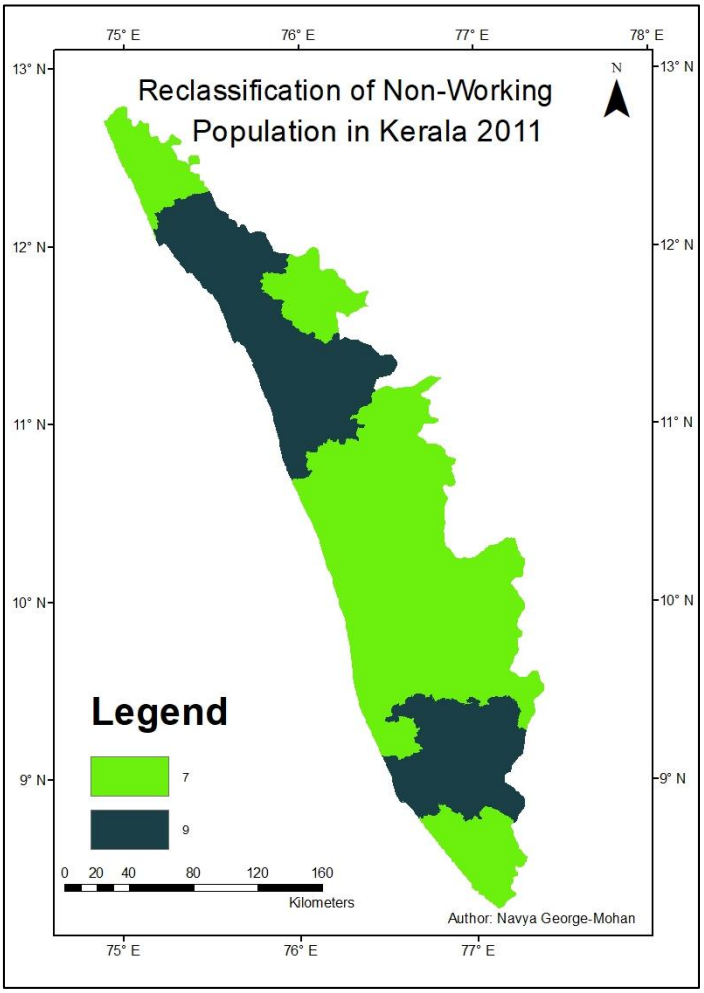

Figure 66: Reclassification of Kerala's non-working population in the year 2011

Figure 67 below depicts the social vulnerability of the State. The social vulnerability ranges between medium to very high. The regions are mainly made up of high to very high vulnerability regions.

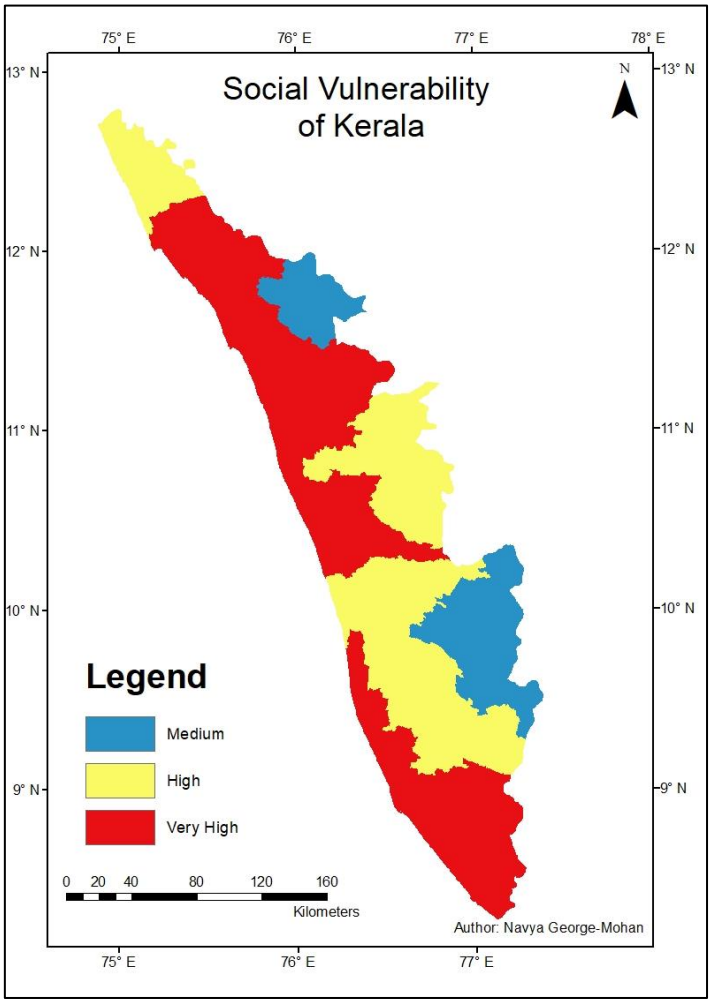

Figure 67: Social Vulnerability of Kerala

4.3.3 Copying Vulnerability

This section looks at the coping vulnerability variables – measured by distance to health centres and the literacy rate of the State. The compiled coping vulnerability is shown too.

Figure 68 below reflects the distance to health centres. Most of the State is in close proximity to hospitals. As most of the State is labelled as '1' - which means very low distance to hospitals – it is categorised as having low vulnerability. Areas that are very high in vulnerability (9) are visible but are not as prominent. An explanation of such low distances to health centres can

be explained by the State's investment in health care as early as the 1950s which only expanded over the years. This is explained in chapter 2.4.5

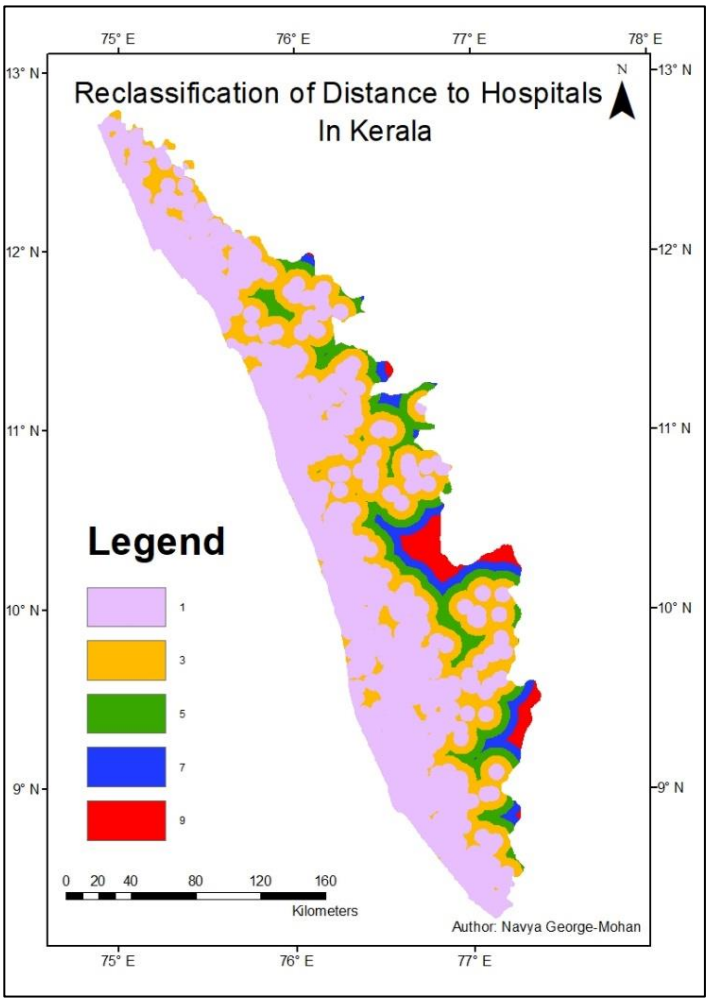

Figure 68: reclassified distances to health centres in Kerala

One of the aspects of social development is literacy. Figure 69 below presents the literacy rate of Kerala. The literacy rate of the State results in very low vulnerability as the State has a high literacy rate. This is supported by the findings of Tharamangalam (1988) who states that the social development of Kerala is far ahead of the other States. Figure 12 in chapter 2.6.5 compares the literacy rate of Kerala with the rest of India. This shows Kerala is ahead of the other States when it comes to literacy.

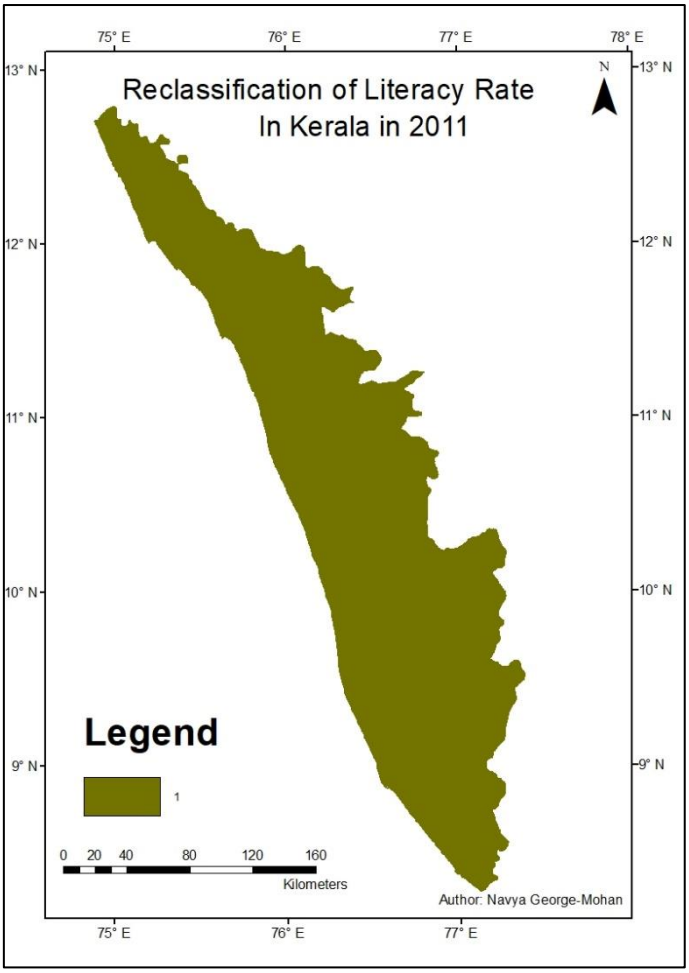

Figure 69: Reclassification of Kerala's literacy rate in the year 2011

Figure 70 below shows the coping vulnerability of Kerala. The coping vulnerability ranges between very low to medium vulnerability. Most of the State has a very low coping vulnerability with notable regions of low and medium vulnerability. The medium vulnerability regions are seen on the highlands of the state where the population density ranges between very low to medium (figure 63) which could explain why the copying vulnerability is medium in those areas as it not highly dense.

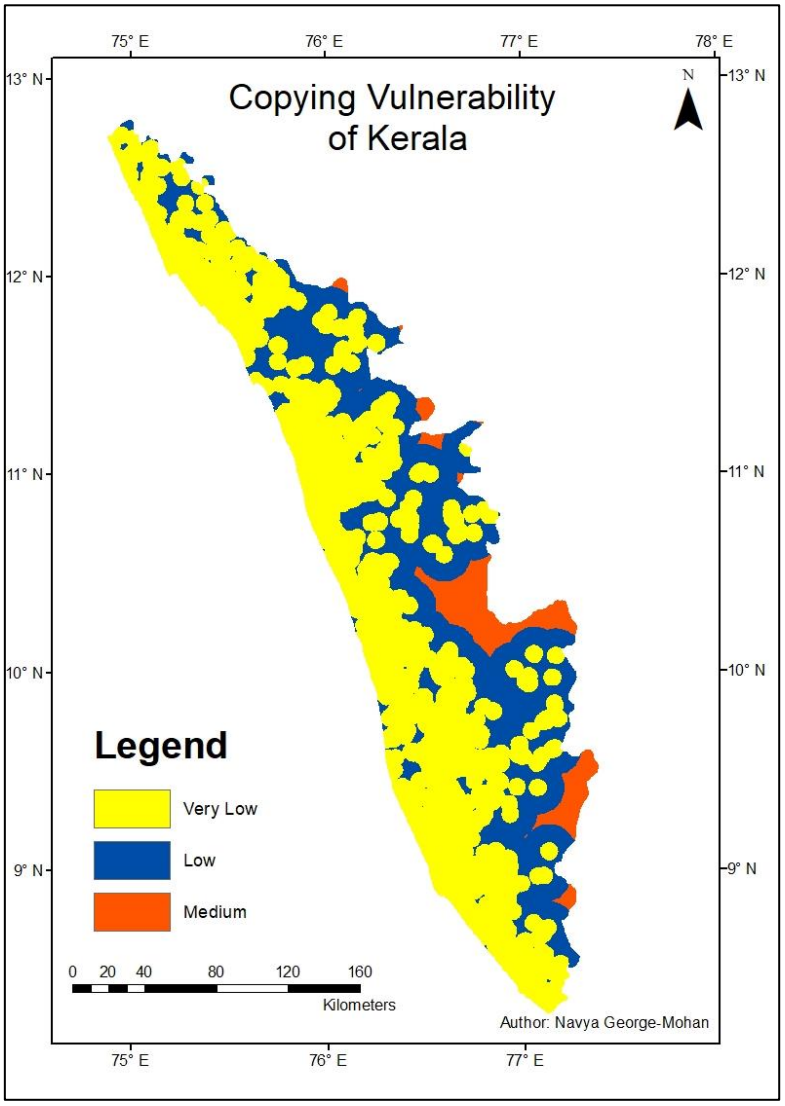

Figure 70: Copying vulnerability of Kerala

4.3.4 Composite Flood Vulnerability

This section presents the overall vulnerability of the State. The variables mentioned in chapter 3.4 and Table 16 have all been processed to produce Figure 71 below.

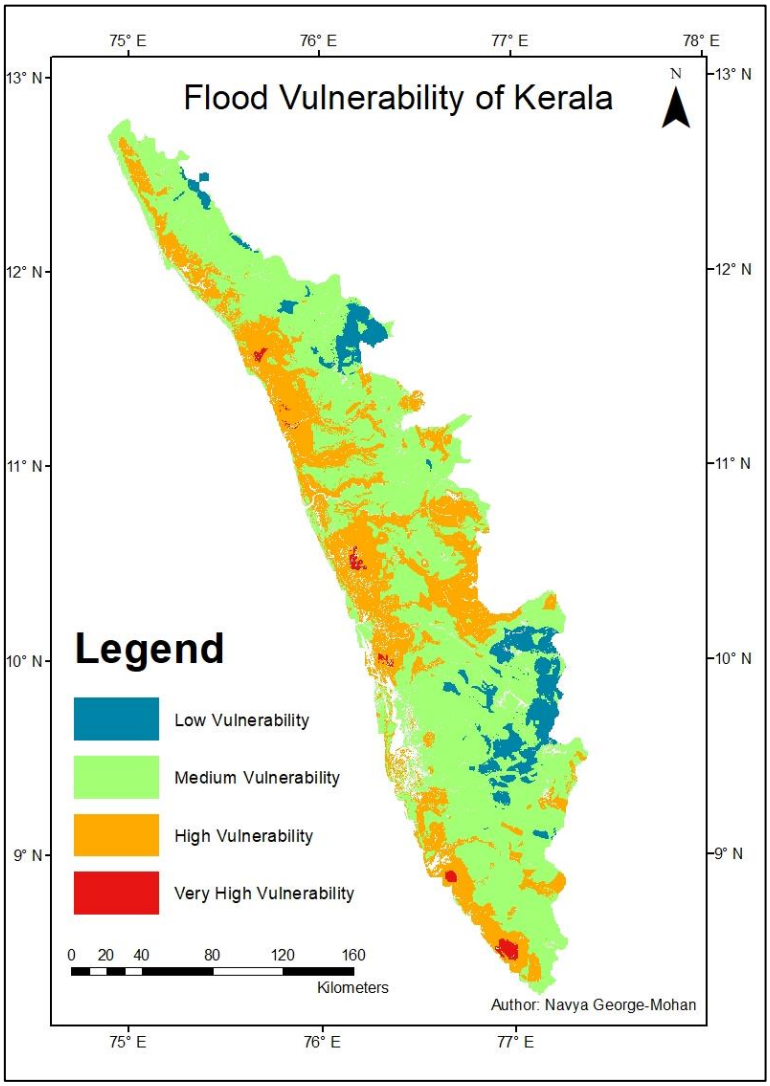

Figure 71: Flood Vulnerability of Kerala

One can see from Figure 72 above that most of the State is classified as medium vulnerability which is prominent in mid to high range areas, followed by high vulnerability regions. High

vulnerability regions are predominantly found in the east coast (low lying areas). The medium to low flood vulnerability is found on the highlands.

4.3.5 Flood Vulnerability Statistics

This section analyses the results of the flood vulnerability statistically. Table 36 below presents the area and percentage of each vulnerability class. Figure 72 depicts percentage area for each vulnerability level.

Table 36: Flood vulnerability areas in hectares and their percentages

Vulnerability	Area(ha)	Percentage
Low	266874.80	7.08%
Medium	2282407.48	60.59%
High	1072775.00	28.48%
Very High	25637.49	0.68%
Other	119580.58	3.17%
	3767275	100%

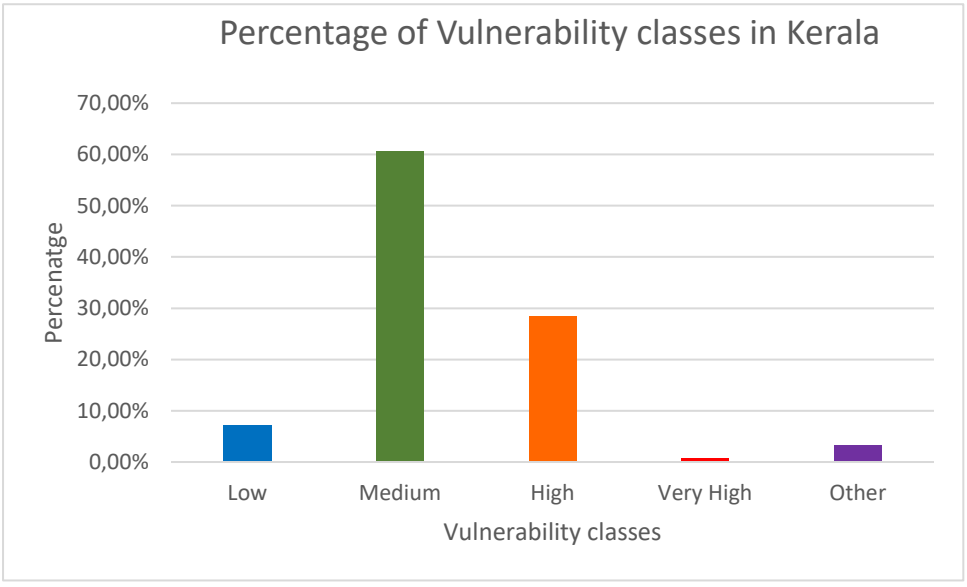

Figure 72: Percentage of Vulnerability classes in Kerala

Figure 72 and Table 36 above show that medium vulnerability is most prominent in the State. This is followed by high, low and then very high vulnerability regions. The last flooding events in Kerala were in the years 1961 and 1924 which not much data is available. However, Unnithanan (2018) states that all districts in the state were put under high alert. These studies results are therefore valid as medium and high vulnerability zones take up majority of the state with the other vulnerability zones having a very low percentage. This study took the average annual rainfall and did not focus on just the monsoon period which could explain why the entire state is not classified as Very high or High. These results show that the state is at risk for future floods and should make sure it is prepared and monitors flood possibilities in the future.

Chapter Five

5 CONCLUSION AND RECOMMENDATIONS

This thesis aimed to determine time series analysis of land use/cover between the years 1973 to 2018, model flood susceptibility during that period and lastly to determine the flood vulnerability for the year 2018. The time series analysis was achieved by classifying Landsat images of the State. Flood susceptibility was attained by processing variables such as drainage density, rainfall, soil types, lithology, the earlier mentioned land use/cover and slope. Once processed it underwent the multi-criteria decision-making approach which helped produce the flood susceptibility map. The flood vulnerability model was attained by taking into account infrastructure, social, coping mechanisms and flood susceptibility characteristics. All these results were attained by using GIS and Remote Sensing techniques.

There has been a definite change in land use/cover which has increased the flood susceptibility areas. The bare land has decreased by 305467.69 ha since 1973 up to the year 2018. The built-up area has increased by 704149.75 ha since 1973. The forest area has also decreased by 830968.79 ha. The crop land increase by 601882.90 ha in 2001 and decreased by 449787.55 ha in 2018.

The biggest increase in built-up area is seen between the years 1973 to 2001 and this can be attributed to the economic reform which took place in the 1990s. The forest areas saw a rapid decrease between the years 1973 to 2001 as the forest areas were turned into areas for plantation. The highest increase in crop land is seen between the years 1973 to 2001 because there was a shift to use the land for vegetation. The decrease in crop land by year 2018 can be explained by the change in culture of the local people towards farming.

The amount of rainfall over the years has changed. The range of the average rainfall has increased from 1973 to 2018 which means the amount of rainfall has increased. The year 2018 saw higher volumes of high to very high rainfall compared to the previous years. During the monsoon period, Kerala experiences long periods of high amounts of rainfall.

The increase in built-up area, decrease in forest and bare land and the increase in rainfall has contributed to the increase in flood susceptibility regions. By the year 2018 the high susceptibility regions was 1082687.10 ha, compared to 1973 which was just 618932,05 ha. There is an increase of 463755.05 ha. The medium susceptibility has increased from 1973 but has decreased from 2001 as more areas could be classified as high susceptibility regions.

The composite vulnerability map composed of infrastructure, social, copying vulnerability and flood susceptibility (physical vulnerability). Low infrastructural vulnerability was found in the midlands and highlands whereas medium infrastructural vulnerability was found in the low-lying areas. Medium to high social vulnerability was found in the high lands and very high social vulnerability was found in the lowlands. Very low copying vulnerability is found in the low-lying areas, low to medium copying vulnerability is found in the mind and high lands.

The areas which are highly flood vulnerable are along the west coast which are low lying areas of the State. Literature supports this finding as low-lying areas are usually flood prone. Other reasons that it is highly vulnerable is because it highly dense in population and built-up area when compared to the rest of the state. However, most of the State is found to be in the medium vulnerability regions (60.59%). This is mostly seen in the midland and highlands where crop land is high, and the density of the population and built-up areas is comparatively lower than the west coast.

A state-wide flood susceptibility and vulnerability map has not been produced and therefore this is a starting point. This data can be added to the research. The results of this study, though satisfactory, are not rigorous enough, due to errors inherent in data sets used. More accurate results can be obtained by using more accurate census, rainfall and geological data. Improved land use/cover mapping in the future will also contribute to more accurate flood vulnerability modelling over Kerala and elsewhere.

References

Abboud, J., Ryan, M. C. & Osborn, G. D., 2018. *Groundwater Flooding in a River-Connected Alluvial Aquifer,* Calgary: University of Calgary.

Abebe, Y., Kabir, G. & Tesfamariam, S., 2018. Assessing urban areas vulnerability to pluvial flooding using GIS applications and Bayesian Belief Network model. *Journal of Cleaner Production,* Volume 174, pp. 1629-1641.

Aggarwal, S. P., Thakur, P. K. & Dadhwal, V., 2009. Remote sensing and GIS Applications in Flood Management. *Journal of Hydrological Research and Development,* Volume 24, pp. 145-158.

Aized, S. & Awan, A., 2017. Classification techniques in machine leraning: applications and issues. *Basic and Applied Sciences,* Volume 13, pp. 459-465.

Ali, A., 2010. *Remote Sensing.* Iraq: University fo Technology,Iraq.

Anderson, E. & Brackenridge, R., 2006. *Modis-based flood detectiob, mapping and measuremnet: The potential for operational hydrological applications,* Netherlands: Springer.

Arseni, M. et al., 2017. Flood Hazard Monitoring using GIS and Remote Sensing observations. *Carpathian journal of earth and environmental sciences ,* 12(2), pp. 329-334.

Ayog, N., 2018. *The New Indian Express.* [Online]
Available at: https://www.newindianexpress.com/business/2018/feb/10/kerala-best-in-healthcare-tamil-nadu-third-health-index-report-1771163.html
[Accessed 25 January 2021].

Bai, L. et al., 2018. Accuracy of CHIRPS Satellite-Rainfall Products over Mainland China. *Remote Sensing,* 2(10), p. 362.

Balasubramanian, A., 2007. *India-Topography and slope,* Mysore: University of Mysore.

Balasubramanian, A., 2017. *Digital Elevation Model(DEM) in GIS,* Mysore: Centre for Advanced Studies in Earth Science, University of Mysore.

Baxter, N. & Williamson, J., 2001. *Know your soils- Part 1 introduction to soils.* 1 ed. State of Victoria: State of Victoria, Department of Natural Resources and Environment.

Bayliss, A. C. & Reed, D. W., 2001. *The use of historical data in flood frequency estimation,* Wallingforf: Centre for Ecology and Hydrology.

Benito, G. & Hudson, P. F., 2017. *Flood hazards: the context of fluvial geomorphology,* New York: New York University.

Bhatta, N. & GeethaPriya, M., 2016. *RADAR and its Applications.* Thuckalay, International Science Press.

Bindu, C. & Mohamed, A. R., 2016. Water bodies as a catalyst to growth and development-The case of Kodungallur town, Kerala. *ScienceDirect,* Volume 24, pp. 1790-1800.

Birkmann, J., 2007. of an indicator-based methodology for debris-flow hazards: Applicability, usefulness and policy implications. *Environmental hazards,* Volume 7, pp. 20-31.

Blösch, G. et al., 2015. Increasing river floods: Fiction or reality?. *Water,* 4(2), pp. 1-16.

Boopendranath, M. R., 2006. *Fishing effort management in Kerala,* Kochi: Central Institute of Fisheries Technology.

Brito, M. M. d., Evers, M. & Höllermann, B., 2017. Prioritization of flood vulnerability, coping capacity and exposure indicators through the Delphi technique: a case study in Taquari-Antas basin, Brazil. *International Journal of Disaster Risk Reduction,* Volume 24, pp. 119-128.

Bruijn, K. M. d. et al., 2016. *Flood vulnerability of critical infrastructure in Cork, Ireland.* s.l., European Conference on Flood Risk Management .

Bukhari, S. I. A. & Rizvi2, S. H., 2015. Impact of Floods on Women: With Special Reference to Flooding Experience of 2010 Flood in Pakistan. *Journal of Geography and Natural Disasters,* 5(2), pp. 1-5.

Carvalho, L. M. T. et al., 2007. *Weighted Overlay, Fuzzy Logic and Neural Networks for Estimating Vegetation Vulnerability within the Ecological Economical Zoning of Minas Gerais, Brazil,* Campos do Jordão: Brazilian Symposium on GeoInformatics.

Chan, Y. & Koo, V., 2008. An Introduction To Synthetic Aperture Radar (SAR). *Progress in Electromagnetic Research,* Volume 2, pp. 27-60.

Chapi, K., Shirzadi, A., Himan, S. & Singh, V., 2017. A novel hybrid artificial intelligence approach for flood susceptibility assessment. *Environmental Modelling and Software,* Volume 95, pp. 229-245.

Chen, A. S., Djordjević, S., Leandro, J. & Savić, D. A., 2010. An analysis of the combined consequences of pluvial and fluvial flooding. *Water Science and Technology,* 7(62), pp. 1491-1498.

Chrysaida-Aliki & Hatzichristos, T., 2019. *A GIS-based Spatial Multi-Criteria Decision Analysis: Crisp and Fuzzy Methods.* Limmassol, Agile.

Coninx, I. & Bachus, K., 2007. *Integrating social vulnerability to floods in a climate change context ,* s.l.: Catholic University of Leuven.

Cristofari, G., Wenk, M., Fuchs, S. & M, P.-K., 2019. The importance of indicator weights for vulnerability indices and implications for decision making in disaster management. *International Journal of Disiater Risk Reduction,* Volume 36.

D, V., M, S. G. & V, M., 2015. Long-Term Rainfall Trend of Kerala, Tamil Nadu and Pondicherry Using Departure Analysis. *International Journal odd Earth Sciences and Engineering,* 8(1), pp. 452-157.

Dordrecht, S., 2007. *Stream Ecology.* s.l.:Springerlink .

Doswell, C. A., 2003. *Flooding,* Norman: Elsevier Science.

Earle, S., 2015. *Physical Geology.* 2 ed. British Columbia: British Columbia Ministry of Advanced Education, Skills & Training, and the Hewlett Foundation..

Emergency Management Australia.(2002). Australian Emergency Manuals Series. Available at: https:www.ipcc.ch (Accessed: 14 February 2021)

Environment Agency.(2014). *Monthly water situation report.* Available at: https://assets.publishing.service.gov.uk/government/uploads/system/uploads/attachment_data/file/352710/WSR_Aug14.pdf (Accessed: 13 December 2020)

Esau, I. et al., 2016. Trends in normalized difference vegetation index (NDVI) associated with urban development in northern West Siberia. *Atmospheric Chemistry and Physics,* Volume 16, pp. 9563-9577.

Escober, F., Hunter, G., Bishop, L. & Zerger, A., 1999. *Introduction to GIS,* Melbourne: Department of Geomatics, The University of Melbourne.

ESRI. (2016). *Where does the ArcGIS Online Data Enrichment source data come from?. Available at*: https://support.esri.com/en/technical-article/00001223 (Accessed: 13 March 2021)

European Environment Agency. (2015). *WorldClim - Global Climate Data.* Available at: https://www.eea.europa.eu/data-and-maps/data-providers-and-partners/worldclim-global-climate-data (Accessed: 16 January 2021)

Faisal, A.-A., Kafy, A.-A. & Roy, S., 2018. Integration of Remote Sensing and GIS Techniques for Flood Monitoring and Damage Assessment: A Case Study of Naogaon District, Bangladesh. *Journal of Remote Sensing & GIS,* 7(2), pp. 1-5.

Fox, T. A. et al., 2017. Agricultural land-use change in Kerala, India: Perspectives from above and below the canopy. *Agriculture, Ecosystems and Environment,* Volume 245, pp. 1-10.

Joseph, S., 2014. *shodhganaga.* [Online]
Available at: http://shodhganga.inflibnet.ac.in/bitstream/10603/22485/13/13_chapter3.pdf [Accessed 09 07 2018].

Gaur, H., 2020. Research on Flood. *International Journal for Research in Applied Science & Engineering Technology (IJRASET),* Volume 8, pp. 442-443.

Getahun, Y. & Sintayehu, G., 2015. Flood hazard Assessment and Mapping of Flood Inundation Area of the Awash River Basin in Ethopia using GIS and HEC-GeoRAS/HEC-RAS. *Civin and Environmental Engineering,* 5(4), pp. 1-12.

Goodchild, M., 1992. Geographical Information Science. *International Journal of Geographical Information Science,* 16 September, 6(1), pp. 34-45.

Unnithanan, G.P. S., 2018. *India Today.* [Online]
Available at: https://www.indiatoday.in/india/story/kerala-floods-red-alert-withdrawn-from-all-districts-death-toll-touches-357-1317976-2018-08-19
[Accessed 1 March 2021].

Government of India. (2018). Study report: Kerala floods of August 2018. Available at: https://reliefweb.int/report/india/study-report-kerala-floods-august-2018-september-2018 (Accessed: 18 February 2018)

Government of Kerala. (2018). *Study report: Kerala floods of August 2018 (September 2018). Available at: https://reliefweb.int/report/india/study-report-kerala-floods-august-2018-september-2018 (Accessed: 11 January 2021)*

Grases, A. et al., 2020. Coastal Flooding and Erosion under a Changing Climate Implications at a Low-Lying Coast (Ebro Delta). *Water ,* Volume 12.

Gu, Y., Brown, J. F., Verdin, J. P. & Wardlow, B., 2007. A five-year analsyis of MODIS NDVI and NDWI for grassland assessment over the central Gret Plains of the United states. *Geophysical research letters,* Volume 34, pp. 1-6.

Gu, Y. et al., 2014. Evaluation of MODIS NDVI and NDWI for vegetation drought monitoring using Oklahoma Mesonet soil moisture data. *Geophysical Research Letters,* Volume 35, pp. 1-5.

Gu, Y. et al., 2008. Evaluation of MODIS NDVI and NDWI for vegetation drought monitoring using Oklahoma Mesonet soil moisture data. *Geophysical research letters,* Volume 35, pp. 1-5.

Hammami, S. et al., 2019. Application of the GIS based multi-criteria decision analysis and analytical hierarchy process (AHP) in the flood susceptibility mapping (Tunisia). *Geosciences,* Volume 12, pp. 1-16.

Haq, M., Akhtar, M., MuhammadSiddiqi, S. & Rahmatulla, P., 2012. Techniques of Remote Sensing and GIS for flood monitoringand damage assessment: A case study of Sindh province,Pakistan. *The Egyption Journal of Remote Sensing and Space Sciences,* Volume 15, pp. 135-141.

Harley, P. & Samanta, S., 2018. Modeling of inland flood vulnerability zones through remote sensing and GIS techniques in the highland region of Papua New Guinea. *Applied Geomatics,* 10(2), pp. 159-171.

Herring, R. J., 1980. Abolition of Landlordism in Kerala: A Redistribution of Privilege. *Economic and Political weekly ,* 15(26), pp. 61-71.

Hoque, M. A.-A., Tasfia, S. & Ahmed, N., 2019. Assessing Spatial Flood Vulnerability at Kalapara Upazila in Bangladesh Using an Analytic Hierarchy Process. *Sensors,* Volume 19, pp. 1-19.

Houston, D. et al., 2011. *Pluvial (rain-related) flooding in urban areas: the invisible hazard,* s.l.: The Joseph Rowntree.

Huggett, R. J., 2011. *Fundementals of Geomorphology.* 3 ed. Oxon: Taylor & Francis.

Hunt, K. & Menon, A., 2020. The 2018 Kerala floods: a climate change perspective. *Limate Dynamics,* Volume 54, pp. 2433-2466.

Janssen, V., 2009. Understanding coordinate reference systems, datums and transformations. *International Journal of Geoinformatics,* 5(4).

Jaysawal, N. & Bharati, V., 2014. *researchgate.* [Online]
Available at:
https://www.researchgate.net/profile/Neelmani_Jaysawal/publication/264383323_Urbanization_in_India_An_Impact_Assessment/links/5576652d08ae75363751abb9/Urbanization-in-India-An-Impact-Assessment.pdf?origin=publication_detail
[Accessed 10 07 2018].

Joy, B. H., Lee, M. Y. & Mizzi, A., 2020. nsights into the Teaching of Gradient from an Exploratory Study of Mathematics Textbooks from Germany, Singapore, and South Korea. *International Electronic Journal of Mathematics Education,* 15(3), pp. 1306-3030.

Kainz, W., 2014. *Geographich Infromation Science.* Vienna: Universität Wien .

Kandiannan, K., 2018. *Annual and monthly rainfall trend in plantation and spice farming Western Ghats districts.* [Online]
Available at:
https://www.researchgate.net/publication/326082441_Annual_and_monthly_rainfall_trend_in_plantation_and_spice_farming_Western_Ghats_districts
[Accessed 22 April 2020].

Kannan, K. P., 2005. Kerala's Turnaround in Growth Role of Social Development, Remittances and Reform. *Economic and Political Weekly,* 40(6), pp. 5-11.

Keiler, M., Totsching, R., Gade, T. & Papathoma-Kohle, M., 2012. Improvement of vulnerability curves using data from extreme events: debris flow event in South Tyrol. *Natural hazards,* Issue 64, pp. 2083-2105.

Kerala State of environment and Related issues. (2021). *Geological formations in Kerala. Available at:*
http://www.kerenvis.nic.in/Database/Geological_1345.aspx#:~:text=Three%20main%20geological%20formations%20are,These%20have%20North%2DSouth%20alignment.(Accessed: 1 March 2021)

Kerala State of Environment and Related Issues. (2020). *Land.* Available at: http://www.kerenvis.nic.in/Database/Land_817.aspx(Accessed: 8 October 2020)

Kohavi, R. & Provost, F., 1998. *Applied Research in machine Learning,* New York: Colunbia Univeristy.

Kotsiantis, S., 2007. Supervised Machine Learning: A Review of Classification. *Informatica,* Volume 31, pp. 249-268.

Krishnakumar, G., 2019. *The Hindu.* [Online]
Available at: https://www.thehindu.com/news/cities/Kochi/waterbodies-gasping-for-breath/article28090725.ece
[Accessed 6 August 2020].

Krishnakumar, K., Prasada Rao, G. & Gopakumar, C., 2008. Rainfall trends in twentieth century over Kerala, India. *Atmospheric Environmnet,* Volume 43, pp. 1940-1944.

Kshetri, T. B., 2018. *NDVI, NDBI & NDWI Calculation Using Landsat 7, 8.* [Online]
Available at: https://www.linkedin.com/pulse/ndvi-ndbi-ndwi-calculation-using-landsat-7-8-tek-bahadur-kshetri/
[Accessed 3 March 2020].

Kumar, B. M., 2005. Land use in Kerala: Changing scenarios and shifting paradigms. *Journal of Tropical Agriculture,* Volume 1, pp. 1-12.

Kumar, S., 2000. *Basics of Remote Sensing and GIS.* 1 ed. Chennai: Laxmi publishers.

Kundzewicz, Z. W., Hirabayashi, Y. & Kanae, S., 2010. River Floods in the Changing Climate—Observations. *Water Resouce Management,* Volume 24, pp. 2633-2646.

Kuruvilla, y. Z., 2018. *researcchgate.* [Online]
Available at:
https://www.researchgate.net/publication/265552035_Census_Towns_in_Kerala_Challenges_of_Urban_Transformation

Lappas, I. & Kallioras, A., 2019. Flood Susceptibility Assessment through GIS-based multi-criteria approach and analytical hierarchy process (AHP) in a river basin in Central Greece. *International Research Journal of Engineering and Technology (IRJET),* 6(3), pp. 738-758.

Lauda, J., Zoller, G. & Theiken, A., 2020. Flash floods versus river floods – a comparison of psychologicalimpacts and implications for precautionary behaviour. *Natural Hazards ad Earth SYstem Sciences,* Volume 20, pp. 999-1023.

Len, N. L. S. et al., 2018. Flood Vulnerability Index for Critical Infrastructure Towards Flood Risk Management. *American Society for Microbiology,* 11(3), pp. 132-146.

Len, N. L. S. et al., 2018. FLOOD VULNERABILITY OF CRITICAL INFRASTRUCTURES - REVIEW. *Malaysian Journal of geosciences,* 2(1), pp. 31-34.

Macdonald, A., 2019. *Jbarisk.* [Online]
Available at: https://www.jbarisk.com/news-blogs/using-historical-data-for-flood-estimation/
[Accessed 20 September 2020].

Macdonald, D., Dixon, A., Newell, A. & Hallaways, A., 2012. Groundwater flooding within an urbanised flood plain. *Journal of Flood Risk Management,* Volume 5, pp. 68-80.

Madhusoodanan, M., 2018. *Dynamical Downscaling of Regional Climate: Simulation of Extreme Rainfall Events and Their Impacts over the State of Kerala in the Near-Future,* Amritapuri: Amrita Center for Wireless Networks and Applications (AmritaWNA).

Madore, A., Rosenberg, J., Dreisbach, T. & Weintraub, R., 2018. *Positive Outlier: Health Outcomes in Kerala, India over Time,* s.l.: Harvward Medical School.

Maidment, D. R. & Tarboton, D., 2011. *Computation of Slope,* Austin: University of Texas.

Maqsood, T. et al., 2017. *Development of flood vulnerability models for cmmerical buildings in Australan Central Business Districts,* Sydney: The City of Sydney Council.

Marchi, M., Sinjur, I., Bozzano, M. & Westergren, M., 2019. Evaluating WorldClim Version 1 (1961–1990) as the Baseline for Sustainable Use of Forest and Environmental Resources in a Changing Climate. *Sustainability,* Volume 11, pp. 1-14.

McVicar, T. & Korner, C., 2012. On the use of elevation, altitude, and height in the ecological and climatological literature. *Oecologie,* Volume 171, pp. 335-337.

Melesse, A., Weng, Q., Thenkabail, P. & Senay, G., 2007. Remote Sensing Sensors and Applications in Environmental. *Sensors,* pp. 3209-3241.

Mibei, G., 2014. *Introduction to types of classification of rocks.* Lake Bogoria and Lake Naivasha, Geothermal Development Company.

Mou, D., Liu, Z., Wang, Z. & Xu, S., 2014. *The igneous rock lithology and logging curve characteristics of the eastern sag of liaohe basin.* Changchun, 2014 International Conference on Mechatronics, Electronic, Industrial and Control Engineering.

Mundhe, N., 2018. Multi-Criteria Decision Making for Vulnerability Mapping of Flood Hazard: A Case Study of Pune. *Journal of Geographical Studies,* 2(1), pp. 41-52.

Nasiri, H., Yusof, M. J. M. & Ali, T. A. M., 2016. *An overview to flood vulnerability assessment methods.* [Online]
Available at:
https://www.researchgate.net/publication/301664250_An_overview_to_flood_vulnerability_assessment_methods
[Accessed 27 February 2018].

National Academy of Sciences. 2001. *Growing Populations, Changing Landscapes: Studies from India, China, and the United States*. Washington, DC: The National Academies Press. https://doi.org/10.17226/10144

Nath, S., Mishra, G., Kar, J. & Chakraborty, S., 2014. A Survey of Image Classification Methods and Techniques. *International Conference on Control, Instrumentation, Communication and Computational Technologies,* pp. 554-557.

Noble, W. A., 2019. *Encyclopedia Britannica.* [Online]
Available at: https://www.britannica.com/place/Kerala
[Accessed 18 Fevruary 2019].

Ozcelik, C. & Gorokhovich, Y., 2020. An Overland Flood Model for Geographical Information Systems. *Water,* 9(12), pp. 1-20.

Ozeklan, E., 2019. Water body detection analysis using NDWI indices deried from landsat-8 OLI. *Pol. J. Environ. Stud,* 29(2), pp. 1-10.

Padmanabhan, D. N., 2011. *FORMATION OF KERALA SOCIETY AND CULTURE,* Calicut: University of Calicut.

Palubinskas, G., Reinartz, P. & Müller, R., 2003. Mosaicking of optical remote sensing imagery. *IEEE,* Volume 6, pp. 3955-3957.

Papathoma-Kohle, M., 2016. Vulnerability curves vs. vulnerability indicators: application of an indicator-based methodology for debris-flow hazards. *Natural hazards ad earth System Sciences,* pp. 1771-1790.

Paravath, B., 2019. *Mathrabumi.* [Online]
Available at: https://english.mathrubhumi.com/news/kerala/unemployment-rate-increasing-in-kerala--1.3882551
[Accessed 20 January 2021].

Paredes-Trejo, F. et al., 2020. *Assessment of the CHIRPS-Based Satellite Precipitation Estimates.* [Online]
Available at: https://www.intechopen.com/online-first/assessment-of-the-chirps-based-satellite-precipitation-estimates
[Accessed 20 AUgust 2020].

Ramachandran, R. & Reddy, C., 2016. Monitoring of deforestation and land use changes (1925–2012) in Idukki district, Kerala, India using remote sensing and GIS. *Indian Society of Remote Sensing,* Volume 10.

Ramerini, M., 2016. *colonialvoyage.* [Online]
Available at: https://www.colonialvoyage.com/dutch-malabar/#
[Accessed 8 July 2018].

Reddy, M., 2008. *Remote Sensing and Geographical Information systems.* 3 ed. Hyderbad: BS Publications.

Reinhardt, W., 2000. *Principles and Application of Geographic Infromation Systems and Internet/Intranet Technology,* Munich: University of the Federal Armed Forces Munich .

Richar & Bamler, R., 1999. *The SRTM mission: A world-wide 30 m resolution DEM from SAR interferometry in 11 days,* Stuttgart: University of Stuttgart.

Ritter, P., 1987. A Vector-based Slope ANd Aspect Generation Algorithm. *Photogrammteric Engineering and Remote Sensing,* 53(8), pp. 1109-1111.

Roder, G., Sofia, G., Wu, Z. & Tarolli, P., 2017. Assessment of Social Vulnerability to floods in the floodplain of northern Italy. *Weather, Climate, and Society,* 4(9), pp. 717-737.

Saaty, T., 1980. *The Analytic Hierarchy Process: Planning, Priority Setting, Resource Allocation.* 1 ed. s.l.:McGraw-Hill International Book Company.

Sanz-Ramos, M. & Amengual, A., 2018. *Flood forecasting using a coupled hydrological and hydraulic model (based on FVM) and high-resolution meteorological model.* Barcelona, s.n.

Sauvaget, C. et al., 2011. Socio-economic factors & longevity in a cohort of Kerala State, India. *Indian Journal of Medical research,* 5(133), pp. 479-486.

Scheuer, S., Haase, D. & Meyer, V., 2010. Exploring multicriteria flood vulnerability by integrating economic, social and ecological dimensions of flood risk and coping capacity: from a starting point view towards an end point view of vulnerability. *Natural hazards,* Volume 58, pp. 731-751.

Seenath, A., 2018. Effects of DEM Resolution on Modelling Coastal Flood Vulnerbaility. *Marine Geordesy,* 41(6), pp. 581-604.

Setler, L., 2014. *Geomorphology,* s.l.: ScienceDirect.

Sharma, P., 2018. *India Today.* [Online]
Available at: https://www.indiatoday.in/magazine/special-report/story/19950930-a-look-at-how-four-cities-promise-to-lead-indias-business-in-the-next-decade-808250-1995-09-30

Simon, S., 2018. *The New Indian Express.* [Online]
Available at:
https://www.newindianexpress.com/cities/thiruvananthapuram/2018/nov/26/reviving-keralas-rural-water-bodies-1903176.html
[Accessed 6 August 2020].

S, J. S. & C, M. S., 2016. Spatio-Temporal Dynamics of Urban Expansion of Cochin City Region in GIS based on Buffer Gradient Analysis. *International Journal of Science and Reserach ,* pp. 325-331.

Sowmya, K., John, C. & Shrivasthava, N., 2014. Urban flood vulnerability zoning of Cochin City, southwest coast of India, using remote sensing and GIS. *Journal of the International Societyfor the Prevention and Mitigation of Natural Hazards,* 73(1-18).

Standing Committee on Water Resources. (2017). *SIXTEENTH REPORT. Available: http://164.100.47.193/lsscommittee/Water%20Resources/16_Water_Resources_16.pdf.(Accessed: 7 December 2020)*

Stephenson, G., 2010. *A COMPARISON OF SUPERVISED AND RULE-BASED OBJECTORIENTATED,* Stellenbosch: Stellenbosch University.

Swain, K., Singha, C. & Nayak, L., 2020. Flood Susceptibility Mapping through the GIS-AHP Technique Using the Cloud. *Geo-Informtion,* Volume 9.

Taherkhani, M. et al., 2020. Sea-level rise exponentially increases coastal flood frequency. *Scientific Reprots ,* 1(10).

Tang, J. & Pilesjo, P., 2001. Estimating slope from raster data: a test of eigt different algorithms in flat, undulating and steep terrain. *WIT transactions on Ecology and the Environment,* Volume 146, pp. 143-154.

Tascón-González, L., Ferrer-Julià, M., Ruiz, M. & 1, E. G.-M., 2020. Social Vulnerability Assessment for Flood Risk Analysis. *Water,* Volume 12, pp. 1-25.

Teng, J. et al., 2017. Flood inundation modelling: A review of methods, recent advances and uncertainty analysis. *Environmental Modelling and Software,* Issue 90, pp. 201-216.

Teng, J. et al., 2017. *Flood inundation modelling: A Review of methods, recent advances and uncertainty analysis,* Canberra: Elsevier Ltd.

Tharamangalam, J., 1998. The perils of social development without economic growth: The development debacle of Kerala, India. *Bulletin of Concerned Asian Scholars,* 30(1), pp. 23-34.

Th, . I. A., M, . D. A. & N, H. S., 2014. Coupling GIS and Photogrammetry for the Development. *Journal of geoscience and geomatics ,* Volume 2, pp. 1-10.

Thomas, A., 2000. *Physiography, Climate and Vegetation of Kerala ,* Calicut: University of Calicut.

Thomas, K. A., 2000. *Physiography, CLimate and Vegetation of Kerala,* Calicut: University of Calicut.

Tingsanchali, T., 2012. Urban flood Disatser management. *Proceda Engineering,* Volume 32, pp. 25-37.

Tsapanou, A., Poulos, S., Oikonomou, E. & Drakopoulos, P., 2018. *The Sentinel-2A age for Earth and Ocean Observation: Preliminary implementation in the North-East Aegean Sea, Greece..* Athen, Hellenic Geographical Society Conferenc.

Ukrainski, P., 2017. *50northspatial.* [Online]
Available at: http://www.50northspatial.org/pick-best-supervised-classification-method/
[Accessed 19 07 2018].

United States Environment Protection Agency. (2020). *Climate Change Indicators: Coastal Flooding.* Available at: https://www.epa.gov/climate-indicators/climate-change-indicators-coastal-flooding (Accessed on: 12 December 2020)

Unnithan, P. (2018.). Rains wreak havoc in Kerala with more than 34,000 people marooned. [online] India Today. Available at: https://www.indiatoday.in/india/story/kerala-rains-schools-shut-waterlogging-train-traffic-highway-1288316-2018-07-17 [Accessed 21 Aug. 2021]

Vajsova, B. & Astrand, P., 2015. *New sensors benchmark report on Sentinel-2A,* s.l.: Europian Union.

Vázquez-Quintero, G. et al., 2020. GIS-Based Multicriteria Evaluation of Land Suitability for Grasslands Conservation in Chihuahua, Mexico. *Sustainability,* Volume 12, pp. 185-204.

Vishnu, C. et al., 2019. Satellite-based assessment of the August 2018 flood in parts of Kerala, India. *Geomatics, Natural Hazards and Risk,* 10(1).

Vojtek, M. & Vojtekova, J., 2019. Flood Susceptibility Mapping on a National Scale in Slovakia Using the Analytical Hierarchy Process. *Water,* Volume 11, pp. 1-17.

Votjek, M. & Vojtekova, J., 2019. Flood Susceptibility Mapping on a National Scale in Slovakia Using the. *Wayter,* 2(11).

Wacker, A. & Landgrebe, D., 1972. *Minimum Distance Classification in Remote Sensing.* [Online]
Available at:
https://www.researchgate.net/publication/38118906_Minimum_Distance_Classification_in_Remote_Sensing
[Accessed 19 07 2018].

Wulder, M. et al., 2016. The Global Landsat Archive: Status, Consolidation, and Direction. *Remote Sensing of Environment,* Volume 185, pp. 271-283.

Wu, Z. & Abdul-Nour, G., 2020. Comparison of Multi-Criteria Group Decision-Making Methods for Urban Sewer Network Plan Selection. *CivilEng,* Volume 1, pp. 26-48.

Yin, H. et al., 2012. How Normalized Difference Vegetation Index (NDVI) trends from Advanced Very High Resolution Radiometer (AVHRR) and Système Probatoire d'Observation de la Terre Vegetation (SPOT VGT) Time Series Differ in Agricultural Areas: An Inner Mongolian Case Study. *Remote Seinsing,* Volume 4, pp. 3364-3389.

Yin-Loh, W., 2011. Classification and regression trees. *WIREs Data Mining and Knowledge Discovery,* Volume 1, pp. 14-22.

Zhang, L., 2006. Engineering properties of rocks. *Elsevier Geo-Engineering Book Series,* Volume 4, pp. 231-252.

Zhang, L., 2013. *Aspects of rock permeability,* Arizona: Department of Civil Engineering and Engineering Mechanics, University of Arizona.

Zhou, Q., 2017. *Digital Elevation Model and Digital Surface Model,* Hong Kong: Hong Kong Baptist University.